

VISIBILIS



CALIBRATION AND VALIDATION OF
PARTICULATE MATTER SENSORS

André van der Wiel
Dieter Pientka



Version 1.2 - compact
26 December 2019



Acknowledgements

We would like to acknowledge RIVM and particular Marita Voogt for arranging the project location at Berghaven. This gave us the unique opportunity to execute the project in the presence of official monitors.

We would like to acknowledge DCMR and particular Ed van der Gaag and Wilfred van Vliet for the pleasant cooperation and the expert assistance with the installation of the sensor case at Berghaven location.

We would like to acknowledge CAMO Norway and particular Joseph McCurley for providing 'The Unscrambler X' for developing of the calibration models and statistical analysis.

We would like to acknowledge Teus Hagen and Joost Wesseling for reviewing the concept version.

Without the friendly help of everyone, this project could not be successfully completed.

Summary

"Visibilis" is the Latin word for visible. It is the core message of a citizen science project started in May 2018. It is about making visible the invisible particles in the air that largely determine the quality of the air.

The aim of this study is to increase the reliability of relatively cheap particulate matter sensors by means of a model in which the output of the sensor is calibrated against the BAM1020 monitor.

The project was conducted at an official air quality measuring location in Hoek van Holland. A weatherproof case full of different types of sensors and peripheral equipment has been installed on the roof of the measuring location, next to the official particulate matter (PM) monitors BAM1020 and Leckel. Data is collected from the 16th of May 2018 till the 26th of January 2019.

The reliability of the sensor can be improved by using the multiple linear regression (MLR) technique. The PM value from the sensor is read in by the model and the output of the model is the prediction for the PM value as it was measured by the official monitor Met One BAM1020. The MLR model corrects the calibrated PM value for the temperature and relative humidity of the ambient air, which further improves the reliability of the PM sensor.

The accuracy of the calibration models for the Plantower PMSA003- and Nova SDS011 sensors is 4 µg/m³ for PM2.5 and 8 µg/m³ for PM10. The accuracy of the PM2.5 models is good in line with the reproducibility of 4 µg/m³ of the BAM1020 monitor. The PM10 calibration models show an overall bad performance, possibly due to lack of sensitivity for particles >2.5 µm. The validation of the models show an accuracy of 4 µg/m³ for PM2.5 and 8 µg/m³ for PM10.

The accuracy of the MLR calibration models can be further improved by performing the calibration on the particle number (PN) concentrations. This is only possible for the PMSA003- and Dylos DC1100 sensors where the Dylos DC1100 sensor only supports PN. The accuracy of the calibration models for the PMSA003 sensors is 3 µg/m³ for PM2.5 and 6 µg/m³ for PM10. For the Dylos DC1100 sensor the accuracies are respectively 5 µg/m³ for PM2.5 and 9 µg/m³ for PM10. The validation of the models for the PMSA003 sensor show an accuracy of 3 µg/m³ for PM2.5 and 6 µg/m³ for PM10. The validation of the models for the Dylos DC1100 sensor shows an accuracy of 5 µg/m³ for PM2.5 and 8 µg/m³ for PM10.

The extent to which the models are transferable between the PMSA003 sensors has been investigated. This appears to be successful for the model based on mass concentration of particulate matter. The transferability for the model based on particle concentrations can be improved by standardizing the particle classes to a standard sensor.

Table of Contents

Acknowledgements.....	3
Summary.....	4
1 Introduction.....	6
2 Location Berghaven.....	7
3 Sensor Case Construction.....	8
4 Particulate matter sensors and official monitors.....	9
5 Data collection.....	11
6 Database.....	12
7 Data exploration.....	13
7.1 Particulate matter.....	13
7.2 Meteorology.....	24
8 Calibration & Validation.....	26
8.1 Plantower algorithm.....	26
8.2 Calibration of the sensors against BAM1020.....	29
8.3 Improvement of MLR model performance by ASTM D6708.....	38
8.4 Validation MLR models.....	41
8.4.1 <i>MLR validation results based on "PM+RH+T"</i>	42
8.4.2 <i>MLR validation results based on "PN+RH+T"</i>	46
8.5 MLR model transfer between Plantower sensors.....	50
8.5.1 <i>Real-time experiment model transfer PMSA003 sensor</i>	51
8.6 Standardization of the MLR Calibration Model based on particle numbers.....	54
9 Conclusions & Recommendations.....	58
9.1 Improvement of the model.....	58
9.2 Transferability of the model.....	58
9.3 Recommendations.....	59
Contact.....	60
License.....	60
Tables.....	61
Figures.....	62
Appendix 1.....	65
References.....	66

1 Introduction

"Visibilis" is the Latin word for visible. It is the core message of a citizen science project started in May 2018. It is about making visible the invisible particles in the air that largely determine the quality of the air. With the help of RIVM (National Institute for Public Health and the Environment) and DCMR (Rijnmond Environmental Service), the unique opportunity was obtained to use the "Berghaven" measuring location in Hoek van Holland. A weatherproof case full of sensors and peripheral equipment has been installed on the roof of the measuring location, next to the official particulate matter (PM) monitors BAM1020 and Leckel. With an official monitor it is meant that the monitor is calibrated and maintained by DCMR.

The composition of the sensor case is as follows:

- 1 x Dylos DC1100 Pro connected (serial/USB) to Raspberry Pi
- 1 x Nova SDS011 connected (serial/USB) to Raspberry Pi
- 1 x Nova SDS011 as Luftdaten variant with NodeMCU / Wifi linked to Raspberry Pi
- 3x Plantower PMSA003 to Wemos D1 Mini Pro with Wifi linked to Raspberry Pi
- 3x Bosch meteo BME280 on Wemos D1 Mini Pro with Wifi linked to Raspberry Pi
- 1x Dallas DS18B20 One Wire GPIO connected to Raspberry Pi (outside temperature)

The set-up at this location offers the possibility to compare the performance of the sensors with each other and with the measurement results of the official measuring equipment. If we know what the performance of the sensors are and how they relate to each other, then it becomes interesting to look at the possibility of calibration and validation procedures against the official measuring equipment. The output of a particulate matter sensor is sensitive to air humidity and temperature, these parameters are included in the calibration process. The aim was to collect sufficient data to achieve a representative variation in the particulate matter and weather conditions. The aim of this study is to increase the reliability of the particulate matter sensor by means of one conversion algorithm applied to the raw sensor output data.

2 Location Berghaven

The project was conducted at the 'Berghaven' DCMR location in Hoek van Holland. This location is close to the Nieuwe Waterweg and surrounded by lawns. It is partly residential- and industrial area. There are no high buildings in the direct surroundings. The industrial activity is high south to the location, there is open sea west to the location and a small harbor is situated east to the location. The Nieuwe Waterweg south to the location, is a very busy route for all kind of (cruise) ships and tankers as main route to and from the port of Rotterdam. There are three restaurants located to the west of the location at a distance of 250 to 750 meters. The influence of these restaurants on the air quality at the location is estimated to be limited and is only important in a western wind.

Due to the nature of this location it is expected that all kind of artificial and airborne particles can be present, also strongly depending on the wind direction. With a southeast to southwest wind, high concentrations of particulate matter from ships can occur temporarily. Because the station is close to the sea, the chances are high that salt crystals will be present in the air with a southwest to northwest wind direction.

The sensor case was installed on the flat roof of the analyzer house. The roof is covered with black rubber mats.

The location of the analyzer house is presented as a blue marker in figure 1 and 2.

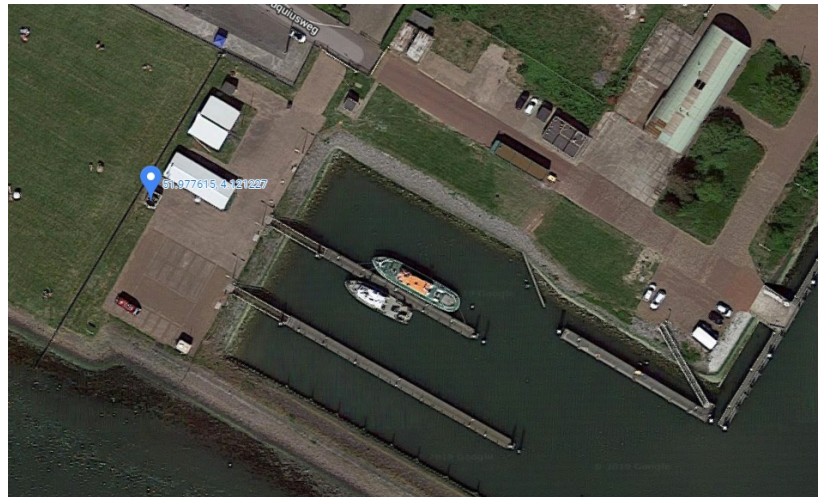


Figure 1: Location Visibilis Project

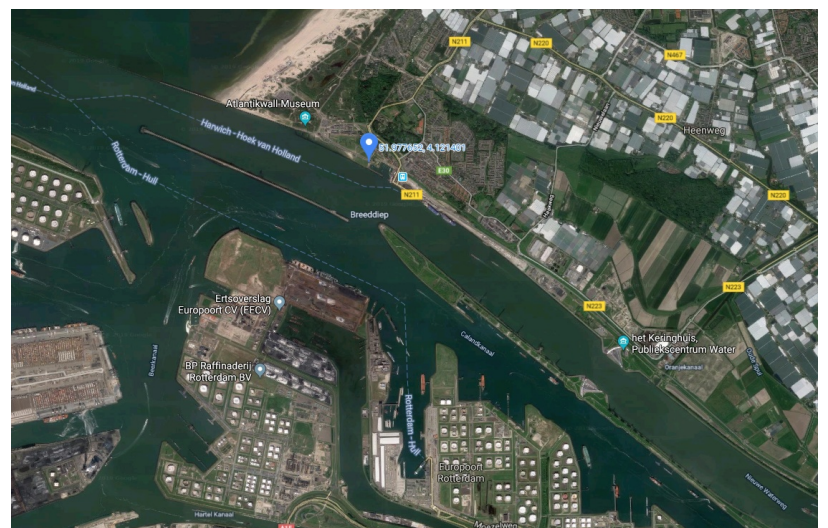


Figure 2: Berghaven, Hoek van Holland

3 Sensor Case Construction

The sensor case is constructed from an original black plastic single walled Dylos case. The bottom and lower side walls of the case are provided with 20 round holes of 25 mm diameter. The holes are needed for extra ventilation in the case because a micro climate is to be expected. The case is mounted on 4 rubber door stoppers of 5 cm high, attached to every corner of the bottom of the case. This causes extra ventilation through the bottom of the case and it will prevent water leakage into the case during heavy rain or melting snow. The inside bottom and side walls of the case are covered with insect gauze, 1 mm² mesh size, to prevent insects and dust coming into the case.

The sensors are mounted in modules per sensor type, where the Dylos is mounted in a metal construction to prevent obstruction of the internal Dylos ventilator. The Raspberry Pi is used to collect the sensor data. A power supply unit is mounted inside the case to feed the different sensor modules, Raspberry Pi and Dylos. An extra ventilator is mounted inside the sensor case against one of the 20 available holes, actively sucking outside air into the case. The extra generated airflow is needed for continuous 'fresh' air into the box and also to stimulate extra ventilation through all the sensor modules and to remove heat generated by the electronics.

The Raspberry Pi is connected to the LAN via an ethernet cable. The power supply cord is led outside the case via a rubber manchet. The external Dallas temperature sensor and the LAN ethernet cable are led outside the case via an open hole.

An upside down sample crate was put on the top of the sensor case and the crate was secured by a stone tile. The crate prevents rain or snow coming into the sensor case. A picture of the sensor case is given in figure 3.



Figure 3: Sensor case

4 Particulate matter sensors and official monitors

At DCMR location "Berghaven" multiple particulate matter (PM) monitors are operational. The following PM monitors are installed at Berghaven:

- Sven Leckel SEQ 47/50 gravimetric Reference Sampler for PM10 (not for PM2.5)
- Met One BAM1020 for PM10 (beta ray attenuation)
- Met One BAM1020 for PM2.5 (beta ray attenuation)

For this project the BAM1020 is chosen as official monitor for both the calibration and validation of the particulate matter sensors. The main reason for this choice is the fact that the BAM1020 monitors can give hourly measurements for both PM2.5 and PM10, while the Leckel monitors only give 24 hours measurements. The BAM1020 monitor has been proven to be equivalent to the Leckel monitor for 24 hours measurements for both PM2.5 and PM10.

The lower detection limit for hourly measurements of PM2.5 and PM10 with the BAM1020 is $4 \mu\text{g}/\text{m}^3$ (24 hours: $1 \mu\text{g}/\text{m}^3$). This means for hourly measurements that results $<4 \mu\text{g}/\text{m}^3$ should be considered as noise. The measurement uncertainty of the BAM1020 for hourly measurements is $4 \mu\text{g}/\text{m}^3$ ⁽³⁾.



Figure 4: Sven Leckel SEQ47/50
(www.leckel.de)



Figure 5: Met One BAM1020
(www.metone.com)

The properties of the particulate matter sensors, as stated in the factory manuals, are given in table 1. For all particulate matter sensors, the measuring principle is based on laser technology.

Sensor Type	Minimum detectable diameter (μm)	Counting efficiency (%)	Accuracy (%)
PMSA003	0.3	50 ($0.3\mu\text{m}$); 98 ($\geq 0.5\mu\text{m}$)	10
SDS011	0.3	70 ($0.3\mu\text{m}$); 98 ($\geq 0.5\mu\text{m}$)	15
Dylos DC1100	0.5	≥ 90	na

Table 1: Properties of the particulate matter sensor

All sensors have a good counting efficiency for particles $\geq 0.5\mu\text{m}$. The accuracy of the Dylos DC1100 sensor is not specified by the vendor.

The Dylos DC1100 sensor gives the particle concentration for two classes (particles/0.01 cubic foot) for $>0.5\mu\text{m}$ and $>2.5\mu\text{m}$. The PMSA003- and SDS011 sensors use an internal factory algorithm to convert the particle concentration to a mass concentration. In addition to mass concentration, the PMSA003 sensor also gives particle concentrations for six classes (particles/0.1L) for $>0.3\mu\text{m}$, $>0.5\mu\text{m}$, $>1.0\mu\text{m}$, $>2.5\mu\text{m}$, $>5.0\mu\text{m}$ and $>10.0\mu\text{m}$. The cut-off borders of the six classes are not known.

The properties of the meteorological sensors, as stated in the factory manuals, are given in table 2.

Bosch BME280	Unit	Range	Accuracy	Resolution	Noise (RMS)
Temperature	$^{\circ}\text{C}$	-40 - 85	0.5	0.01	0.005
Relative Humidity	%	0 - 100	3	0.008	0.02
Air Pressure	hPa	300 - 1100	1.0	0.12	0.2
Dallas DS18B20					
Temperature	$^{\circ}\text{C}$	-55 - 125	0.5	0.0625	na

Table 2: Properties of the meteorological sensors

The follow up for the BME280 is the BME680 with better accuracy.

5 Data collection

The sensor case was installed at DCMR location Berghaven on the 7th of May 2018. The first week was used to test the sensors for their stability under real time conditions. During that week small issues were resolved, mainly data collection problems on the Raspberry Pi and the data webserver. On the 16th of May 2018 the official data collection has started. The aim was to collect data for one year of time, but unfortunately the data collection was needed to put on hold on the 26th of January 2019 due to serious communication problems with the Raspberry Pi. This resulted in approximately 8 months of data collection and the winter- and spring period has not been covered completely.

Every sensor has an unique code in the data collection process. This is necessary to distinguish between the different sensor data in the database. The data of the sensors is automatically transferred to the Scapeler data server. The data of the DCMR monitors and KNMI meteorological monitors is made available via an API (Application Programming Interface). The meteorological data collection from the KNMI monitors was started from the 14th of June 2018. The DCMR monitor data are averaged hourly observations and can be retrieved from the 'Luchtmeetnet' website (<https://www.luchtmeetnet.nl/>). Luchtmeetnet is the Dutch governmental air quality measurement network. The KNMI data are averaged hourly observations, based on 6 individual 10 minute observations and are retrieved from the KNMI website (<https://projects.knmi.nl/klimatologie/uurgegevens/selectie.cgi>).

The coding of the sensors and official monitors is given in appendix 1.

One of the Plantower sensors (PMSA003_8F33) started to generate randomly very high spikes and/or very high constant output from the 2nd of August. The pattern looked like an internal technical sensor issue. This problem got worse during the rest of the month. On the 9th of September it was decided to stop the data collection of this sensor, because the abnormal output was present for more than 50% of the time. The sensor was not replaced by a new one.

The PMSA003-, SDS011 basic- and Dylos DC1100 sensors operated in continuous mode where every second the data was sent to the Raspberry Pi. The Raspberry Pi computed 1 minute averages and sent the data to the 'ApriSensor' server (<https://www.scapeler.com/index.php/diensten/aprisensor/>).

The 'Luftdaten' sensor operated with specific firmware (<https://luftdaten.info/en/home-en/>) where every 2.5 minutes the measurement was started and stopped. The data was uploaded to the 'Luftdaten' cloud server and subsequently downloaded by the 'ApriSensor' server.

6 Database

The data is converted to averaged hourly observations by averaging the 1 minute or 2.5 minute observations. The hourly observation of e.g. 10 AM is the average of 60 minute observations from 9:01 AM till 10:00 AM. The database is compiled on the basis of hourly observations, where one hour is considered as one ‘sample’. Every sample has a corresponding value for the official monitors and sensors. The database consists of 6131 samples collected in the period 16 May 2018 0:00 AM till 26 January 2019 10:00 AM. In total 13 “time periods” are defined in the database, each period has a duration of approximately 2 to 3 weeks. The time periods are chosen chronologically.

At random moments in time, the sensors produced missing data, in most occasions for just one minute. The missing data is not taken into account for further analysis. Because of the high resolution of the data, missing data has negligible effect on the hourly averages.

At random moments in time, the DCMR monitors and/or the sensors caused missing or constant data for longer periods. This was caused by LAN-, Wifi- or Raspberry Pi communication problems. This type of data is considered as invalid data and removed from the database.

Sudden very high or very low abnormal values, out of the trend, are considered as spikes and removed from the database. This was for example an issue for the BME280 air pressure sensor returning zero values.

The Plantower PMSA003 sensor has the ability to output the particulate matter in two different ways, that is the concentration of PM1, PM2.5 and PM10 in $\mu\text{g}/\text{m}^3$ and the concentration in particles/0.1 liter (particle number PN). The PN is given for six classes, for $>0.3 \mu\text{m}$, $>0.5 \mu\text{m}$, $>1.0 \mu\text{m}$, $>2.5 \mu\text{m}$, $>5.0 \mu\text{m}$ and $>10.0 \mu\text{m}$. The definition of PN is the number of particles per 0.1 liter of air having a diameter greater than the specified value. For the three PMSA003 sensors, both the PM- and the PN data is incorporated into the database and are taken into account for the calibration and validation of the PMSA003 sensor against the BAM1020.

Data is collected from three Bosch BME280 meteorological sensors. A preliminary study of the Bosch sensors showed a strong consistency in the data for temperature, relative humidity and air pressure. Therefore it was decided to incorporate data of one particular Bosch sensor in the database (BME280_8F33 sensor 1).

7 Data exploration

The construction of the database, exploration, statistics, calibration and validation of the models is worked out by use of the chemometrics software package The Unscrambler® X from CAMO Norway (<https://www.camo.com/unscrambler/>). For all XY-correlation (scatter) plots and model validation plots, the black line is the target line ($Y=X$) and the blue line is the regression line. For all model calibration plots, the black line is the target line and the red line is the regression line.

7.1 Particulate matter

The BAM1020 monitor data for PM2.5 and PM10 is presented in figure 6.

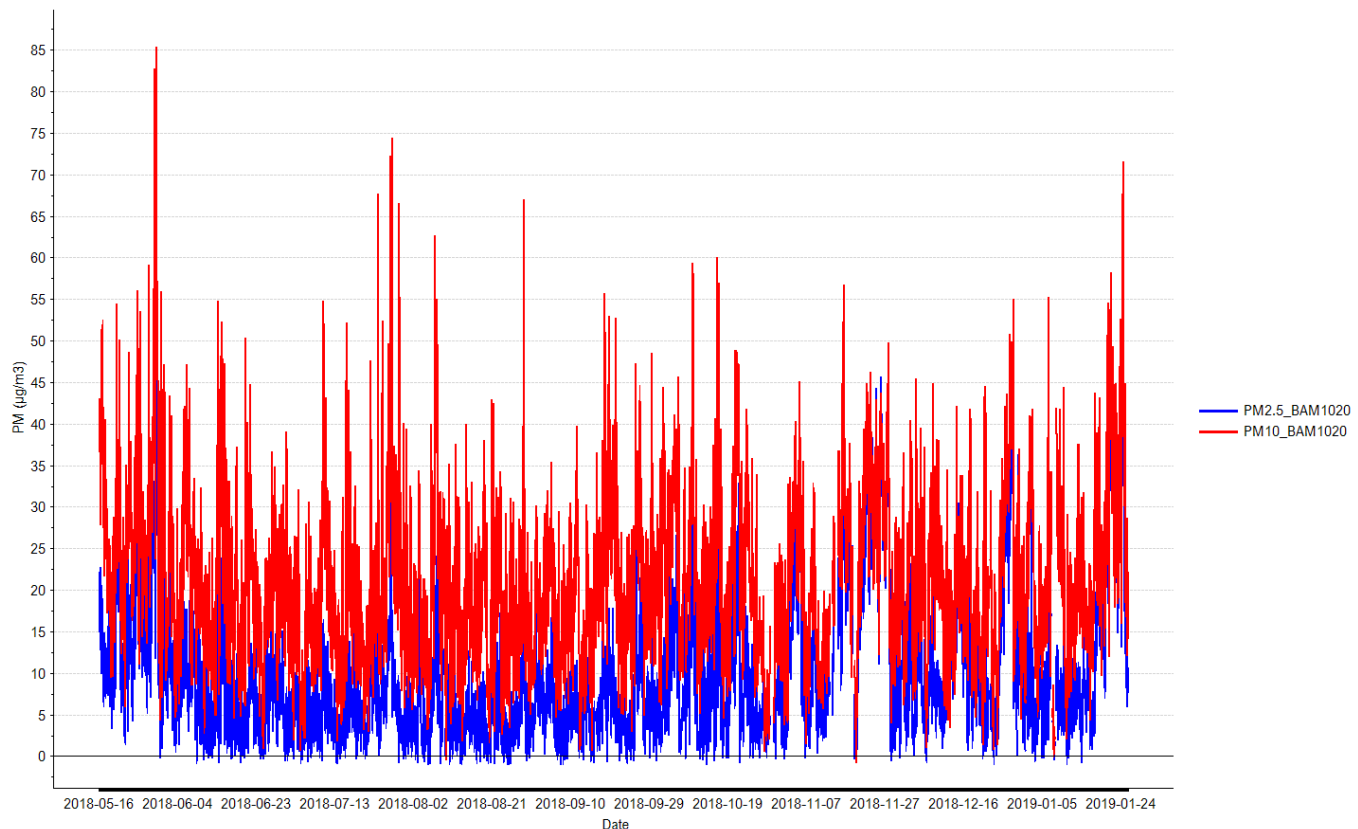


Figure 6: PM2.5 & PM10 data for the BAM1020 monitors at DCMR Berghaven

The average concentration for PM2.5 and PM10 are respectively $9.8 \mu\text{g}/\text{m}^3$ and $21.3 \mu\text{g}/\text{m}^3$ with a standard deviation of respectively $8.5 \mu\text{g}/\text{m}^3$ and $10.3 \mu\text{g}/\text{m}^3$. In general the PM10 value is higher than the PM2.5 value, except for the periods 17 November till 28 November 2018 and 2 January till 26 January 2019 where the PM10 value is almost equal to the PM2.5 value. There is no period with extreme high or low PM concentrations. The variation in concentration is randomly distributed among the seasons. Despite the fact that the project period has not met 1 year of runtime, it is assumed that the variation within the 8-month period is indicative for the project.

The correlation between the BAM1020 hourly data for PM2.5 and PM10 is investigated and based on 6008 data pairs.

- the maximum PM2.5 value is $63 \mu\text{g}/\text{m}^3$

- the maximum PM10 value is $85 \mu\text{g}/\text{m}^3$
- the majority of the data for PM2.5 is $< 15 \mu\text{g}/\text{m}^3$
- the majority of the data for PM10 $< 25 \mu\text{g}/\text{m}^3$
- the squared correlation coefficient (R^2) is weak

The correlation is presented in figure 7.

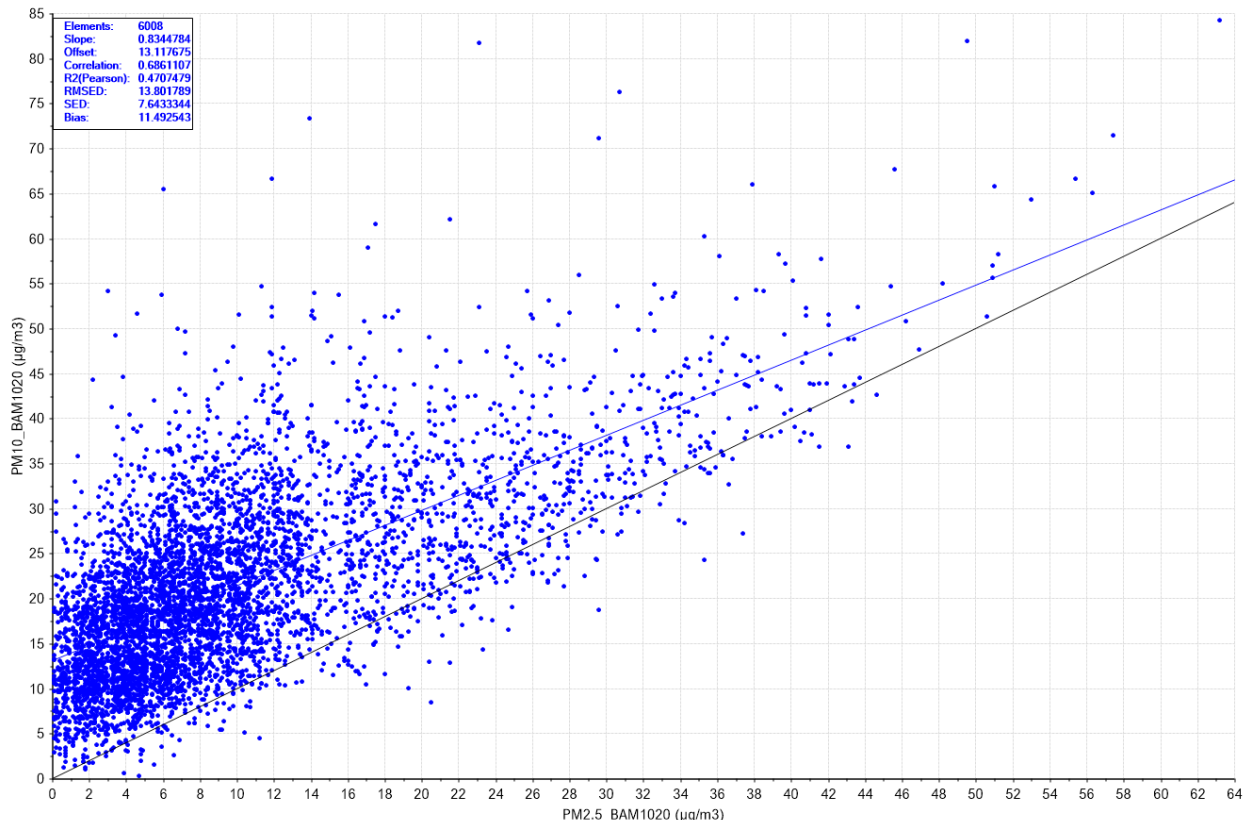


Figure 7: Correlation between PM2.5 & PM10 for the BAM1020 monitors at DCMR Berghaven

The correlation between the raw PM2.5 and PM10 output is also investigated for the sensors. The raw output is directly retrieved by the sensor and not corrected by any pretreatment. The Dylos sensor does not output PM values, therefore the correlation is investigated between particles $> 0.5 \mu\text{m}$ and particles $> 2.5 \mu\text{m}$.

The correlation plots are presented in figures 8, 9, 10 and 11.

The correlations of the PMSA003 sensors show similar performance. The PMSA003_9492 plot is taken as a representative example for the other two sensors.

The PM correlation plots for the sensors all show a 'V-shaped' curve. The V shape is caused by multiple correlation lines present in different data sets. For the Dylos DC1100 sensor, the particle concentrations (PN) are taken as input variables. The V shape is also visible in case the PN classes of the other sensors are taken as input variables. Possible explanations for the V shape could be the origin of the airborne particles or humidity effects or a combination of both. The sensitivity of the sensor laser will be influenced by the composition of the airborne particles. For example, the size of salt crystals is effected by humidity, this effect is known as 'humidity growth'. Location Berghaven is very close to the sea, salt crystals (NaCl) are definitely a part of the airborne particles for this location.

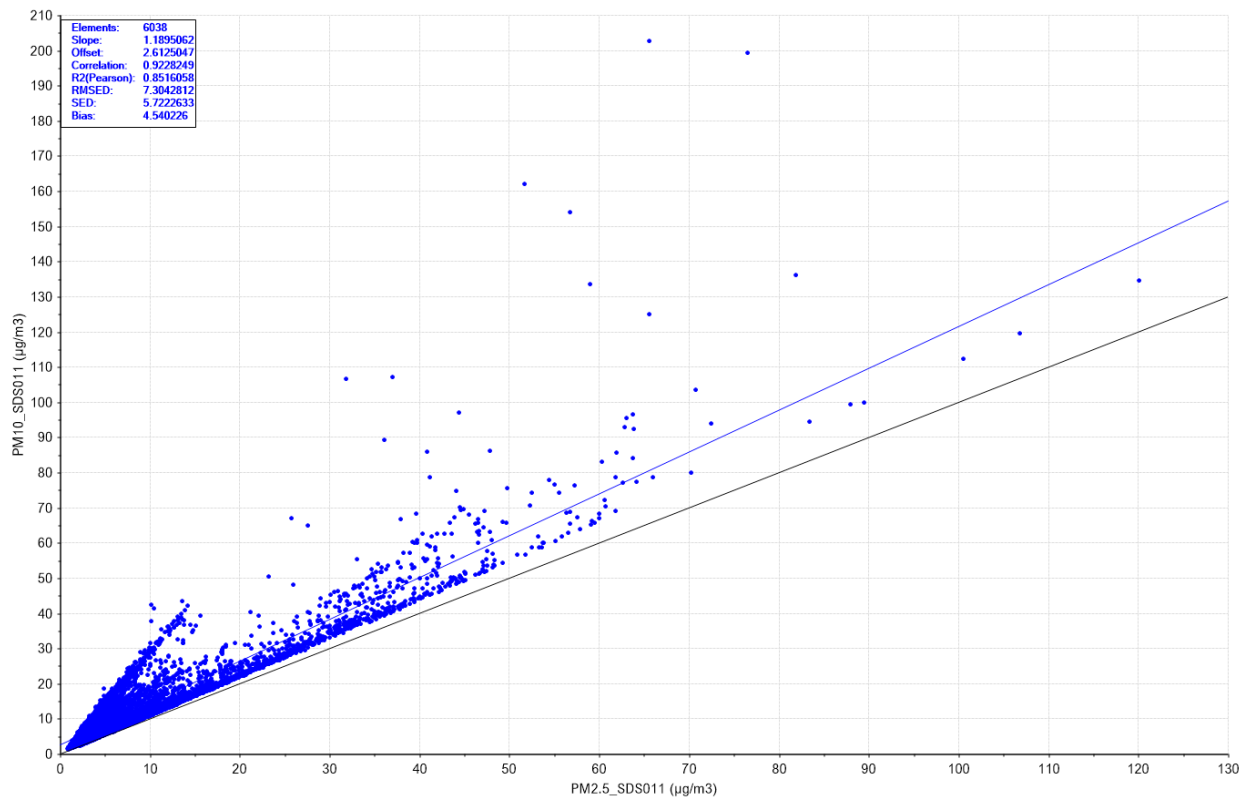


Figure 8: Nova SDS011 correlation plot between PM2.5 & PM10

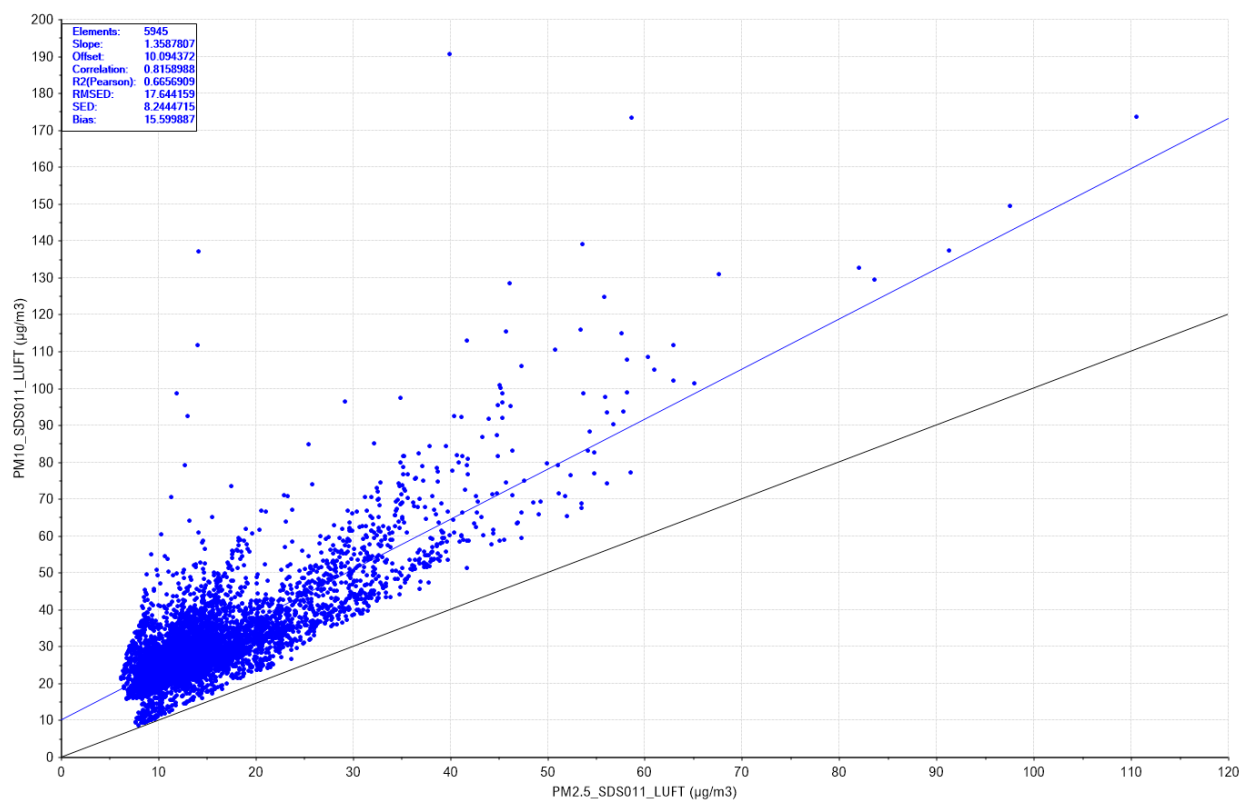


Figure 9: Nova SDS011 'Luftdaten' correlation plot between PM2.5 & PM10

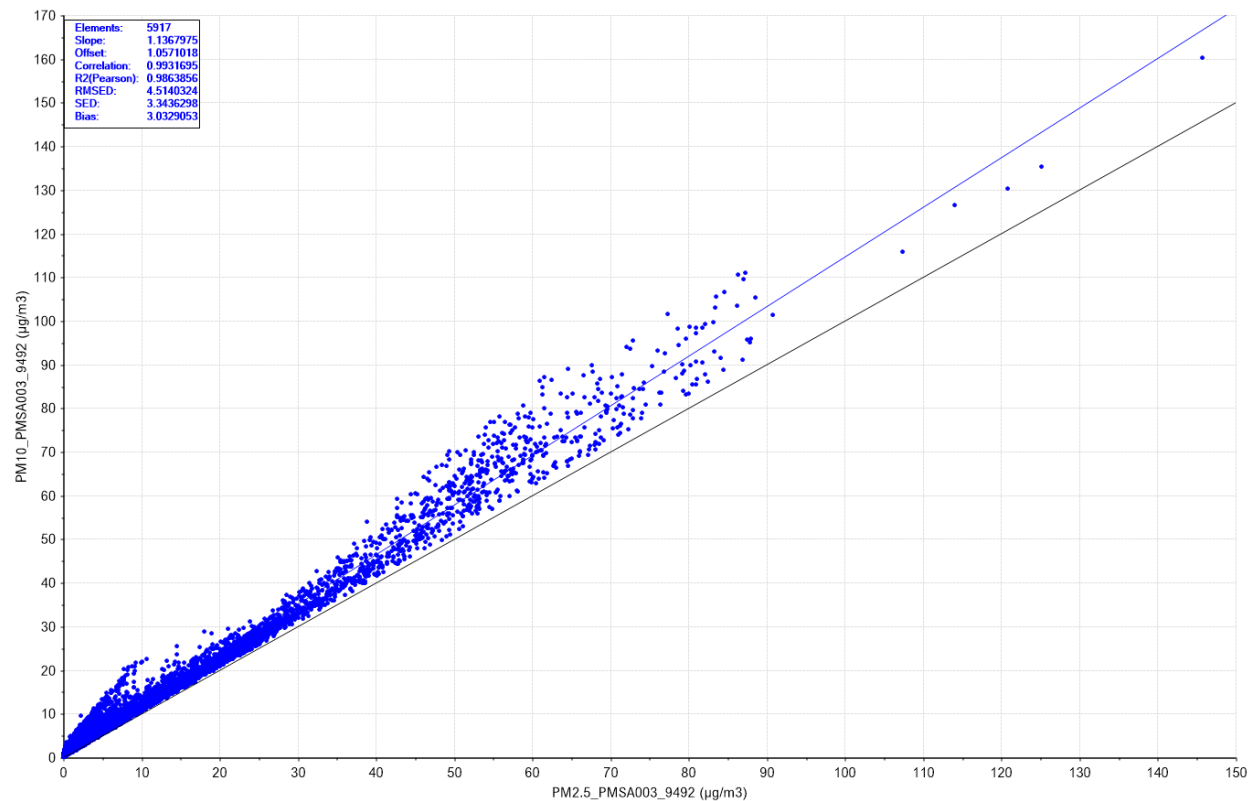


Figure 10: Plantower PMSA003_9492 correlation plot between PM2.5 & PM10

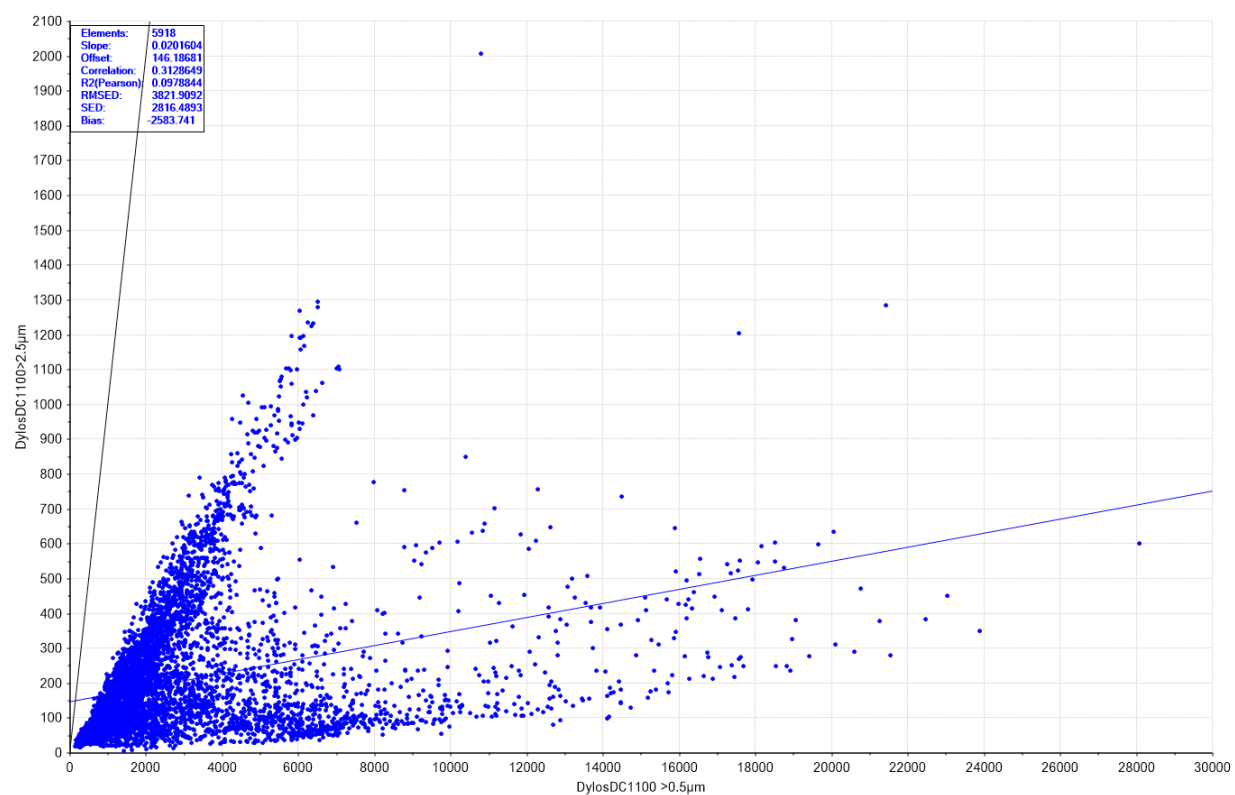


Figure 11: Dylos DC1100 (particles/0.01 cubic foot) correlation plot between PM2.5 & PM10

A comparison between the BAM1020 and PM sensors for respectively PM2.5 and PM10 is presented in 12 and 13. The Y-axis in figure 12 is cut off at $100 \mu\text{g}/\text{m}^3$ and in figure 13 at $140 \mu\text{g}/\text{m}^3$ to achieve better resolution between the lines. During only a few hours, PM2.5 reached a value of a maximum of $150 \mu\text{g}/\text{m}^3$ and PM10 a value of a maximum of $205 \mu\text{g}/\text{m}^3$

The PM2.5 concentration for the Dylos DC1100 is estimated by an empirical equation supplied by the vendor. The raw output of the Dylos DC1100 is particles/0.01 cubic foot. The equation, as specified by Dylos, is as follows:

$$\text{PM2.5 Dylos DC1100 } (\mu\text{g}/\text{m}^3) = (\text{particles} > 0.5 \mu\text{m} \text{ minus particles} > 2.5 \mu\text{m})/250.$$

The original Dylos manual specifies a conversion factor of 150, but this was later revised to 250 and this factor is used in this report

For PM10 this estimation equation is not available. Hence, the Dylos DC1100 is not presented in the graph for PM10.

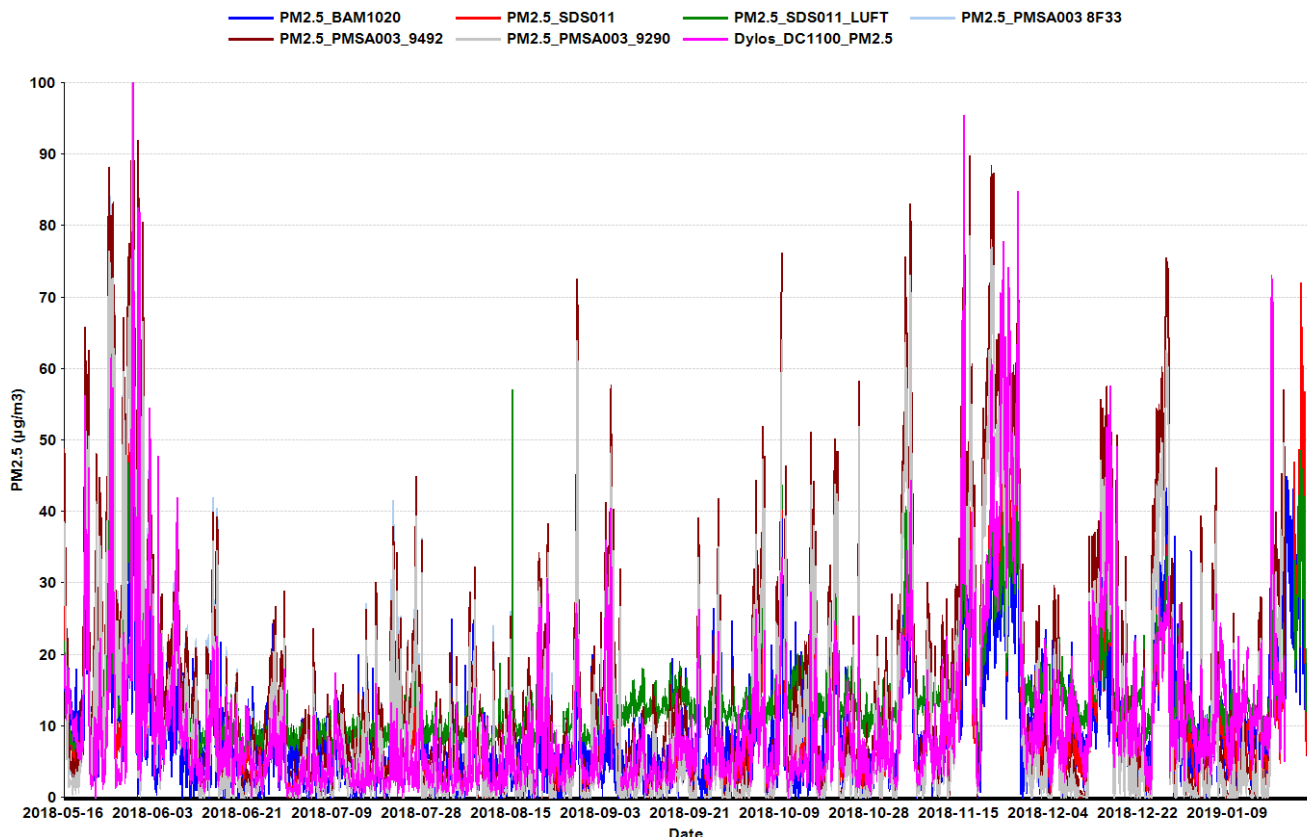


Figure 12: Comparison PM2.5 between BAM1020 and sensors

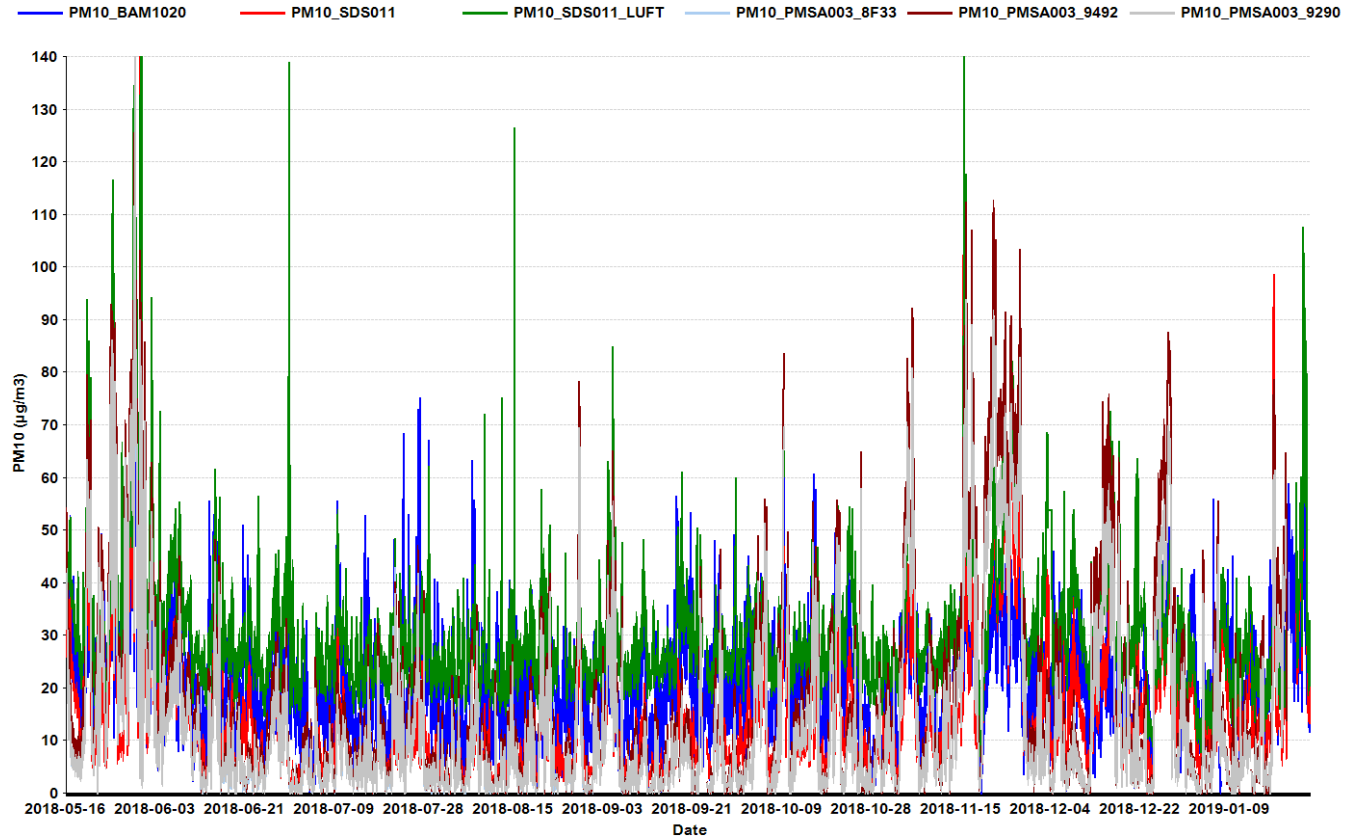


Figure 13: Comparison PM10 between BAM1020 and sensors.

In general, the sensors are biased to each other and the BAM1020. This is more dominant for PM10. There are also multiplicative effects present.

To get a better insight in these effects, the differences are calculated between the sensors and the BAM1020. In the ideal situation, the bias should be zero and the differences should be scattered randomly around zero. The differences are presented in figure 14 and 15 for respectively PM2.5 and PM10.

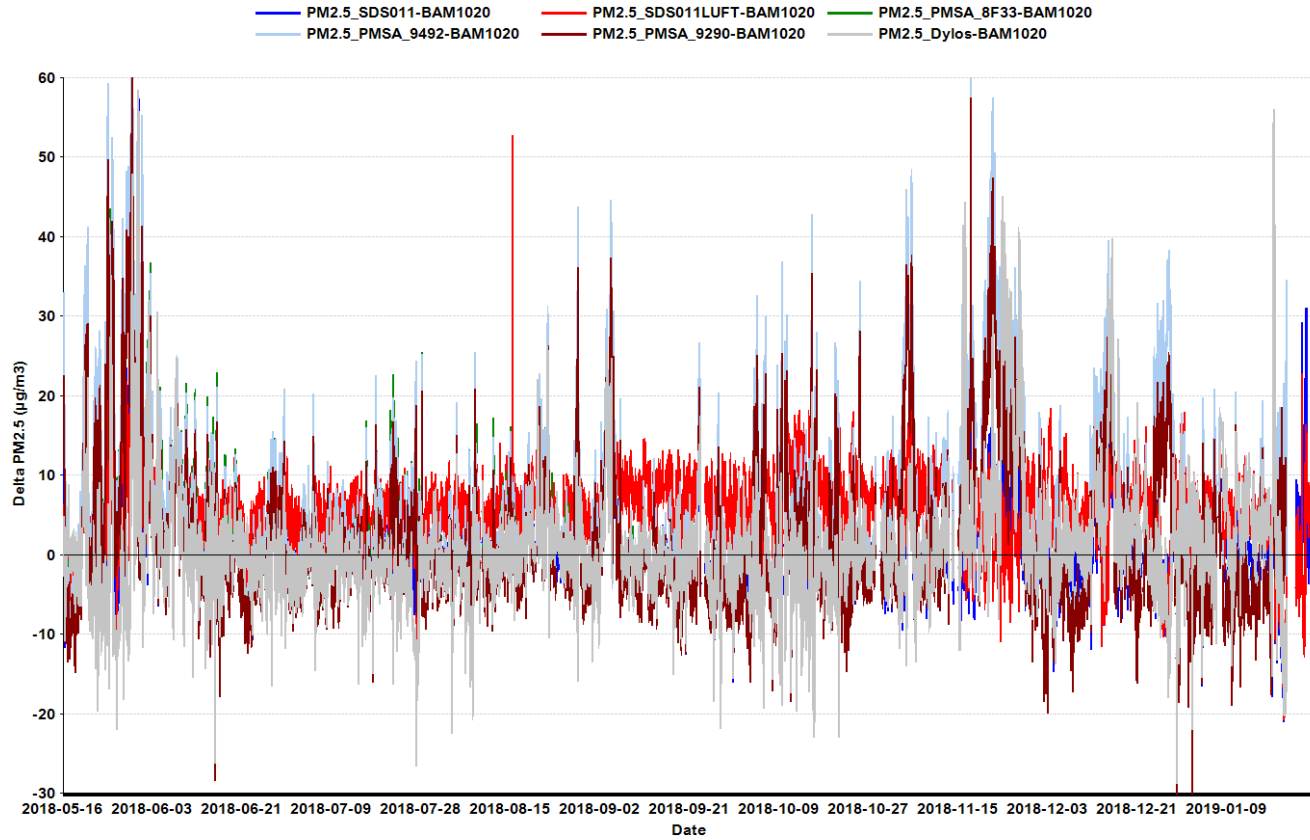


Figure 14: Difference PM_{2.5} between sensors and BAM1020

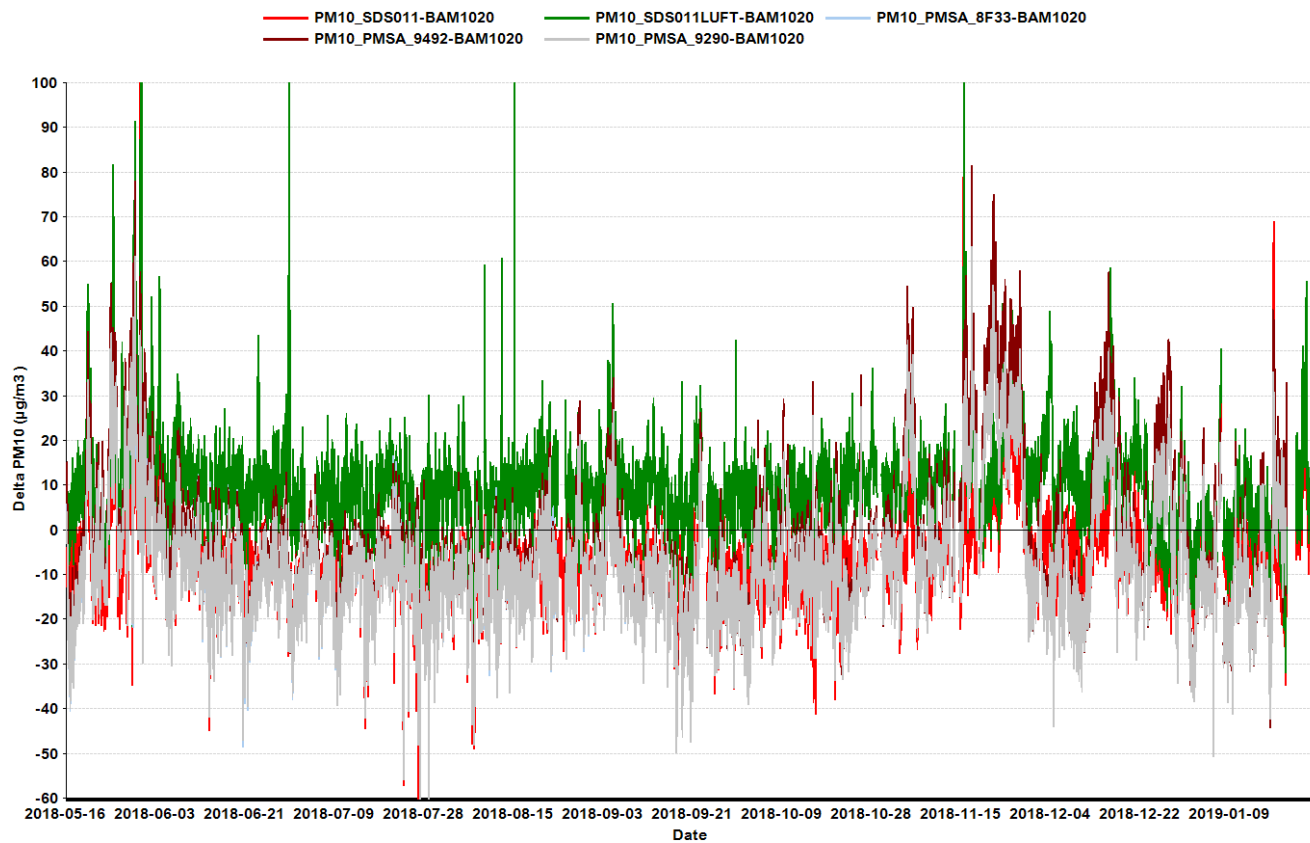


Figure 15: Difference PM₁₀ between sensors and BAM1020

For PM2.5, the SDS011 'Luftdaten' sensor shows the largest positive bias to the BAM1020 and the PMSA003_9290 sensor shows the largest negative bias. A period in May 2018 and November 2018 show higher differences to the BAM1020. This is valid for both PM2.5 and PM10. A possible explanation could be the composition of the airborne particles in those particular periods. The KNMI data from Hoek van Holland shows no correlation between wind direction and increasing bias. There is a weak correlation between the differences and the BAM1020 PM value, this is valid for both PM2.5 and PM10. The higher the BAM1020 PM value, the higher the difference against the PM value of the sensors. This is a multiplicative effect.

Like for PM2.5, the SDS011 'Luftdaten' sensor shows for PM10 the largest positive bias to the BAM1020 and the PMSA003_9290 sensor shows the largest negative bias.

In figure 16, we look more closely into the differences for PM2.5 for the three PMSA003 sensors. It can be clearly seen the sensors show similar performance. This pattern is also visible for PM10, but not shown in a graph.

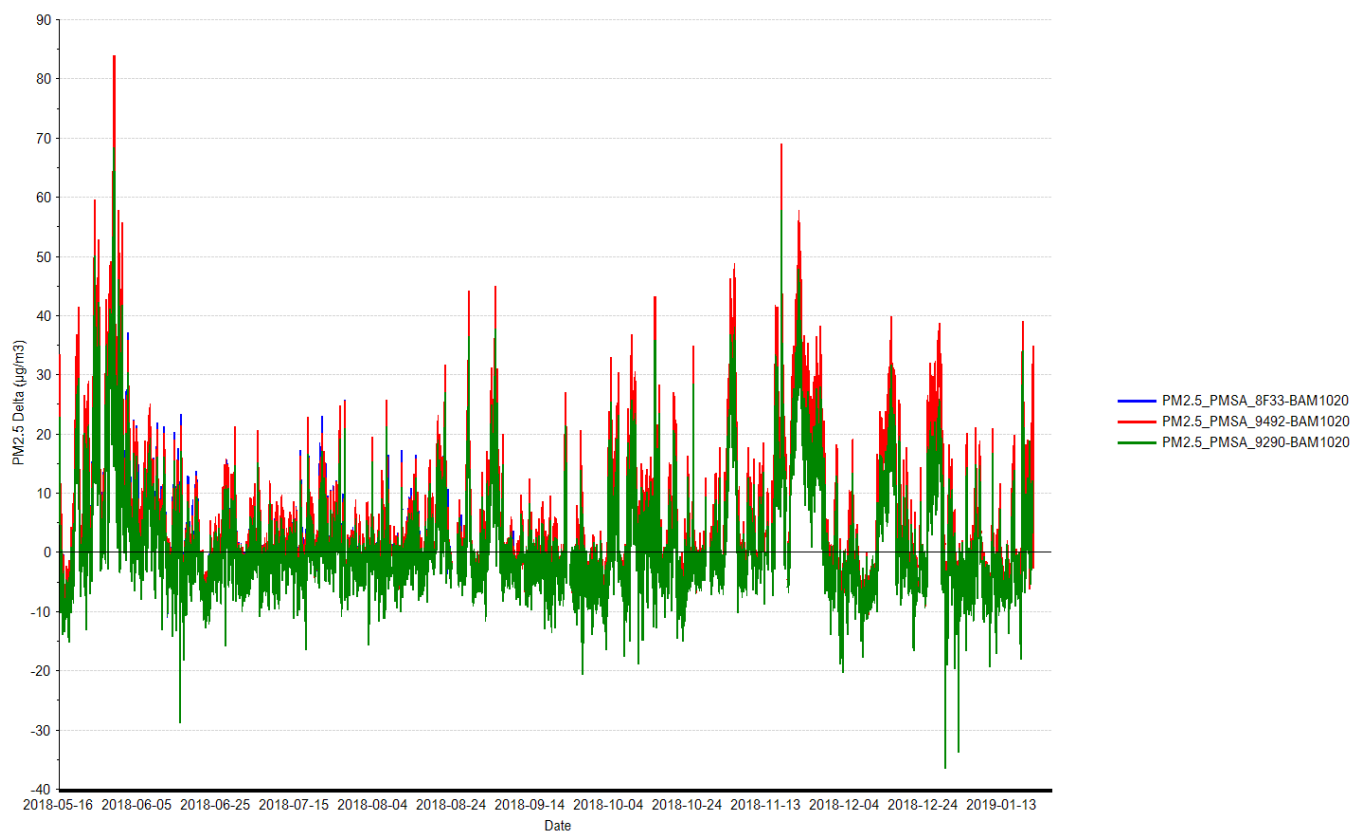


Figure 16: Difference PM2.5 between PMSA003 sensors and BAM1020

The Plantower PMSA003 sensor measures also the PN number for six classes. The three PMSA sensors show similar performance, therefore sensor PMSA003_9492 is taken as a representative example for the plots. The data for the six PN classes is presented in figure 17 and 18.

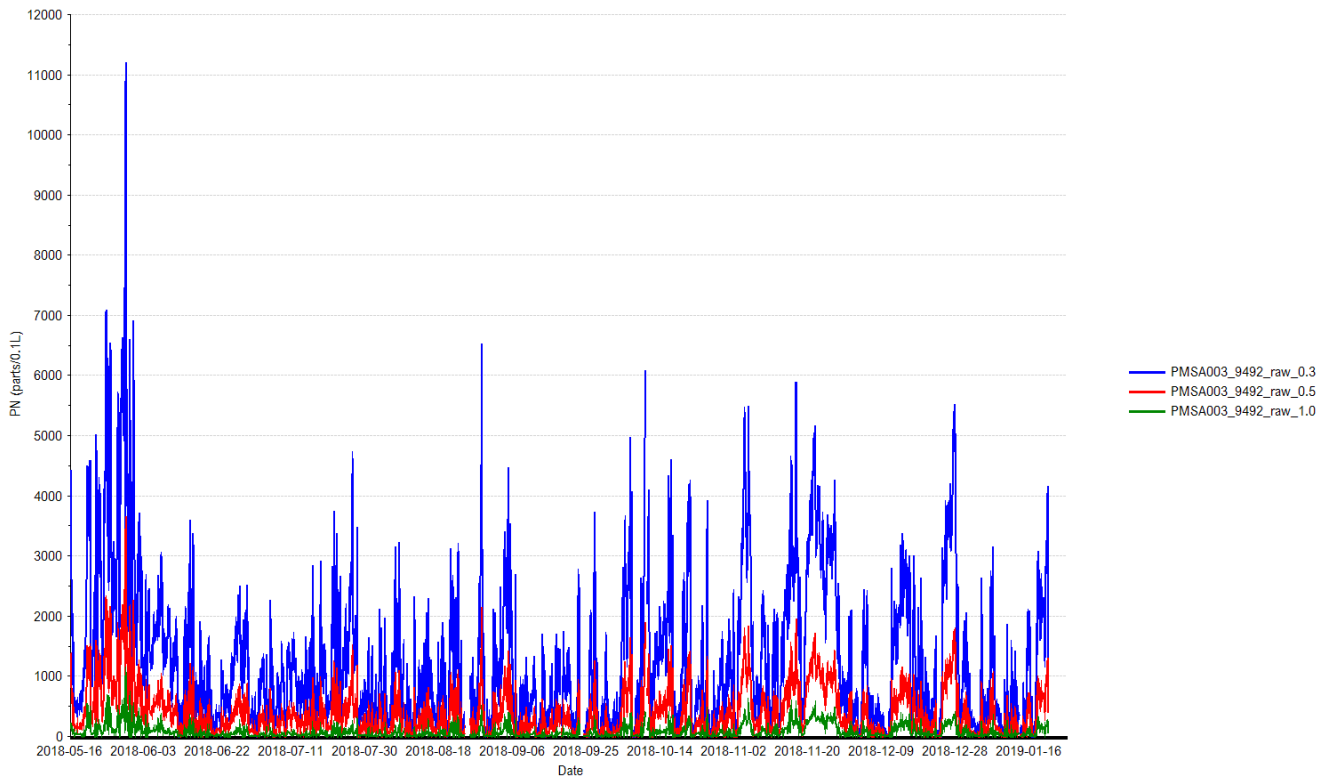


Figure 17: Particle number data of the Plantower PMSA003_9492 sensor $0.3\mu\text{m}$, $0.5\mu\text{m}$ and $1.0\mu\text{m}$ particles

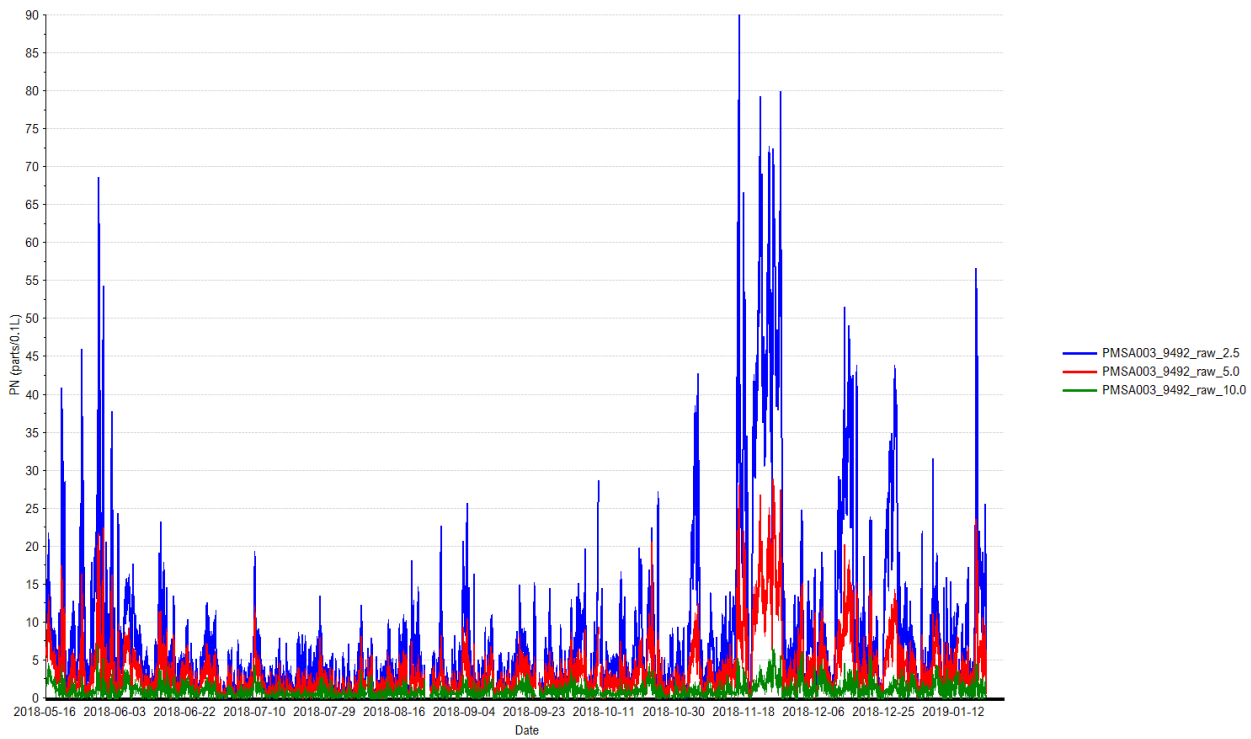


Figure 18: Particle number data of the Plantower PMSA003_9492 sensor $1.0\mu\text{m}$, $2.5\mu\text{m}$ and $10.0\mu\text{m}$ particles

As we have seen before, the correlation plots between PM2.5 and PM10 show a 'V-shaped' curve. This effect is also visible for each correlation between randomly chosen PN classes, but the effect is more dominant for the classes $>1.0\mu\text{m}$. As an example, the correlation plots between PN $1.0\mu\text{m}$ and PN $2.5\mu\text{m}$ for the Plantower sensor PMSA003_9492 is presented in figure 19.

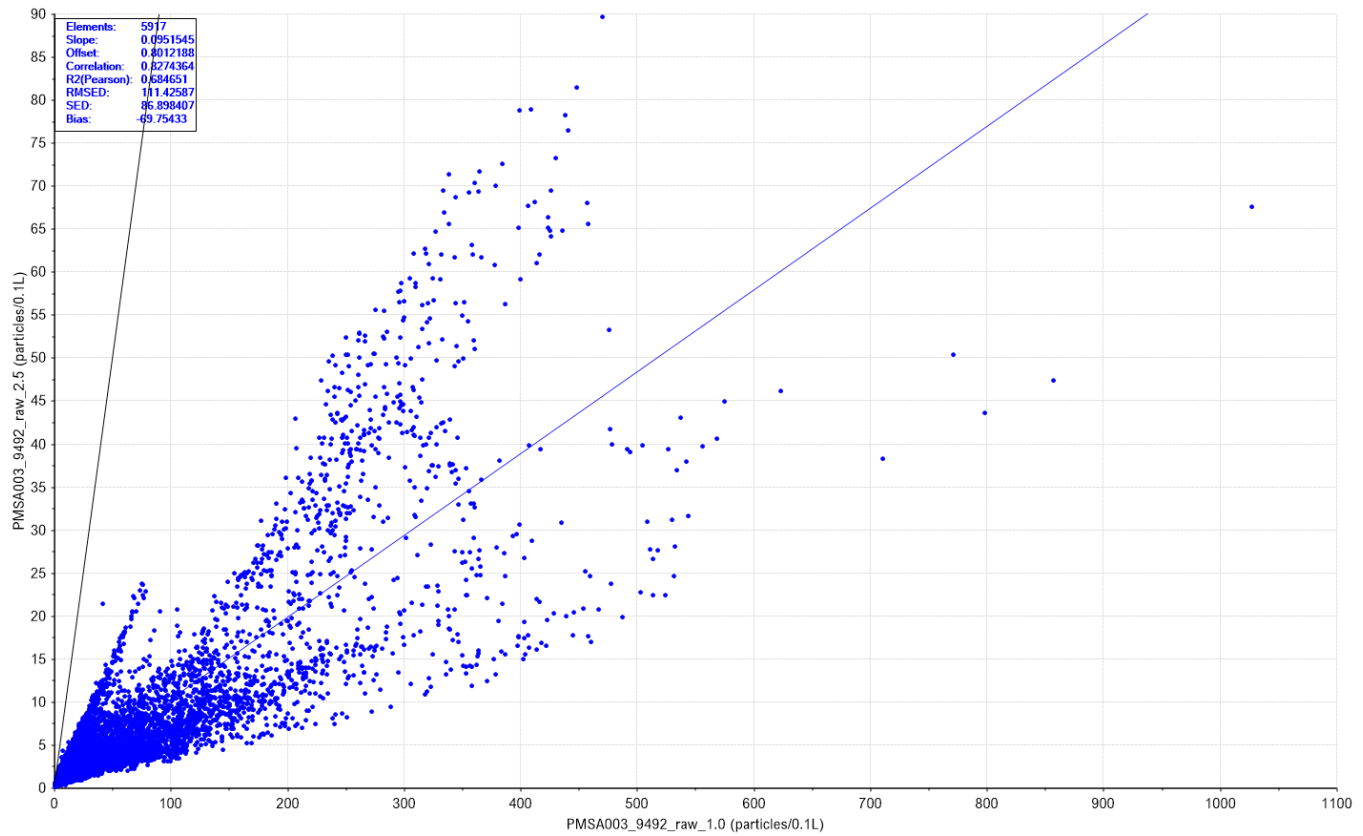


Figure 19: Correlation plot PN $1.0\mu\text{m}$ versus PN $2.5\mu\text{m}$ for sensor PMSA003_9492

The importance of PN number for the calibration of the PMSA003 sensors will be explained in more detail in 8.2.

The correlation of the PMSA003 sensors 9290 and 8F33 against 9492 is investigated for all PN classes. The results are given in table 3.

	Class	N	Slope	Offset	R2 (pearson)	SED	Bias
PMSA9290 versus 9492	0.3µm	5917	1.034	75.5	0.9954	92.2	115.4
	0.5µm	5917	1.046	23.6	0.9952	31.7	40.0
	1.0µm	5917	1.112	12.1	0.9863	14.8	18.7
	2.5µm	5917	1.790	-0.95	0.9244	5.57	3.09
	5.0µm	5917	1.363	-0.92	0.8754	1.57	0.27
	10.0µm	5917	1.591	0.053	0.8463	0.386	0.384
PMSA8F33 versus 9492	Class	N	Slope	Offset	R2 (pearson)	SED	Bias
	0.3µm	2526	1.046	32.5	0.9923	123.4	90.0
	0.5µm	2526	1.012	3.83	0.9929	33.8	8.7
	1.0µm	2526	1.073	-1.12	0.9967	8.61	3.92
	2.5µm	2526	1.211	0.63	0.9668	1.51	1.47
	5.0µm	2526	2.535	-0.11	0.9561	1.48	1.55
	10.0µm	2526	5.680	0.10	0.8421	0.53	0.67

Table 3: Between sensor correlation statistics for the PN classes of the PMSA003 sensors

Explanation of the parameters:

- N : number of observations
- Slope : steepness of the correlation line
- Offset : cut off on the Y-axis
- R2 pearson : Pearson's correlation coefficient
- SED : Standard Error of Determination
- Bias : average difference between Y and X

Due to technical problems with the 8F33 sensor, the number of observations is much less compared to the other sensors. The best correlation is achieved for the lowest PN classes 0.3 µm and 0.5 µm. The lowest classes also deliver the highest PN values. The slope increases among the PN classes with the highest value for the 10 µm class. This is an indication that the sensors differ in terms of sensitivity, but also that the cut-off borders in the PN classes is different.

7.2 Meteorology

For the meteorological parameters temperature and relative humidity, the data of the official KNMI monitors and the sensors is presented in figure 20.

It can be concluded, a micro climate is present inside the sensor case, caused by the heat produced by the sensors and peripheral equipment, but also caused by heat absorption by the black surface of the sensor case. The inside temperature shows a bias of approximately +7°C compared to the external Dallas sensor. The external Dallas sensor correlates good with the official KNMI temperature monitor. The inside relative humidity shows a bias of approximately -30% compared to the official KNMI monitor. The inside temperature varies between +6.1°C and +47.9°C and the relative humidity between 10.4% and 66.4% (drying effect).

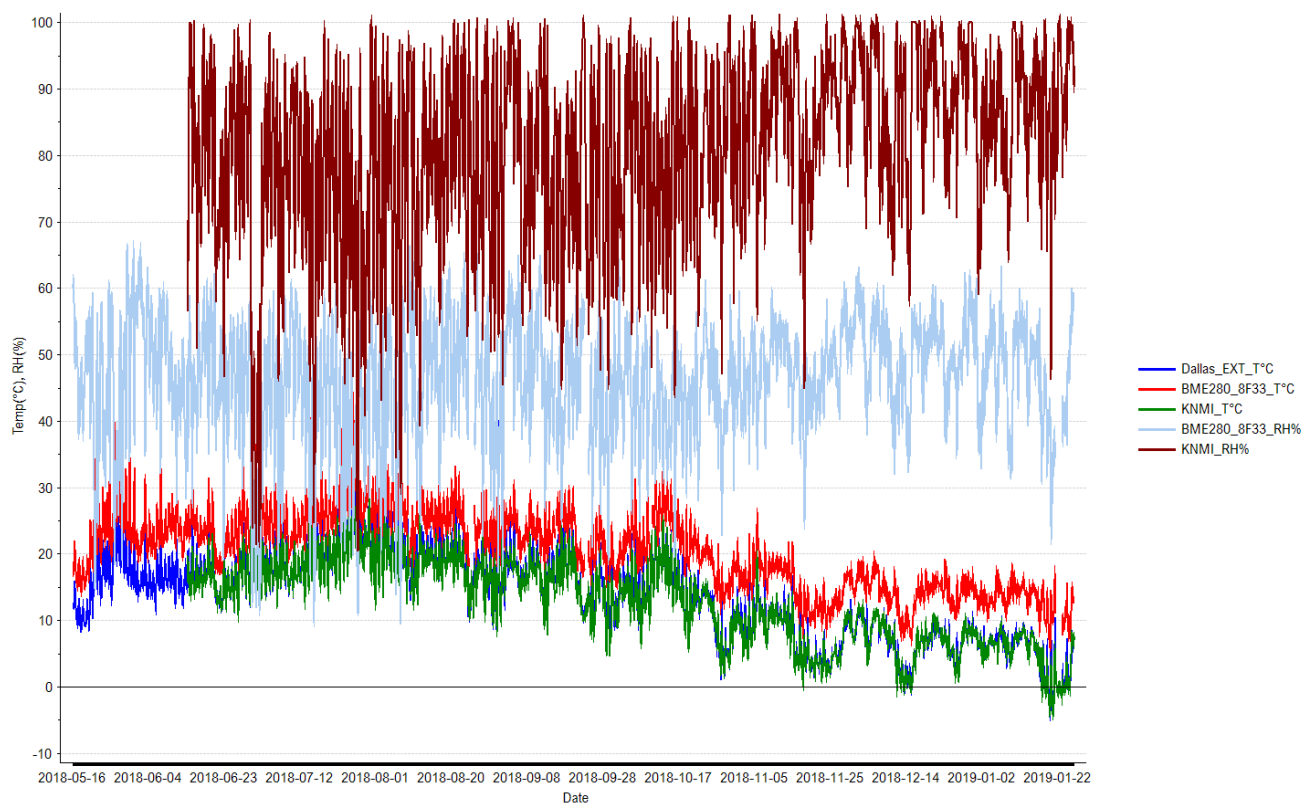


Figure 20: Temperature and relative humidity data of KNMI monitors and sensors

Studies have proven the impact of humidity and/or temperature on the output of laser based PM sensors^{1,2}. Temperature and relative humidity are also taken into account for the calibration and validation of the PM sensors against the BAM1020. Air pressure, wind direction and wind speed are not included in the calibration and validation of the models, because these parameters most likely have no influence on the sensitivity of the sensors. Due to the micro climate in the sensor case, the inside variations in temperature and relative humidity do not match the variations outside the sensor case.

The Bosch BME280 sensor also measures the air pressure. The lowest recorded value is 977.2 hPa and the highest recorded value is 1041.5 hPa. The air pressure is presented in figure 21.

Three BME280 sensors were in use for the data collection. A short study on the output of the three BME280 sensors (id 8F33, 9290 and 9492 see appendix 1) shows that sensor 8F33 gives the average output of the three BME280 sensors (not discussed in this report). The meteorological data used for the calibration and validation of the PM sensors is derived from the 8F33 sensor.

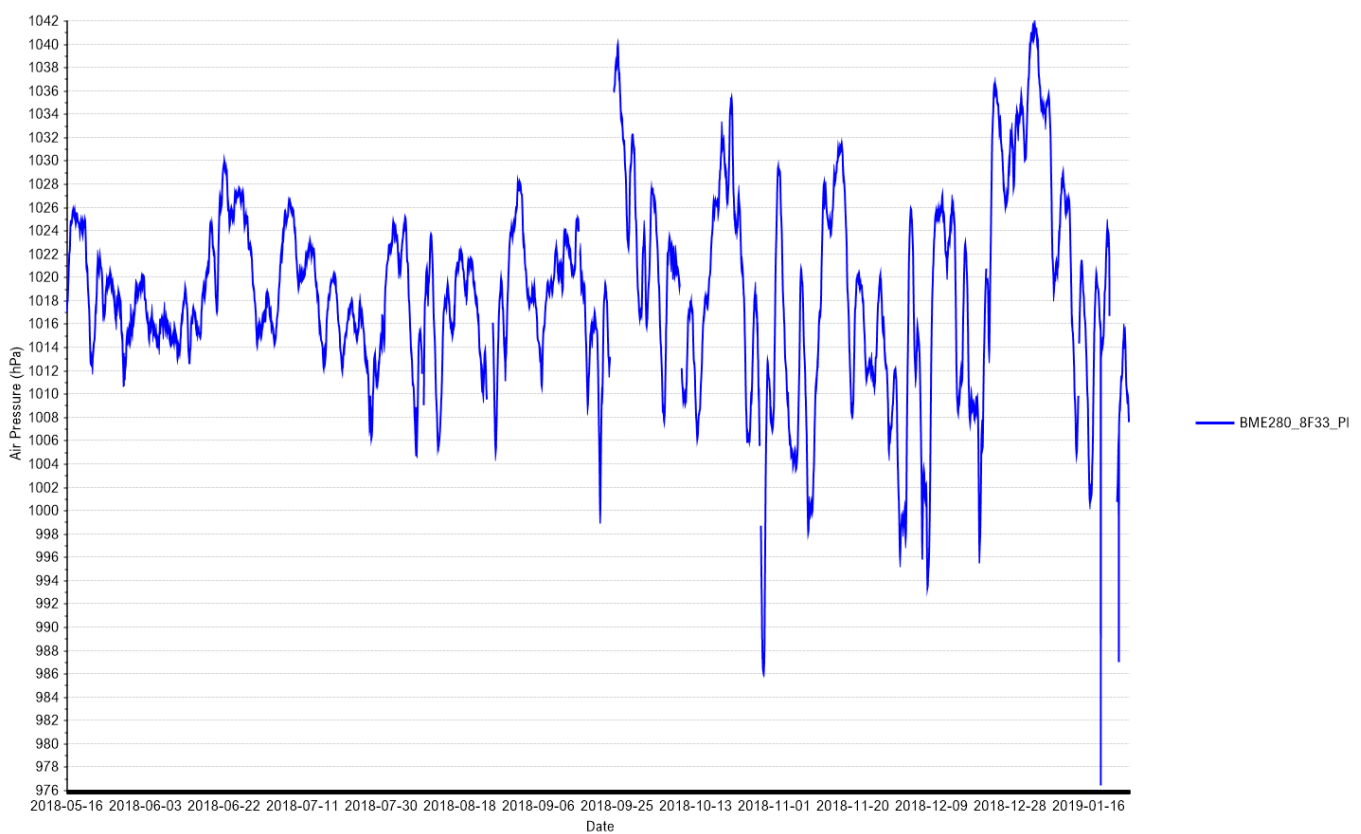


Figure 21: Air pressure Bosch BME280 sensor

8 Calibration & Validation

8.1 Plantower algorithm

The sensor firmware converts the PN classes into a PM2.5- and PM10 concentration. The supplier was not willing to provide information about this algorithm. The algorithm is simulated by calibration of the six PN classes against the PM2.5- or PM10 concentration in $\mu\text{g}/\text{m}^3$. As calibration type, the MLR (Multiple Linear Regression) function is used, assuming all PN classes have a linear relationship with PM2.5 and PM10. Within the MLR models, the six PN classes are used as X-variables. The MLR calibration results for the three PMSA003 sensors show similar performance, therefore sensor PMSA003_9492 is taken as a representative example in the plots.

The MLR models are presented in figure 22 (PM2.5) and 23 (PM10) where the X-axis is the original sensor PM value and the Y-axis is the predicted PM value by the MLR model.

For both PM2.5 and PM10, a very strong correlation, good linearity and perfect slope is present. The Y-residuals tend to bias above the black target line ($Y=X$) when PM2.5 and $\text{PM10} > 90 \mu\text{g}/\text{m}^3$, but in this region there is also lack of data. The accuracy of the calibrations is expressed as RMSEE (Root Mean Square Error of Estimation) and is $1.0 \mu\text{m}^3$ for PM2.5 and $1.2 \mu\text{g}/\text{m}^3$ for PM10. It looks like the MLR models are a good representation of the internal factory algorithm.

The MLR models are validated with an independent set. The accuracy of the validation is expressed as RMSEP (Root Mean Square Error of Prediction), the values are $1.0 \mu\text{g}/\text{m}^3$ for PM2.5 and $1.2 \mu\text{g}/\text{m}^3$ for PM10. The RMSEP values are very good in line with the RMSEE values of the calibration models.

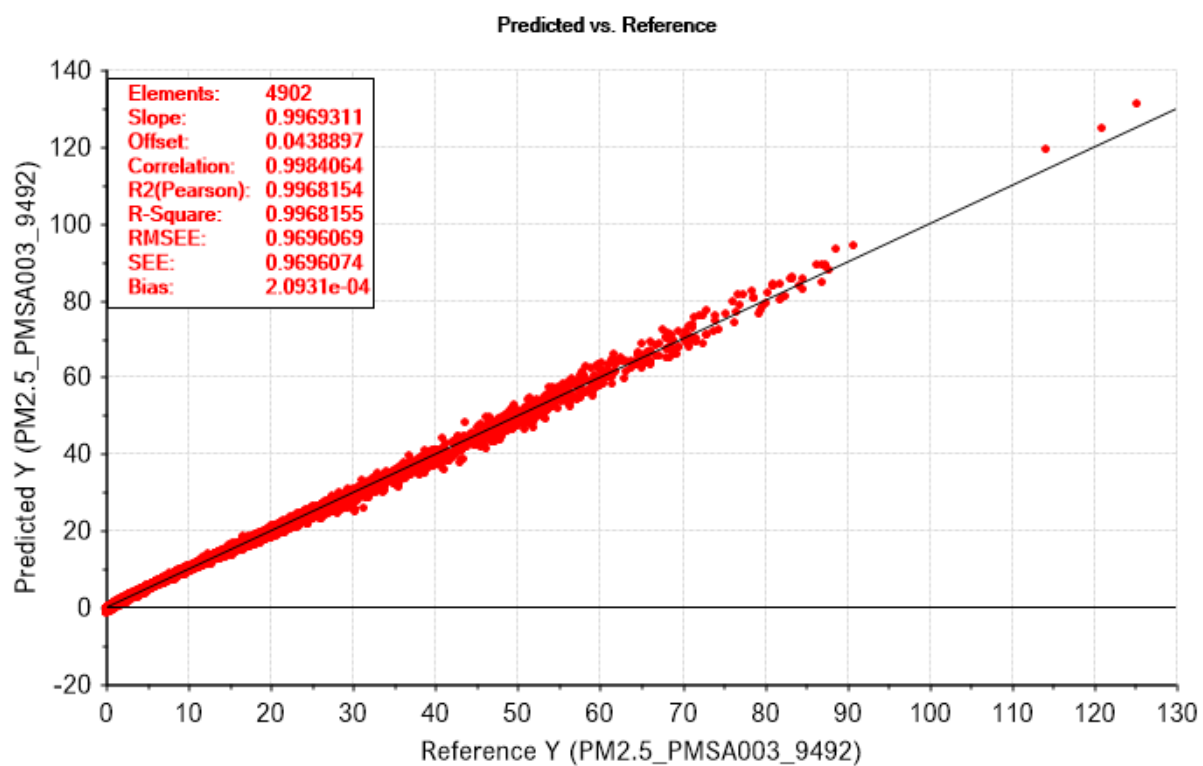


Figure 22: MLR model for PM2.5 against PN, sensor PMSA003_9492

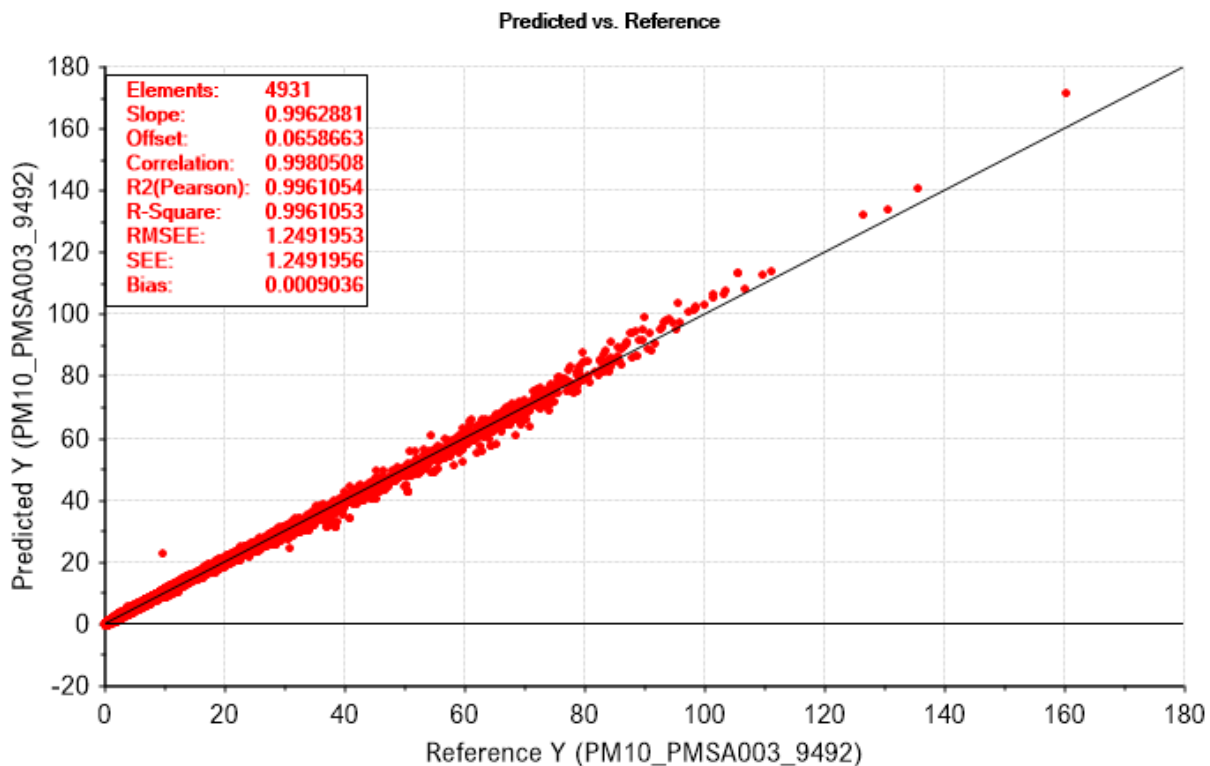


Figure 23: MLR model for PM10 against PN, sensor PMSA003_9492

The regression coefficients of the MLR models show a remarkable difference. The PN class $5.0\mu\text{m}$ shows the largest negative value for the PM2.5 model while for the PM10 model this class has almost no influence. For both PM2.5 and PM10 models, the PN classes $0.5\mu\text{m}$, $2.5\mu\text{m}$ and $10.0\mu\text{m}$ show the most influence on the models. The regression (B) coefficients for the PM2.5- and PM10 model are presented in figure 24 (PM2.5) and 25 (PM10).

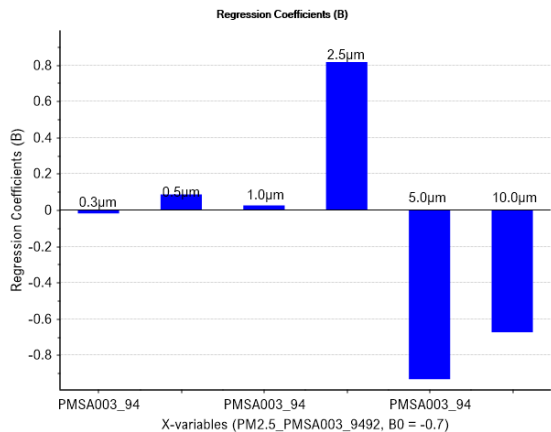


Figure 24: MLR regression coefficients for PM2.5 for sensor PMSA003_9492

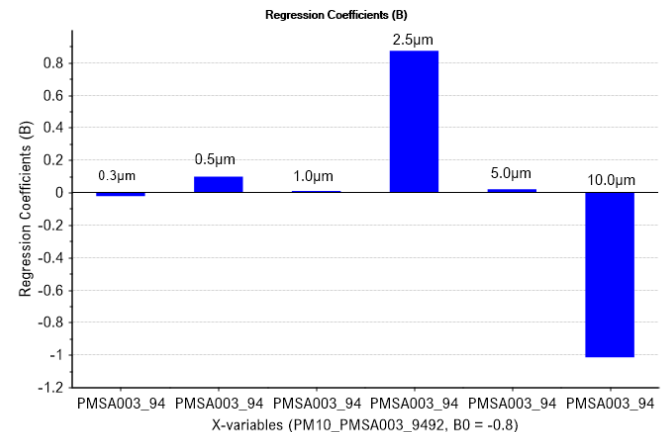


Figure 25: MLR regression coefficients for PM10 for sensor PMSA003_9492

The standard errors in the regression coefficients and intercepts are given in table 4.

Variable	B-coefficient PM2.5	STDerr PM2.5	B-coefficient PM10	STDerr PM10
Intercept	-0.707	0.045	-0.779	0.057
PMSA003_9492_raw_0.3	-0.019	0.002	-0.022	0.003
PMSA003_9492_raw_0.5	0.087	0.008	0.099	0.010
PMSA003_9492_raw_1.0	0.025	0.002	0.011	0.002
PMSA003_9492_raw_2.5	0.817	0.011	0.874	0.014
PMSA003_9492_raw_5.0	-0.933	0.042	0.021	0.051
PMSA003_9492_raw_10.0	-0.674	0.075	-1.015	0.093

Table 4: Standard errors in the regression coefficients and intercepts of the MLR models PM2.5 and PM10

The true internal factory algorithm to convert PN into PM is not known, but it can be assumed, it is a lookalike MLR function where every PN class contributes to the PM concentration.

8.2 Calibration of the sensors against BAM1020

The use of a direct correlation between the PM sensor output and the BAM1020 has little value. The influence of relative humidity and temperature causes a bad fit and poor accuracy of the calibration line.

The aim of this project is to increase the reliability of the particulate matter sensor by means of a model in which the output of the sensor is calibrated against the BAM1020 monitor. A specific model applies to PM2.5 and PM10. Because both relative humidity and temperature of the air influence the output of the sensor, these variables are included in the calibration process. The calibration is performed for each sensor and the robustness of the model is determined by use of validation.

The database is split into a calibration- and validation set. Every 6th sample belongs to the validation set (N=1022), the remaining samples belong to the calibration set (N=5109). One sample is an hourly observation of all available data. The calibration set is used for construction of the models, the validation set is used for the independent validation of the models.

For the calibration of the sensors, it is assumed that the BAM1020 gives the true value. It is also assumed that the influence of RH% and T on the sensor output can be explained by a linear model. For the calibration, the MLR type was chosen and that stands for Multiple Linear Regression. There are many more regression techniques available like PLS (Partial Least Squares) or non-linear regression techniques or even machine learning techniques (e.g. Random Forest). For this project the MLR method is chosen to keep it less complex and explainable. As experiment, some calibrations were computed using PLS, but the results were not significantly better compared to MLR. These results are not part of this report.

The construction of the MLR model looks like this example below:

$$\text{PM2.5_BAM1020} = \text{constant} + a * \text{PM2.5_sensor} + b * \text{RH\%} + c * T$$

- a : regression coefficient of PM2.5 output in $\mu\text{g}/\text{m}^3$
- b : regression coefficient of Relative Humidity in %
- c : regression coefficient of Temperature in °C
- constant : a constant number

PM2.5_BAM1020 is the Y-variable. PM2.5_sensor, RH% and T are the X-variables. The direction of the regression coefficients and constant can be positive or negative. The value of the regression coefficient and constant determines how important they are for the model.

The MLR model can be seen as an arithmetic post calculation on the output value of the sensor. In this way, the sensor 'predicts' the PM value as if it was measured by the BAM1020. The MLR model has a certain accuracy and it can improve the reliability of the sensor, because the influence of RH% and T are also taken into account. For each sensor a specific MLR model is constructed and validated to test the robustness of the MLR model.

The MLR calibrations are non-orthogonal regressions and are performed in two ways. The first way is calibration against the BAM1020 by using the PM output, RH% and T as X-variables. This is worked out

for all sensors except for the Dylos DC1100. The second way is calibration against the BAM1020 by using the Particle Number (PN) classes, RH% and T as X-variables. This is worked out for the Plantower PMSA003 sensors and the Dylos DC1100 sensor. As discussed in 7.1, the PMSA003 sensor delivers the PN of six classes and the DC1100 delivers the PN for two classes. For the PMSA003 sensor this way returns into a total of 8 X-variables and for the DC1100 into a total of 4 X-variables.

The properties of the MLR calibrations based on PM, RH% and T as X-variables are given in table 5. The errors of the regression coefficients are given in table 6.

	PMSA003_8F33		PMSA003_9290		PMSA003_9492		SDS011_basic		SDS011_Luftdaten	
	PM2.5	PM10	PM2.5	PM10	PM2.5	PM10	PM2.5	PM10	PM2.5	PM10
N	2096	2082	4834	4822	4837	4854	4905	4915	4865	4853
Range ($\mu\text{g}/\text{m}^3$)	0-63.2	1.8-84.3	0-63.2	0-84.3	0-63.2	0-84.3	0-63.2	0-84.3	0-63.2	0-84.3
Slope	0.755	0.461	0.772	0.385	0.777	0.366	0.748	0.464	0.700	0.414
Offset ($\mu\text{g}/\text{m}^3$)	1.93	10.9	2.15	12.8	2.10	13.4	2.44	11.4	2.92	12.4
R-square	0.754	0.460	0.772	0.385	0.777	0.365	0.748	0.462	0.699	0.413
Accuracy ($\mu\text{g}/\text{m}^3$)	3.3	7.1	3.8	8.0	3.7	8.0	4.2	7.5	4.5	7.7
B0	20.6	27.5	15.1	16.0	14.8	14.7	20.0	19.3	14.5	16.3
RegrCoef_PM	0.4076	0.4451	0.4416	0.3728	0.3834	0.3151	0.6399	0.5719	0.8184	0.5105
RegrCoef_RH%	-0.2261	-0.2318	-0.1431	-0.0940	-0.1498	-0.0948	-0.2465	-0.2425	-0.2326	-0.2114
RegrCoef_T°C	-0.2997	-0.1111	-0.1935	0.1929	-0.1905	0.2445	-0.2653	0.2267	-0.3172	-0.0512

Table 5: properties MLR models against BAM1020 with PM, RH% and T as X-variables

	PMSA003_8F33		PMSA003_9290		PMSA003_9492		SDS011_basic		SDS011_Luftdaten	
	PM2.5	PM10	PM2.5	PM10	PM2.5	PM10	PM2.5	PM10	PM2.5	PM10
B0	0.99	2.20	0.44	0.91	0.44	0.97	0.49	0.88	0.54	0.91
RegrCoef_PM	0.0051	0.0107	0.0036	0.0068	0.0031	0.0060	0.0057	0.0088	0.0083	0.0087
RegrCoef_RH%	0.0108	0.0234	0.0068	0.0137	0.0067	0.0145	0.0075	0.0137	0.0082	0.0141
RegrCoef_T°C	0.0234	0.0511	0.0098	0.0201	0.0097	0.0213	0.0106	0.0196	0.0116	0.0195

Table 6: Errors regression coefficients

Explanation of the parameters:

- N : number of observations
- Range : the min-max range of the model
- Slope : steepness of the model regression line
- Offset : cut off on the Y-axis
- R-square : correlation coefficient of the regression line (R^2 -pearson)
- Accuracy : Root Mean Square Error of Estimation (RMSEE)
- B0 : Constant

The accuracy among the different sensors is comparable for both PM2.5 and PM10. The PMSA003 sensors perform slightly better for PM2.5, resulting in a better slope and R^2 . The MLR calibrations for PM10 perform significantly worse compared to PM2.5. The accuracy of the PM2.5 models is approximately $4 \mu\text{g}/\text{m}^3$ and this is equal to the reproducibility of the BAM1020 for hourly observations. The accuracy for the PM10 models is approximately $8 \mu\text{g}/\text{m}^3$.

A graphical presentation of the MLR models from table 5 are given in figures 26, 27 and 28 for PM2.5 and in figures 29, 30 and 31 for PM10. For the PMSA003 sensors, only the 9492 is presented. For all MLR models the black line is the target line ($Y=X$) and the red line is the slope.

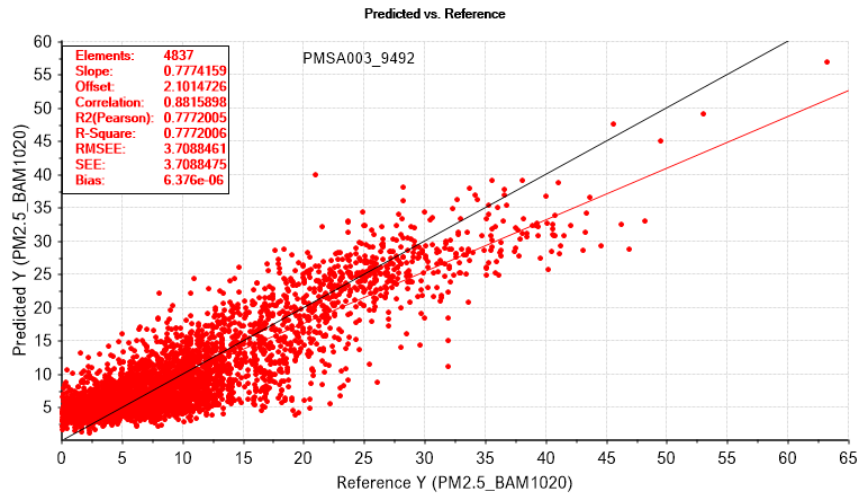


Figure 26: PMSA003 - MLR model PM2.5 against BAM1020 with PM, RH% and T as X-variables

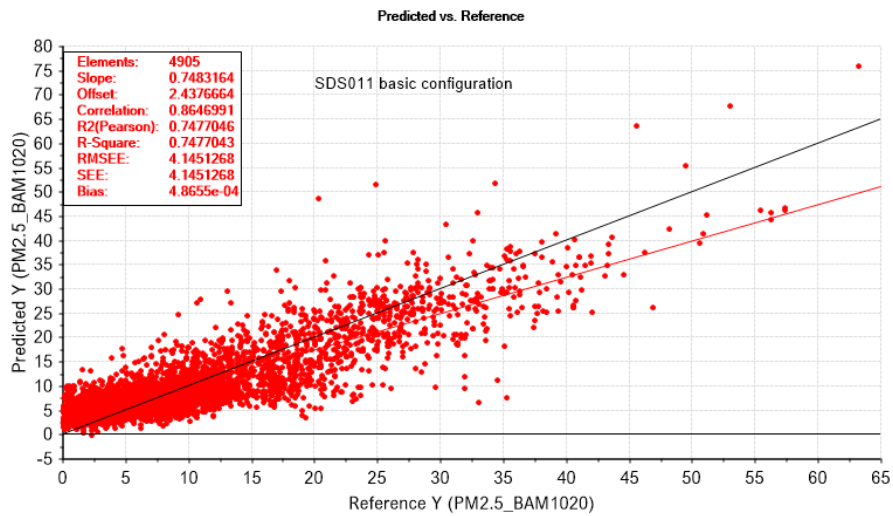


Figure 27: SDS011 basic config - MLR model PM2.5 against BAM1020 with PM, RH% and T as X-variables

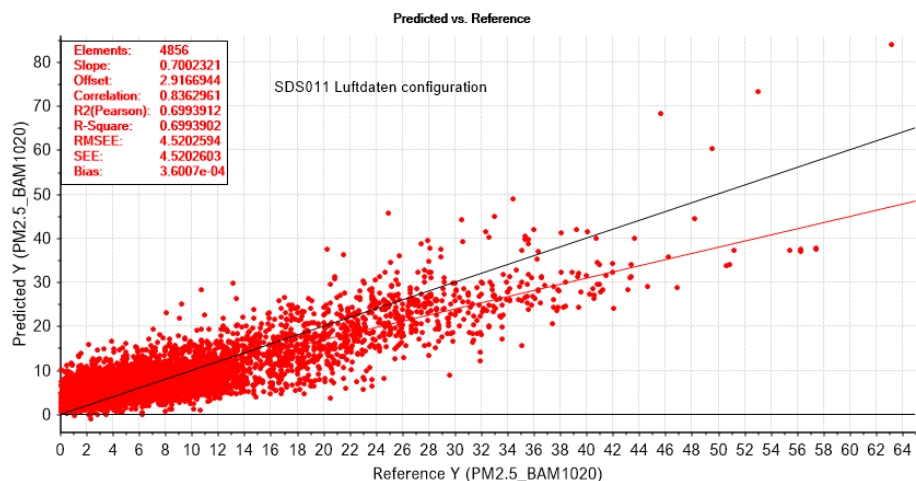


Figure 28: SDS011 Luftdaten - MLR model PM2.5 against BAM1020 with PM, RH% and T as X-variables

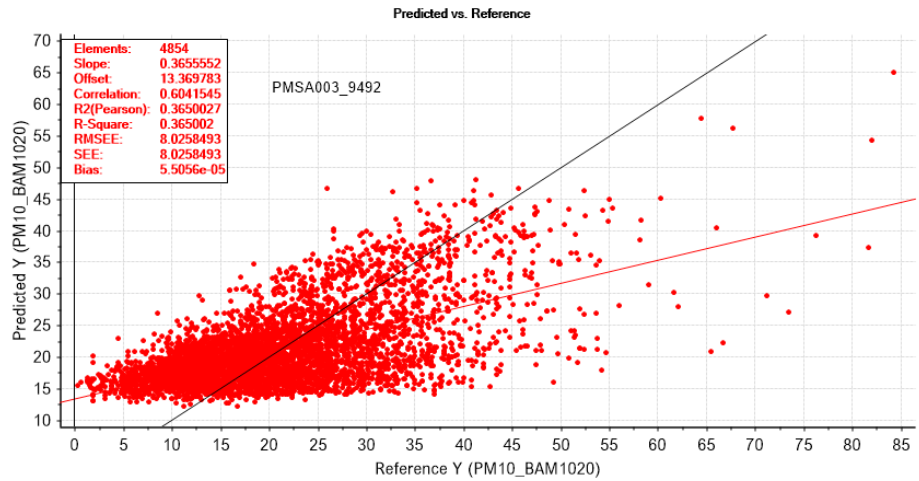


Figure 29: PMSA003 - MLR model PM10 against BAM1020 with PM, RH% and T as X-variables

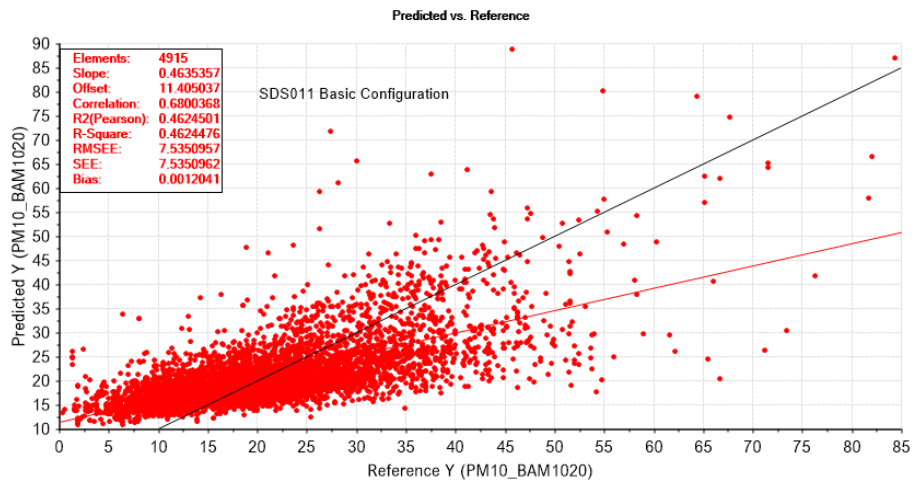


Figure 30: SDS011 basic config - MLR model PM10 against BAM1020 with PM, RH% and T as X-variables

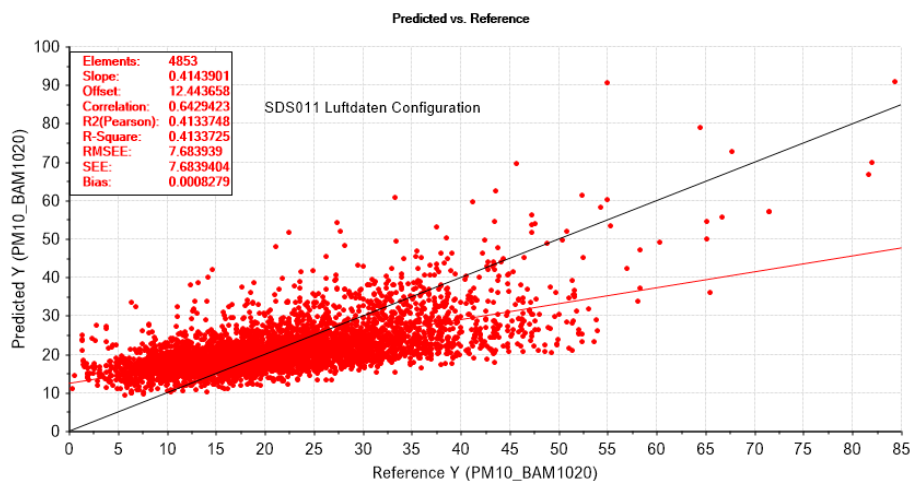


Figure 31: SDS011 Luftdaten - MLR model PM10 against BAM1020 with PM, RH% and T as X-variables

The properties of the MLR calibrations based on PN, RH% and T as X-variables are given in table 7. The errors of the regression coefficients are given in table 8.

	PMSA003_8F33		PMSA003_9290		PMSA003_9492		Dylos_DC1100		Dylos_DC1100	
	PM2.5	PM10								
N	2093	2100	4836	4834	4836	4836	4789	4801	4786	4808
Range ($\mu\text{g}/\text{m}^3$)	0-63.2	1.8-84.3	0-63.2	0.3-84.3	0-63.2	0.3-84.3	0-63.2	0.3-81.7	0.0-63.2	0.3-84.3
Slope	0.797	0.686	0.835	0.656	0.833	0.664	0.641	0.183	0.634	0.337
Offset ($\mu\text{g}/\text{m}^3$)	1.61	6.44	1.56	7.24	1.58	7.06	3.36	17.1	3.42	13.9
R-square	0.795	0.684	0.834	0.655	0.832	0.663	0.640	0.182	0.633	0.336
Accuracy ($\mu\text{g}/\text{m}^3$)	3.0	5.7	3.2	5.8	3.2	5.7	4.6	8.8	4.6	8.0
B0	16.0	10.9	12.8	14.4	12.4	16.9	12.6	23.9	12.7	13.9
RegrCoef_particles (>0.5 μm minus >2.5 μm)							0.0023			
RegrCoef_particles (>2.5 μm)							0.0252			
RegrCoef_particles (>0.5 μm)								0.0023	0.0022	
RegrCoef_0.3 μm	-0.0209	-0.0054	0.1327	0.1810	0.1700	0.2423				
RegrCoef_0.5 μm	0.0817	0.0420	-0.4298	-0.5911	-0.5440	-0.7764				
RegrCoef_1.0 μm	-0.0368	-0.0442	0.0792	0.1502	0.0840	0.1293				
RegrCoef_2.5 μm	0.3975	-1.2745	-0.0143	-1.7346	0.0322	-0.5357				
RegrCoef_5.0 μm	1.2759	11.3487	1.2229	3.6006	-0.0275	-0.3541				
RegrCoef_10.0 μm	1.4172	4.4872	-1.4686	7.0791	2.2161	11.4704				
RegrCoef_RH%	-0.2228	-0.2464	-0.1759	-0.2714	-0.1790	-0.2858	-0.1988	-0.2170	-0.2125	-0.1538
RegrCoef_T°C	-0.2260	0.2352	-0.2070	0.1633	-0.2508	-0.0083	-0.0026	0.0942	0.0042	0.3762

Table 7: Properties MLR models against BAM1020 with "PN+RH+T" as X-variables

	PMSA003_8F33		PMSA003_9290		PMSA003_9492		Dylos_DC1100		Dylos_DC1100	
	PM2.5	PM10	PM2.5	PM10	PM2.5	PM10	PM2.5	PM10	PM2.5	PM10
B0	0.93	1.78	0.41	0.76	0.44	0.78	0.56	1.04	0.56	0.97
RegrCoef_particles (>0.5 μm minus >2.5 μm)							2.66E-05			
RegrCoef_particles (>2.5 μm)							7.72E-04			
RegrCoef_particles (>0.5 μm)								2.66E-05	4.52E-05	
RegrCoef_0.3 μm	0.0088	0.0169	0.0064	0.0118	0.0082	0.0146				
RegrCoef_0.5 μm	0.0277	0.0530	0.0218	0.0399	0.0269	0.0480				
RegrCoef_1.0 μm	0.0072	0.0139	0.0073	0.0133	0.0054	0.0097				
RegrCoef_2.5 μm	0.0872	0.1674	0.0639	0.1167	0.0369	0.0658				
RegrCoef_5.0 μm	0.3940	0.7565	0.1310	0.2429	0.1346	0.2402				
RegrCoef_10.0 μm	2.1488	4.1236	0.3459	0.6504	0.2460	0.4394				
RegrCoef_T°C	0.0222	0.0427	0.0092	0.0169	0.0102	0.0182	0.0128	0.0231	0.0129	0.0222
RegrCoef_RH%	0.0098	0.0188	0.0063	0.0114	0.0064	0.0114	0.0084	0.0167	0.0085	0.0146

Table 8: Errors regression coefficients

PMSA003: For the PMSA003 sensors it can be concluded that the models based on "PN+RH+T" show better overall performance compared to the models based on "PM+RH+T". The accuracy of the models for PM2.5 improves from averaged 3.6 to 3.1 $\mu\text{g}/\text{m}^3$. The accuracy of the models for PM10 improves from averaged 7.7 to 5.7 $\mu\text{g}/\text{m}^3$. The regression coefficients for the models based on "PM+RH+T" show comparable signs and values among the three sensors. Sensor 8F33 shows more deviating regression coefficients, but this is due to a much smaller calibration set. The regression coefficients for the models based on "PN+RH+T" do not show comparable signs and values. It is not clear why this is the case, but it seems, that it is not possible to maintain a 'general' model with averaged regression coefficients.

SDS011: For the SDS011 sensors the models based on "PN+RH+T" could not be constructed, because this sensor does not provide the PN classes.

Dylos DC1100: For the Dylos DC1100 sensor, only the models based on "PN+RH+T" could be constructed, because this sensor does not provide PM values.

The PN classes for the Dylos DC1100 sensor are different compared to the Plantower PMSA003 sensor. The Dylos manual gives information about the relation between the PN class and PM.

According to the manual, "PN class >0.5 μm " minus "PN class >2.5 μm " is a measure for PM2.5 (*PM2.5-Dylos*). This class can be converted to PM2.5 after dividing by a factor (see 7.1). The Dylos manual does not give a measure for PM10, based on a PN class.

The MLR model for PM2.5 is calibrated against the PN class as proposed by the manual, but also against the "PN class >0.5 μm " (*PMtotal_Dylos*), because in theory this class should cover all measured particles which could have a potential contribution to PM2.5.

The MLR model for PM10 is calibrated against the "PN class >2.5 μm " (*PM10-Dylos*), but also against the "PN class >0.5 μm " (*PMtotal_Dylos*), because in theory this class should cover all measured particles which could have a potential contribution to PM10.

In summary, the MLR calibrations are constructed for the following PN classes:

1. PM2.5-Dylos = PN class >0.5 μm minus PN class >2.5 μm
2. PM10-Dylos = PN class >2.5 μm
3. PMtotal-Dylos = PN class >0.5 μm (PM2.5 and PM10)

The overall performance of the Dylos models are worse compared to the PMSA003 sensors. This can be due to the fact that the Dylos sensor provides two PN classes while the PMSA003 sensor provides six PN classes. The PM2.5 model based on PMtotal-Dylos shows comparable performance with the model based on PM2.5-Dylos. The PM10 model based on PMtotal-Dylos shows better performance compared to the model based on PM10-Dylos. Both models for PM10 show very bad slopes, which could mean too low sensitivity of the Dylos sensor for particles >2.5 μm .

A graphical presentation of the MLR models from table 7 are given in figures 32, 33 and 34 for PM2.5 and in figures 35, 36 and 37 for PM10. For the PMSA003 sensors, only the 9492 is presented.

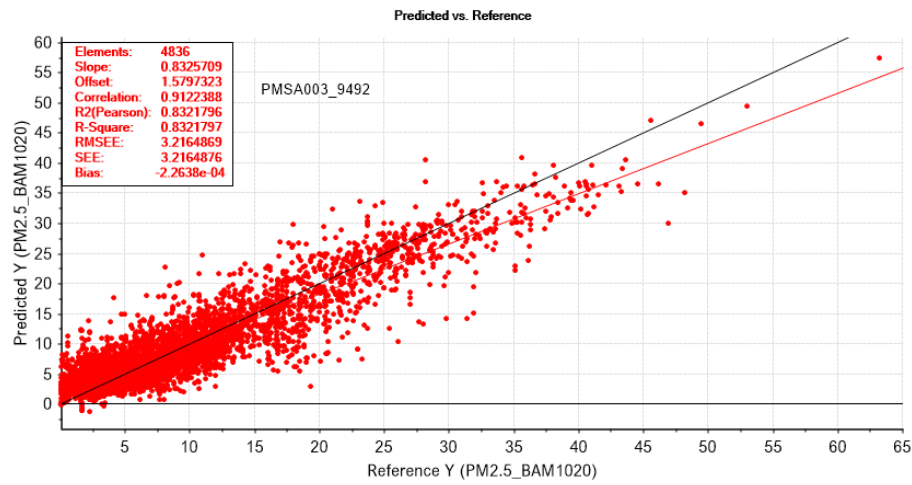


Figure 32: PMSA003 - MLR model PM2.5 against BAM1020 with "PN+RH+T" as X-variables

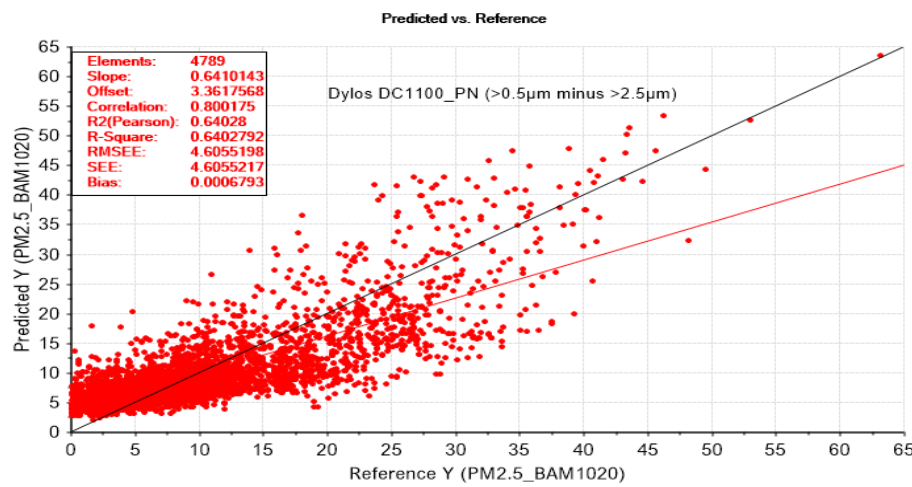


Figure 33: Dylos DC1100 (A) - MLR model PM2.5 against BAM1020 with "PN+RH+T" as X-variables

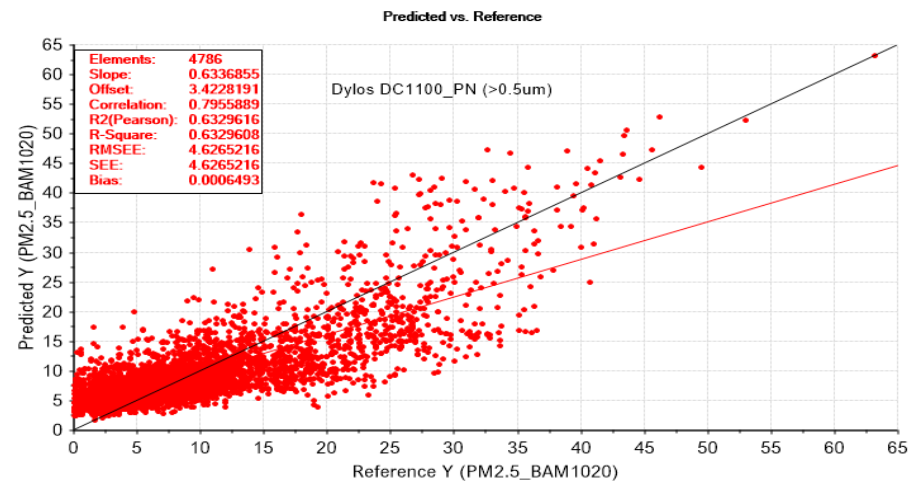


Figure 34: Dylos DC1100 (B) - MLR model PM2.5 against BAM1020 with "PN+RH+T" as X-variables

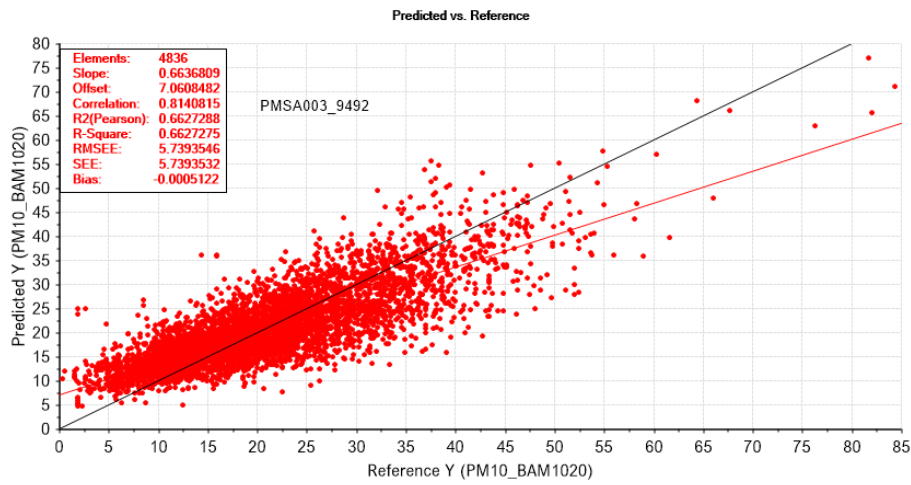


Figure 35: PMSA003 - MLR model PM10 against BAM1020 with "PN+RH+T" as X-variables

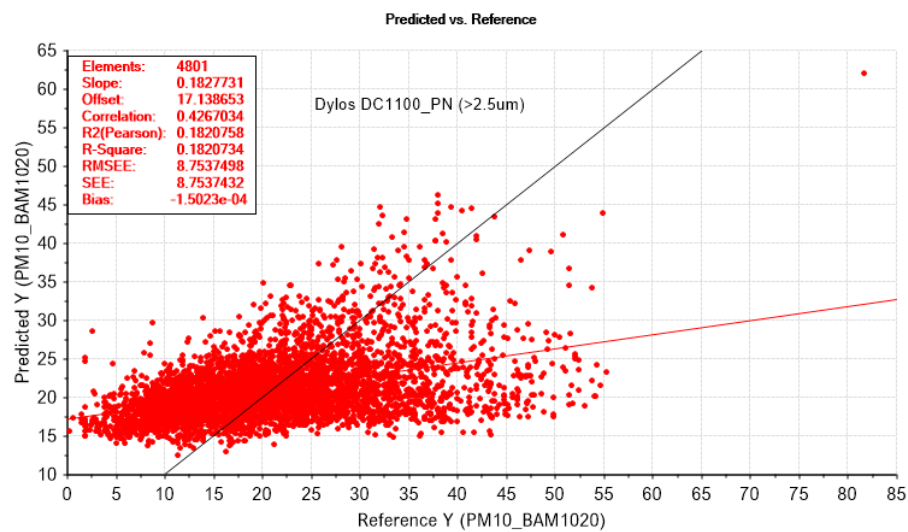


Figure 36: Dylos DC1100 (A) - MLR model PM10 against BAM1020 with "PN+RH+T" as X-variables

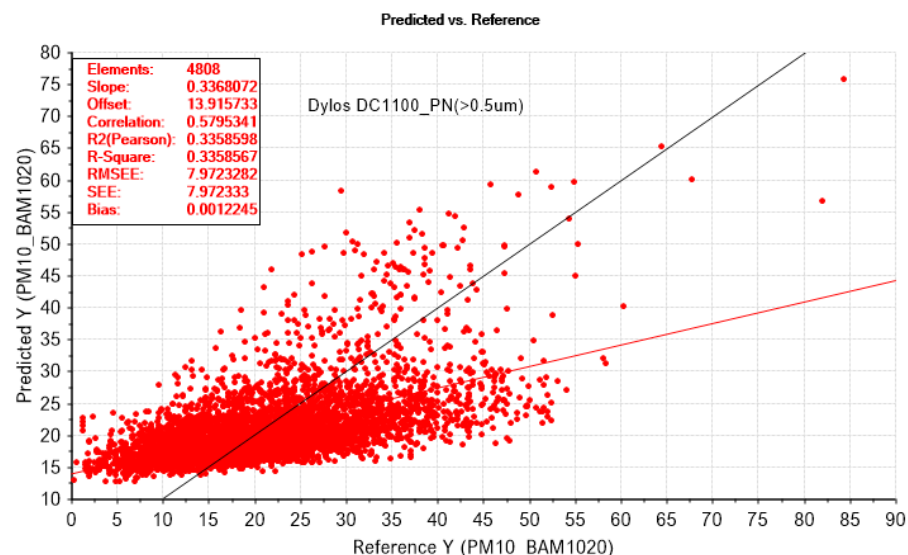


Figure 37: Dylos DC1100 (B) - MLR model PM10 against BAM1020 with "PN+RH+T" as X-variables

8.3 Improvement of MLR model performance by ASTM D6708

In general the slope and fitting of a (multivariate) calibration model can be investigated for improvement by use of ASTM D6708 (standard practice for statistical assessment and improvement of expected agreement between two test methods that purport to measure the same property of a material). This is achieved by the use of a mathematical post processing on the output of the model. The ASTM D6708 assessment can be considered as an extra part of the calibration process of the models.

The following post processing options (classes) can be calculated:

1. Class 0 $Y = X$ (complete equality, no improvement needed)
2. Class 1a $Y = X + b$ (weighed constant)
3. Class 1b $Y = X * b$ (weighed proportional)
4. Class 2 $Y = aX + b$ (weighed linear)

Where X is the output of the calibration model and Y is the output of the post processing according to ASTM D6708.

ASTM D6708 is investigated for the PM2.5 model for sensor PMSA003_8F33 based on "PN+RH+T". The available method to calculate the ASTM D6708 improvements could manage a maximum of 2000 samples. The 8F33 model has 2093 samples and therefore 93 samples with the lowest PM2.5 values were removed from the set. The lowest samples are far below the minimum detection limit of the BAM1020 monitor and are therefore not important for the model. The conclusion of ASTM D6708 is that the model can be improved by use of a Class 2 post calculation. The function of this Class 2 model is $Y = 1.184X - 1.3685$.

In figure 38 the outcome of the different classes is presented. In figure 39 the Y-residuals versus level is presented for the different classes. The 'LAB' value is equal to the BAM1020 monitor value, the X-axis is the BAM1020 value and the Y-axis is the model value. The best slope, fitting and residual distribution is achieved by the Class 2 post calculation. It must be notified that the Class2 post calculation increases the model standard error from $3.0 \mu\text{g}/\text{m}^3$ to $3.2 \mu\text{g}/\text{m}^3$. The Class 0 shows an under prediction effect of the model for PM concentrations $> 35 \mu\text{g}/\text{m}^3$ and an over prediction effect for PM concentrations $< 10 \mu\text{g}/\text{m}^3$. There is a so called scissor around $25 \mu\text{g}/\text{m}^3$. The Class2 post calculation neutralizes this scissor effect. The Y-residuals show a more homogeneous distribution around the different levels of the model after a Class 2 post calculation.

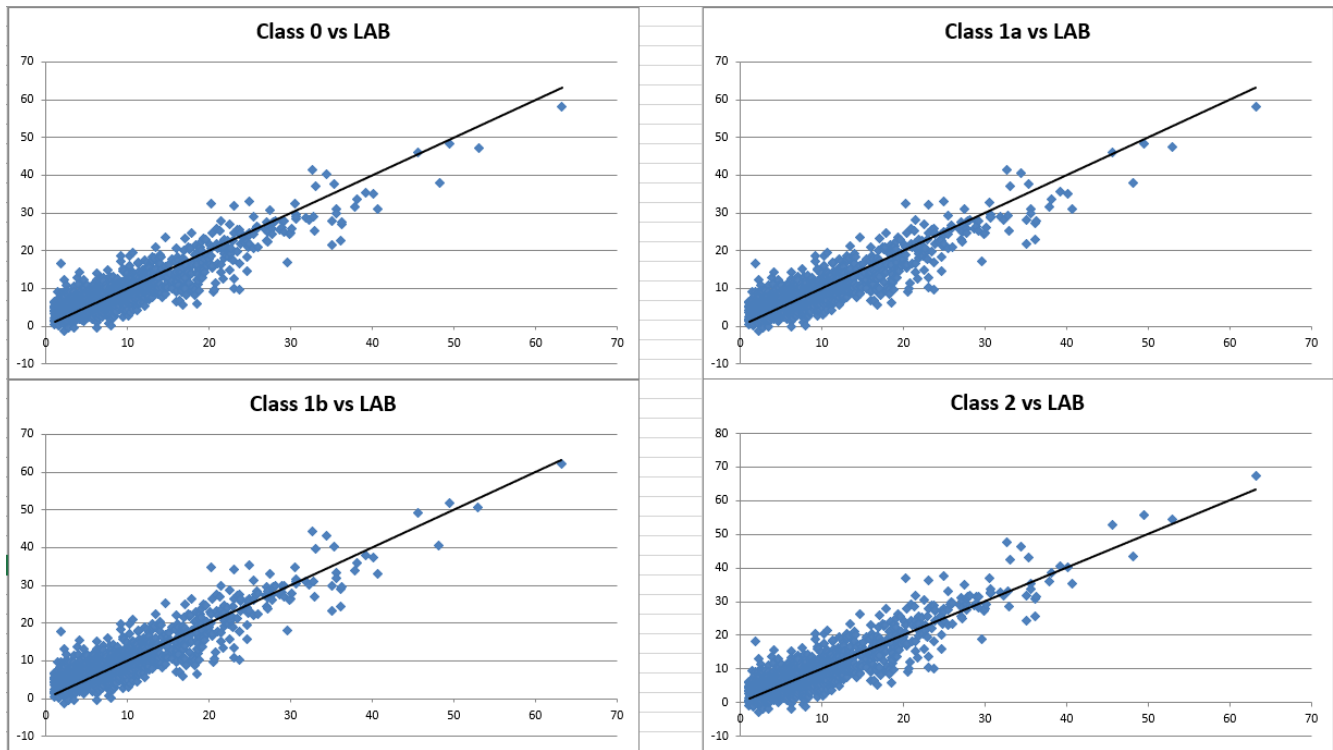


Figure 38: Outcome of ASTM D6708 improvement on PM2.5 model PMSA003_8F33 "PN+RH+T"

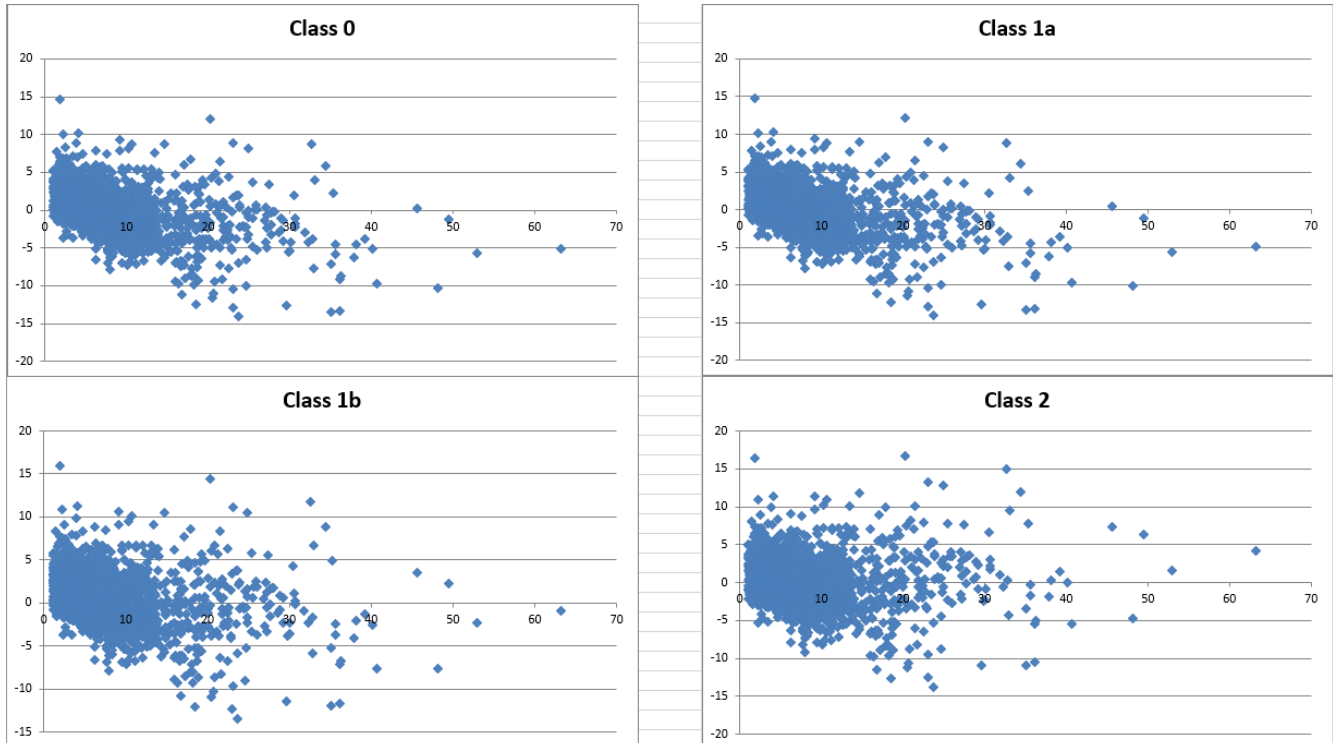


Figure 39: Residuals versus level of different ASTM D6708 calculations on PM2.5 model PMSA003_8F33 "PN+RH+T"

The work out of the MLR model (PM2.5, based on “PN+RH+T”) inclusive the Class 2 post calculation is investigated for the PMSA003_8F33 sensor. The validation set (N=419) is used for this investigation. The PM2.5 results retrieved by the MLR model and the MLR model + Class2 post calculation are compared with the BAM1020 monitor values (figure 40). Also the PM2.5 (Y)-residuals for the MLR model and the MLR model + Class2 post calculation are compared (figure 41).

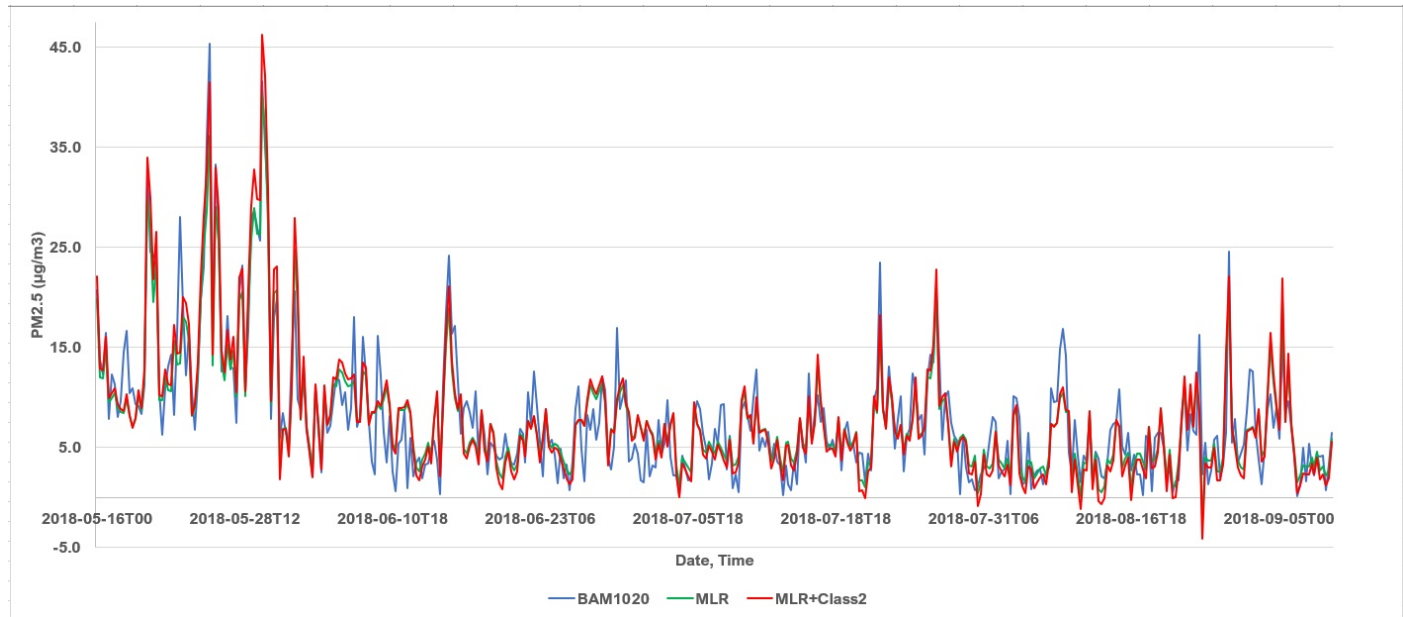


Figure 40: PM2.5 BAM1020, MLR, (MLR+Class2) for PMSA003_8F33 Validation Set



Figure 41: Difference PM2.5 versus BAM1020 for MLR, (MLR+Class2) for PMSA003_8F33 Validation Set

The bias and standard deviation in the differences between the MLR model and BAM1020 on the total validation set are respectively $-0.09 \mu\text{g}/\text{m}^3$ and $2.84 \mu\text{g}/\text{m}^3$. For the "MLR+Class2" model the values are respectively $0.00 \mu\text{g}/\text{m}^3$ and $2.98 \mu\text{g}/\text{m}^3$. The Class2 post calculation reduces the bias to zero but increases the standard deviation with $0.12 \mu\text{g}/\text{m}^3$.

For this investigation, it can be concluded that the ASTM D6708 post calculation does not significantly improve the model performance. However, it is recommended to investigate for the other MLR models if the ASTM D6708 post calculation could improve the model performance.

8.4 Validation MLR models

As discussed in 8.2, the MLR calibration models are validated with an independent validation set to test the accuracy and robustness. The hourly sensor observations of the validation set are used to predict PM2.5 and PM10 by the calibration models and the predicted results are compared with the BAM1020 monitor values.

The accuracy of the validation (SEP: Standard Error of Prediction) is tested against the accuracy of the calibration model (SEC: Standard Error of Calibration). The bias in the validation is tested against the SEP validation. The numbers of samples in the calibration- and validation sets are very big, therefore it makes no sense to use statistical tests for evaluation of the accuracy and bias e.g. the F-test for accuracy and t-test for bias.

The other parameters of the validation are used to check if the calibration model is robust for independent sensor observations.

The validation results for the MLR models based on "PM+RH+T" are given in table 9. The validation results for the MLR models based on "PN+RH+T" are given in table 10.

8.4.1 MLR validation results based on “PM+RH+T”

	PMSA003_8F33		PMSA003_9290		PMSA003_9492		SDS011_basic		SDS011_Luftdaten	
	PM2.5	PM10	PM2.5	PM10	PM2.5	PM10	PM2.5	PM10	PM2.5	PM10
N	420	422	967	968	968	970	981	981	972	974
Range ($\mu\text{g}/\text{m}^3$)	0.1-45.4	2.8-60.3	0.1-50.9	1.0-60.3	0.1-50.9	1.0-60.3	0.1-55.4	1.0-66.7	0.1-55.4	1.0-66.7
Slope	0.762	0.419	0.778	0.374	0.782	0.378	0.763	0.485	0.707	0.426
Offset ($\mu\text{g}/\text{m}^3$)	1.82	11.67	1.97	13.02	1.92	13.15	2.20	10.98	2.75	12.37
R-square	0.765	0.399	0.787	0.358	0.793	0.354	0.765	0.485	0.712	0.394
Accuracy ($\mu\text{g}/\text{m}^3$)	3.2	7.7	3.6	7.7	3.6	7.8	4.0	7.1	4.4	7.7
BIAS ($\mu\text{g}/\text{m}^3$)	-0.1	-0.2	-0.2	0.0	-0.2	0.2	-0.1	0.2	-0.1	0.3

Table 9: Validation results MLR models based on “PM+RH+T”

Explanation of the parameters:

- N : number of observations
- Range : the min-max range of the model
- Slope : steepness of the model regression line
- Offset : cut off on the Y-axis
- R-square : correlation coefficient of the regression line (R^2 -pearson)
- Accuracy : Root Mean Square Error of Prediction (RMSEP)
- B0 : Constant

The accuracy of all validations are good in line with the accuracy of the calibration models. The validation accuracy for the PMSA sensors is better for PM2.5 compared to the SDS011 sensors, but for PM10 they are comparable among all sensors. The bias of all validations is < 10% of the accuracy of the validations and is therefore not significant. The slope of the validations for PM2.5 are good and for PM10 the slopes are weak.

The offsets of all PM2.5 models are within the minimum detection limit of $4 \mu\text{g}/\text{m}^3$ of the BAM1020 monitor. The offsets of all PM10 models are higher than the minimum detection limit of $4 \mu\text{g}/\text{m}^3$ of the BAM1020 monitor.

The R^2 values are comparable with the slope values. The conclusion is clear that PM10 is hard to model against the BAM1020 based on “PM+RH+T” as X-variables. This could possibly be improved with other regression techniques.

A graphical presentation of the validations from table 9 are given in figures 42, 43 and 44 for PM2.5 and in figures 45, 46 and 47 for PM10. For the PMSA003 sensors, only the 9492 is presented. For all MLR validations the black line is the target line ($Y=X$) and the blue line is the slope. The X-axis (Y Reference) is the BAM1020 value, the Y-axis (Predicted Y) is the MLR model value.

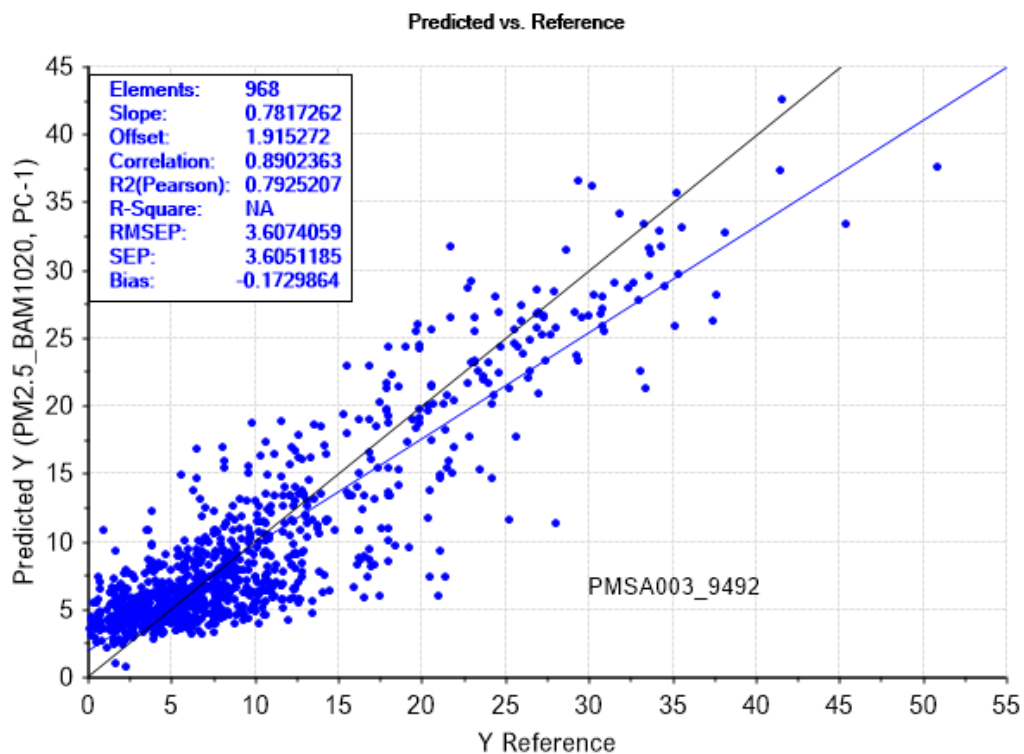


Figure 42: PMSA003 - Validation of MLR model PM2.5 against BAM1020 with "PM+RH+T" as X-variables

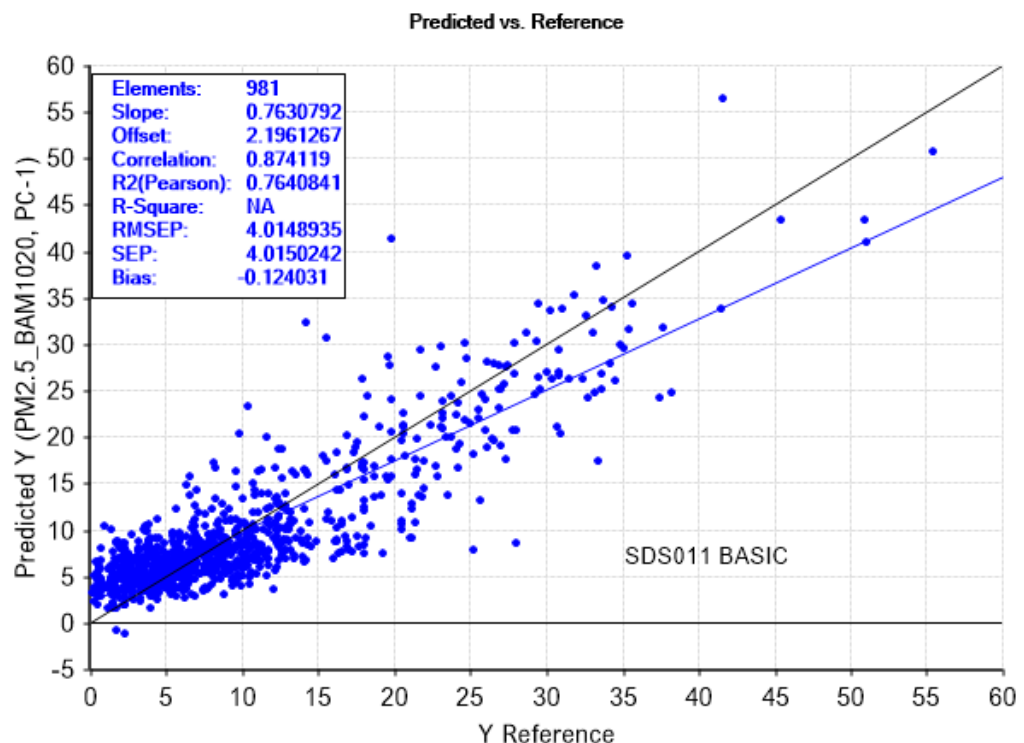


Figure 43: SDS011 basic config - Validation of MLR model PM2.5 against BAM1020 with "PM+RH+T" as X-variables

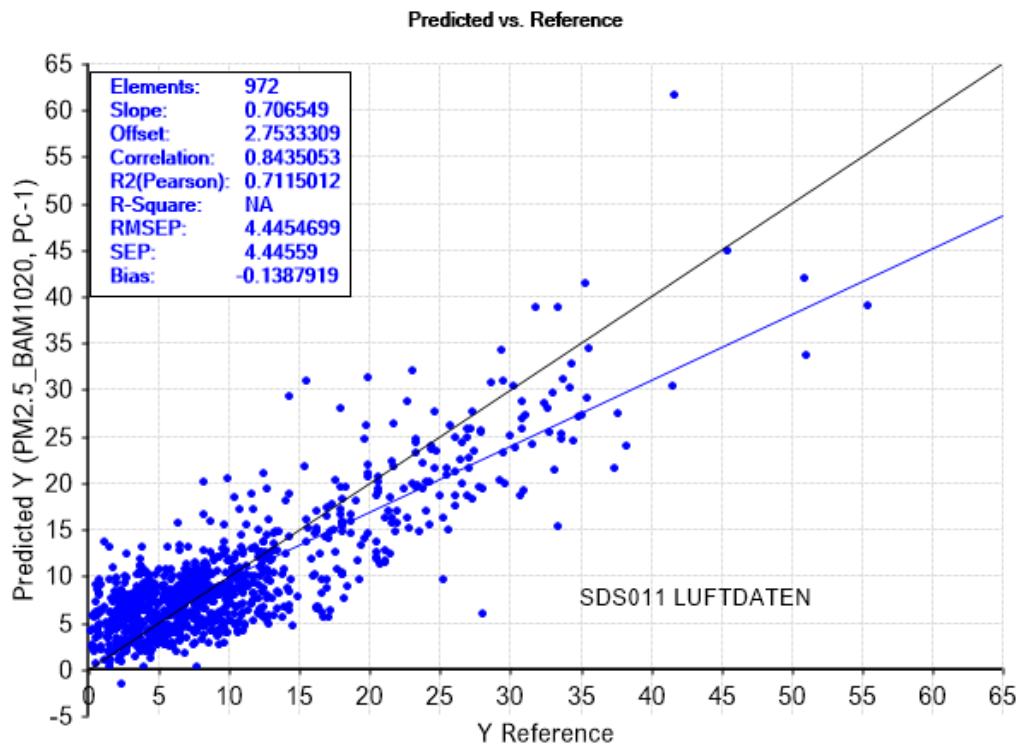


Figure 44: SDS011 Luftdaten - Validation of MLR model PM2.5 against BAM1020 with "PM+RH+T" as X-variables

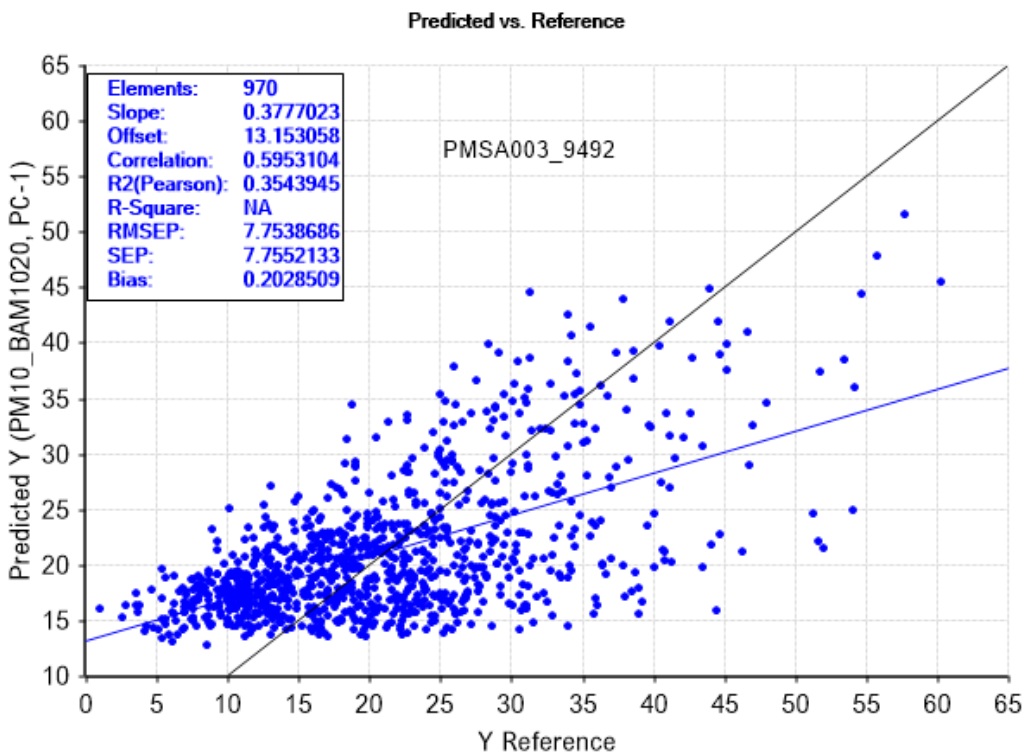


Figure 45: PMSA003 - Validation of MLR model PM10 against BAM1020 with "PM+RH+T" as X-variables

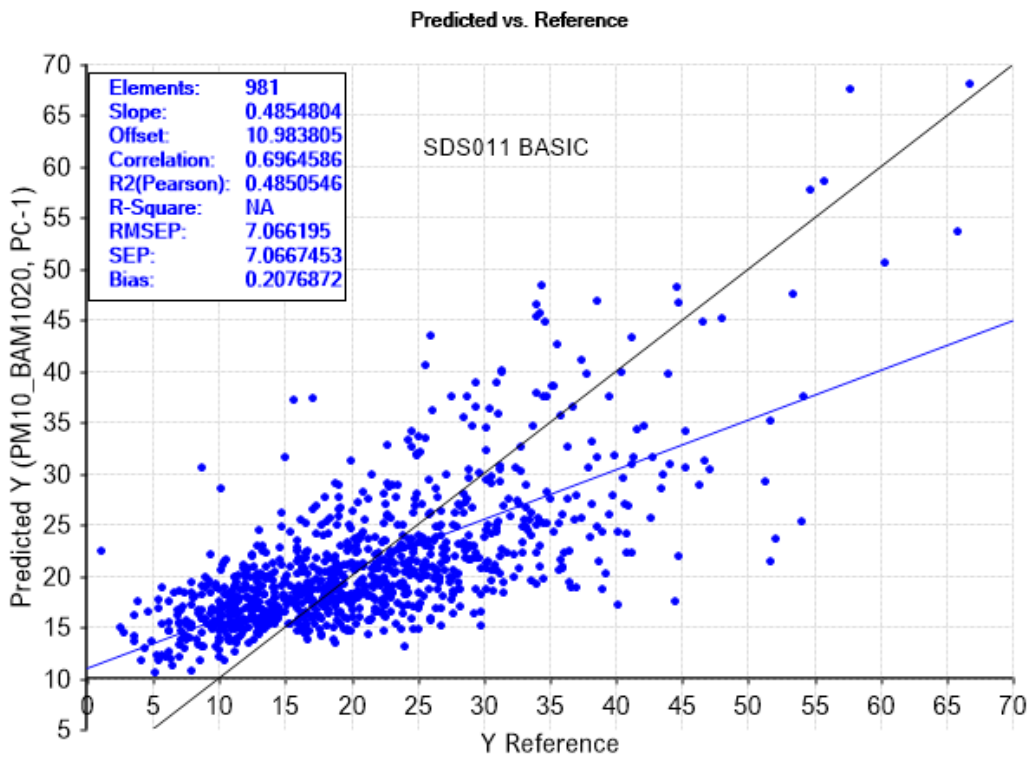


Figure 46: SDS011 basic config - Validation of MLR model PM10 against BAM1020 with "PM+RH+T" as X-variables

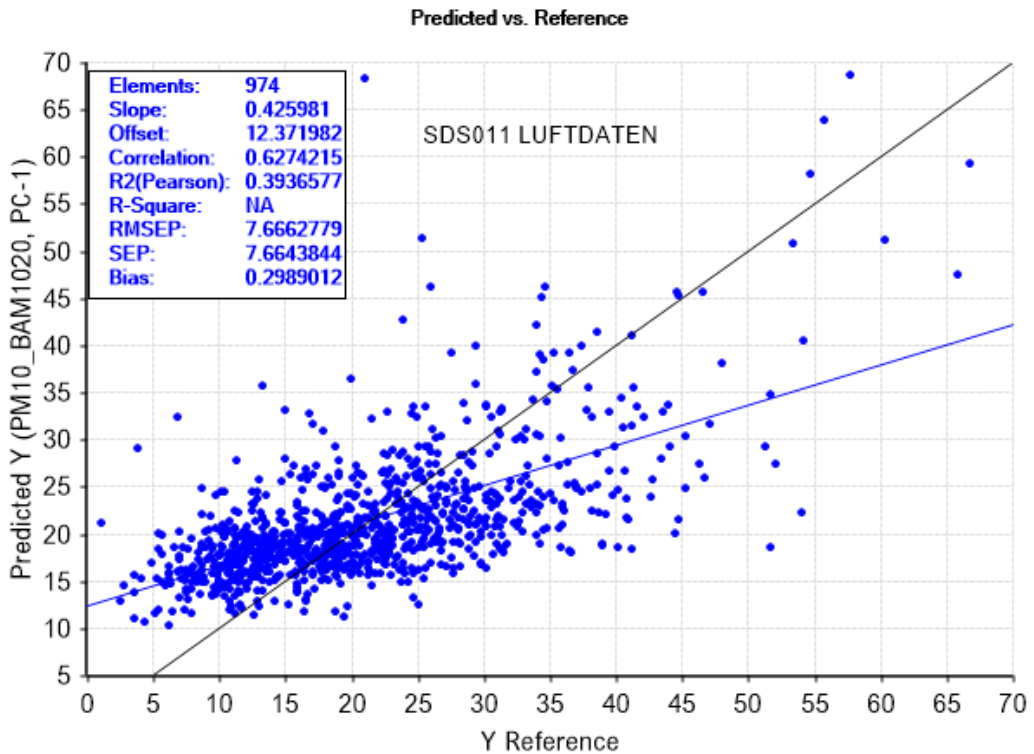


Figure 47: SDS011 Luftdate - Validation of MLR model PM10 against BAM1020 with "PM+RH+T" as X-variables

8.4.2 MLR validation results based on “PN+RH+T”

	PMSA003_8F33		PMSA003_9290		PMSA003_9492		Dylos_DC1100		Dylos_DC1100 (>0.5µm)	
	PM2.5	PM10	PM2.5	PM10	PM2.5	PM10	PM2.5 (>0.5µm->2.5µm)	PM10 (>2.5µm)	PM2.5	PM10
N	420	422	968	970	968	970	962	963	962	964
Range ($\mu\text{g}/\text{m}^3$)	0.1-45.4	2.8-60.3	0.1-50.9	1.0-60.3	0.1-50.9	1.0-60.3	0.2-50.9	2.5-60.3	0.2-50.9	1.0-60.3
Slope	0.799	0.676	0.831	0.651	0.831	0.654	0.623	0.183	0.614	0.340
Offset ($\mu\text{g}/\text{m}^3$)	1.52	6.77	1.42	7.35	1.39	7.23	3.38	17.12	3.45	13.86
R-square	0.818	0.645	0.851	0.615	0.85	0.621	0.646	0.183	0.641	0.342
Accuracy ($\mu\text{g}/\text{m}^3$)	2.8	5.9	3.1	6.0	3.1	5.9	4.7	8.7	4.8	7.8
BIAS ($\mu\text{g}/\text{m}^3$)	-0.1	0.2	-0.2	0.1	-0.2	0.0	-0.2	0.1	-0.2	0.1

Table 10: Validation results MLR models based on “PN+RH+T”

The accuracy of all validations are good in line with the accuracy of the calibration models. The validation accuracy for both PM2.5 and PM10 for the PMSA003 sensors is significantly better compared to the Dylos DC1100 sensor.

The slope of the validations for PM2.5 are good for the PMSA003 sensors and moderate for the Dylos DC1100 sensor. The slope of the validations for PM10 are moderate for the PMSA003 sensors and very weak for the Dylos DC1100 sensor.

The validation of the Dylos DC1100 sensor also proofs that the PM10 model is very weak in performance.

The offsets of all PM2.5 models are within the minimum detection limit of $4 \mu\text{g}/\text{m}^3$ of the BAM1020 monitor. The offsets of all PM10 models are higher than the minimum detection limit of $4 \mu\text{g}/\text{m}^3$ of the BAM1020 monitor.

The R^2 values are comparable with the slope values. The bias of all validations is < 10% of the accuracy of the validations and is therefore not significant.

The overall performance of the validations for the PMSA003 MLR models based on “PN+RH+T” is better compared to the MLR models based on “PM+RH+T”. It looks like that information gets lost due to the internal PMSA algorithm converting the PN classes to PM values. This information is of importance and used by the MLR models based on “PN+RH+T”.

The validation results for the Dylos DC1100 sensor show that the performance for the PM2.5 model is not improved by choosing the particles $>0.5\mu\text{m}$ instead of $(>0.5\mu\text{m} - >2.5\mu\text{m})$. However, the PM10 model based on particles $>0.5\mu\text{m}$ shows an improved performance compared to the model based on particles $>2.5\mu\text{m}$.

A graphical presentation of the validations from table 10 are given in figures 48, 49 and 50 for PM2.5 and in figures 51, 52 and 53 for PM10. For the PMSA003 sensors, only the 9492 is presented.

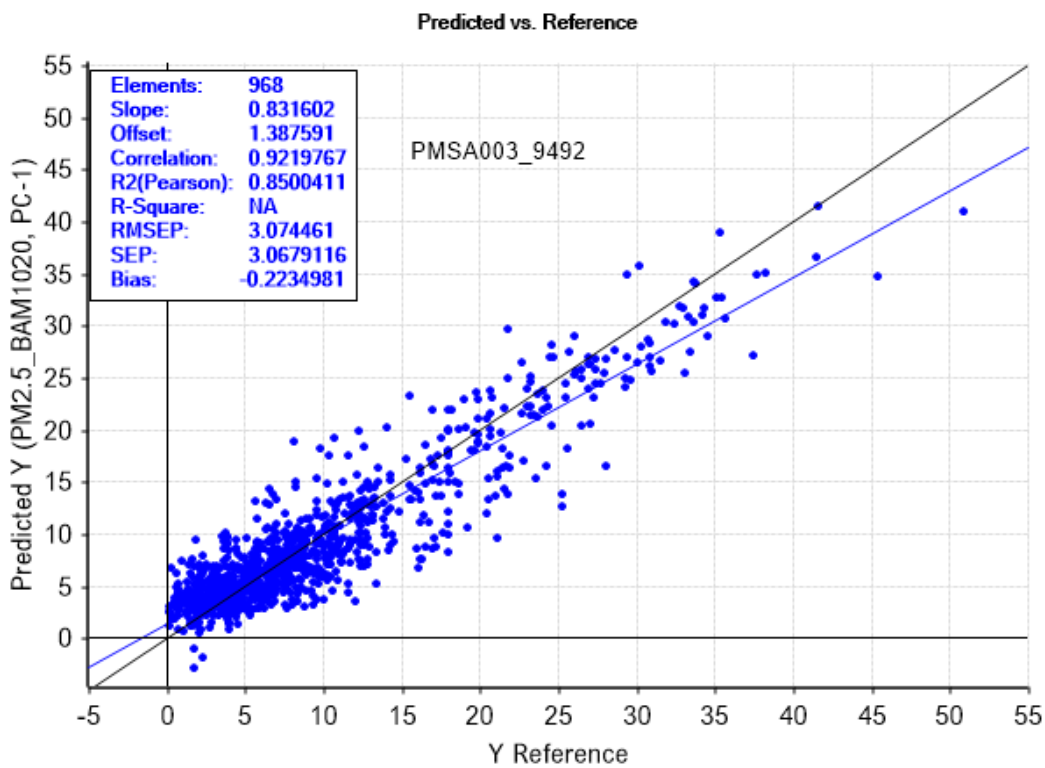


Figure 48: PMSA003 - Validation MLR model PM2.5 against BAM1020 with "PN+RH+T" as X-variables

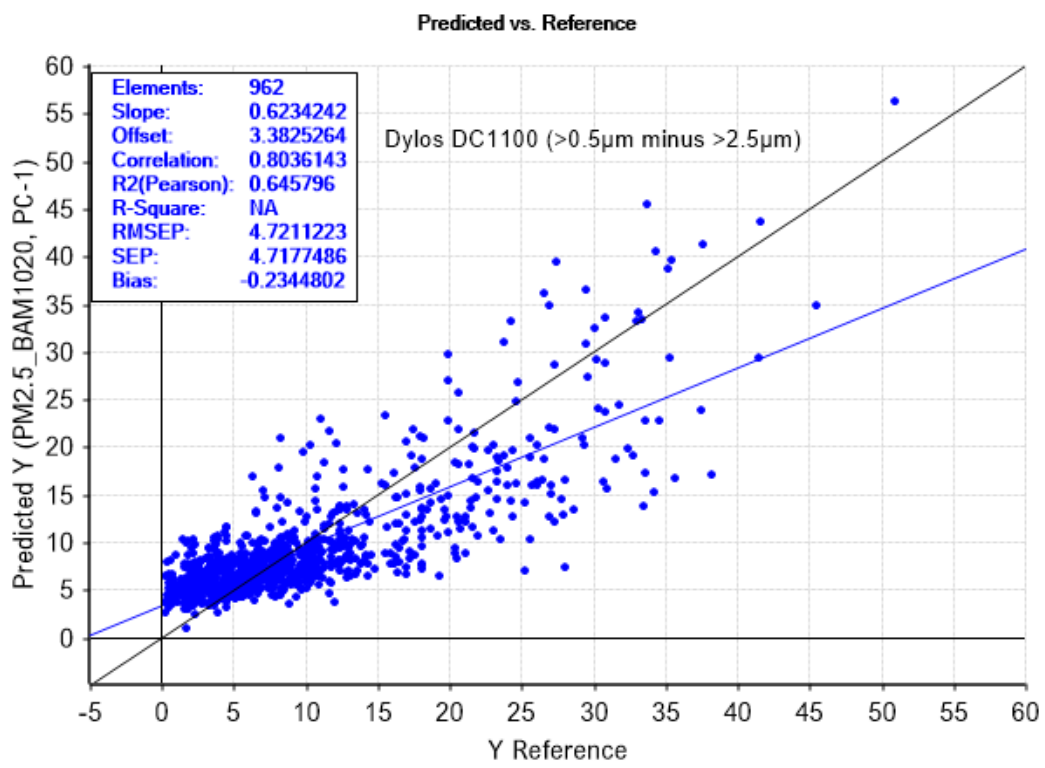


Figure 49: Dylos DC1100 (A) - Validation MLR model PM2.5 against BAM1020 with "PN+RH+T" as X-variables

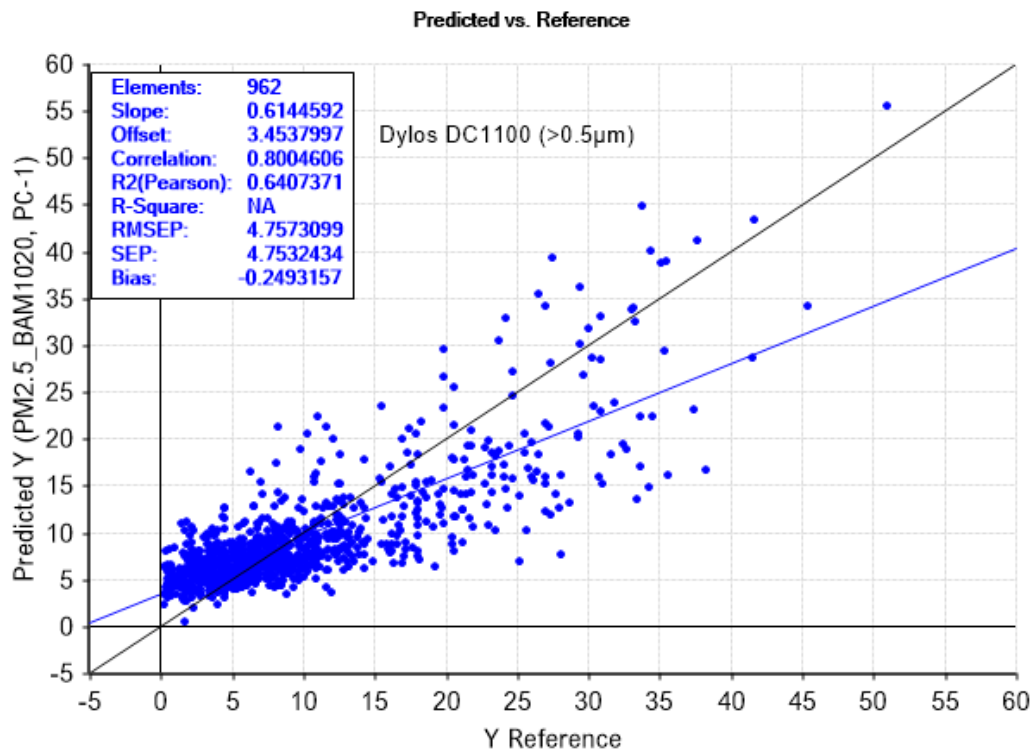


Figure 50: Dylos DC1100 (B) - Validation MLR model PM2.5 against BAM1020 with "PN+RH+T" as X-variables

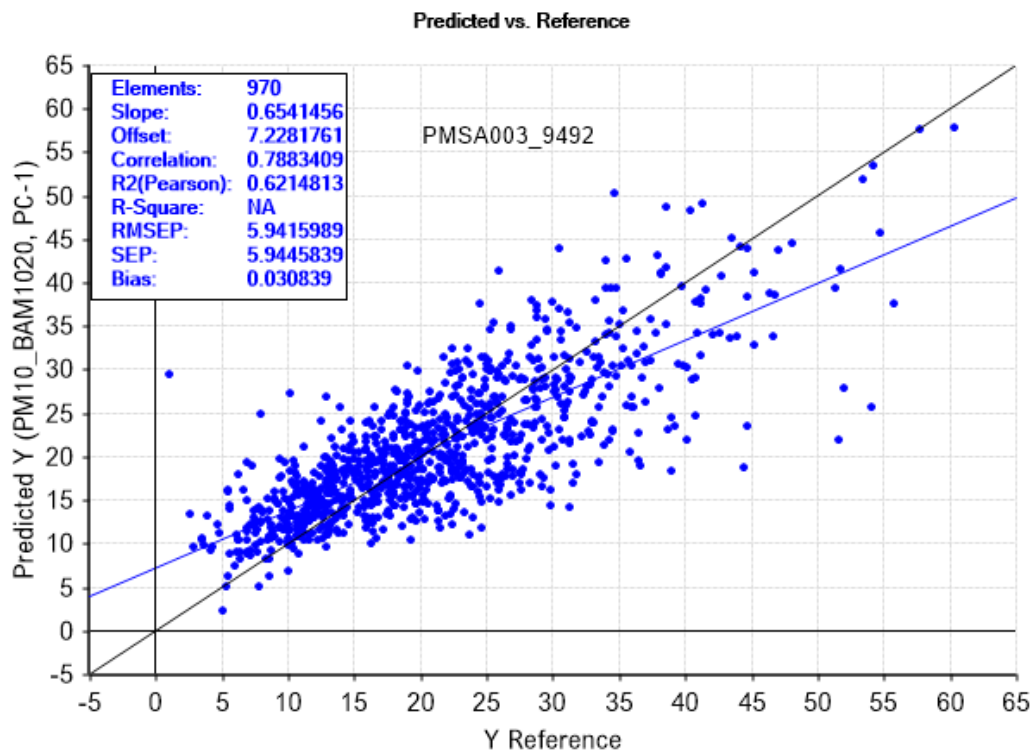


Figure 51: PMSA003 - Validation of MLR model PM10 against BAM1020 with "PN+RH+T" as X-variables

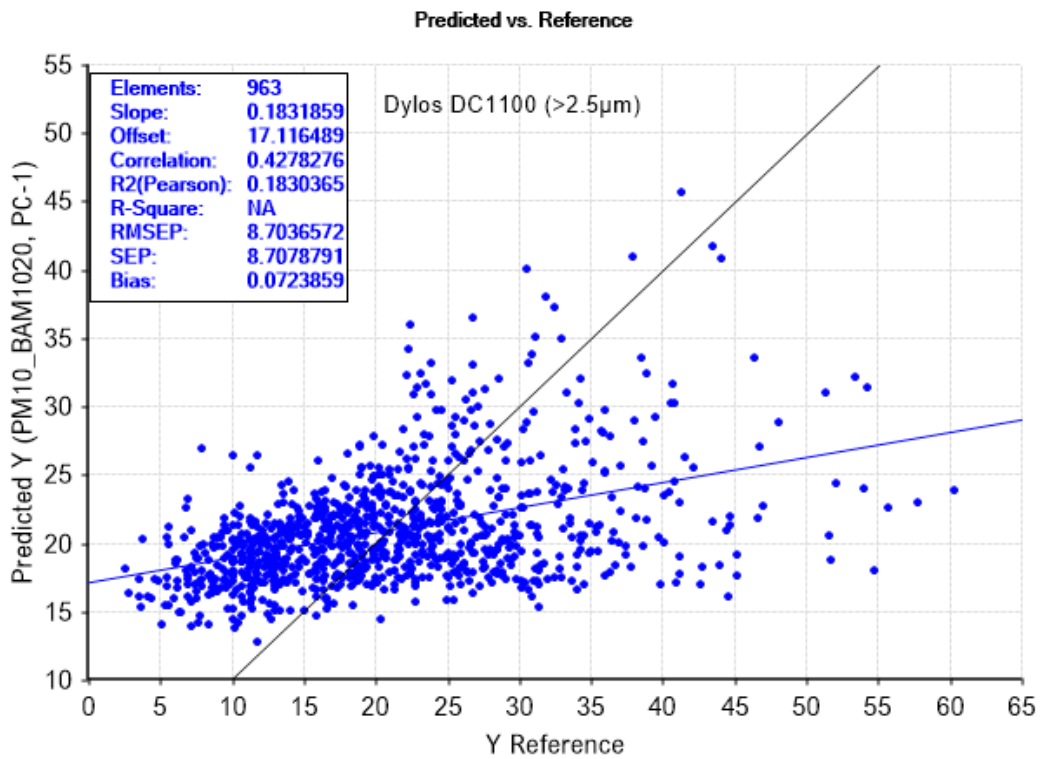


Figure 52: Dylos DC1100 (A) - Validation of MLR model PM10 against BAM1020 with "PN+RH+T" as X-variables

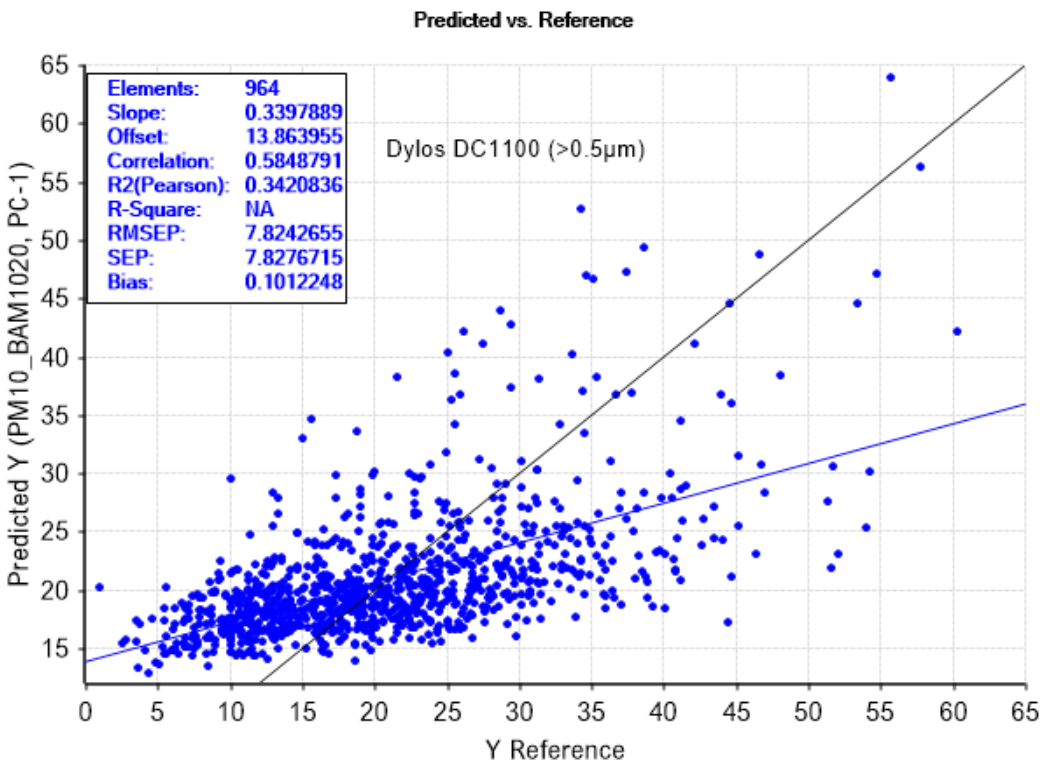


Figure 53: Dylos DC1100 (B) - Validation of MLR model PM10 against BAM1020 with "PN+RH+T" as X-variables

8.5 MLR model transfer between Plantower sensors

The models are developed per sensor and are also validated per sensor. It has been investigated to what extent the models are transferable between the Plantower sensors, because three of this type of sensor have been calibrated. Transferability has been assessed on the validation results of the model transferred from sensor PMSA003_9492 to sensors PMSA003_9290 and PMSA003_8F33. This is done for PM2.5 and PM10 based on “PM+RH+T” and “PN+RH+T”. The validation results after the transfer are compared with the primary validation results of the individual models for sensor PMSA003_9290 and PMSA003_8F33.

The results for the models based on “PM+RH+T” are given in table 11 and for “PN+RH+T” in table 12.

	PMSA003_9290 via 9492 model		PMSA003_8F33 via 9492 model	
	PM2.5	PM10	PM2.5	PM10
N	967	969	420	422
Range ($\mu\text{g}/\text{m}^3$)	0.1-50.9	1.0-60.3	0.1-45.4	2.8-60.3
Slope	0.679	0.316	0.725	0.308
Offset ($\mu\text{g}/\text{m}^3$)	1.7	13.29	2.24	14.56
R-square	0.786	0.351	0.763	0.376
Accuracy ($\mu\text{g}/\text{m}^3$)	4.0	7.8	3.2	7.9
BIAS ($\mu\text{g}/\text{m}^3$)	-1.4	-0.9	0.0	0.5

Table 11: Validation results transfer of PMSA003_9492 models “PM+RH+T” to other PMSA003 sensors

The validation results for sensor PMSA003_9290 are comparable with the primary validation results as given in table 9, except for the bias which is >10% of the accuracy and therefore significant. The validation results for sensor PMSA003_8F33 are comparable with the primary validation results as given in table 9.

	PMSA003_9290 via 9492 model		PMSA003_8F33 via 9492 model	
	PM2.5	PM10	PM2.5	PM10
N	968	970	420	422
Range ($\mu\text{g}/\text{m}^3$)	0.1-50.9	1.0-60.3	0.1-45.4	2.8-60.3
Slope	0.911	0.701	-0.218	-0.243
Offset ($\mu\text{g}/\text{m}^3$)	0.35	4.43	-2.65	4.00
R-square	0.803	0.492	NA	NA
Accuracy ($\mu\text{g}/\text{m}^3$)	3.7	7.4	8.5	13.3
BIAS ($\mu\text{g}/\text{m}^3$)	-0.5	-1.8	-12.4	-21.3

Table 12: Validation results transfer of PMSA003_9492 models “PN+RH+T” to other PMSA003 sensors

The validation results for sensor PMSA003_9290 are not as good as the primary validation results as given in table 8. However, for PM2.5 the slope and R^2 are good and the accuracy is just 0.6 $\mu\text{g}/\text{m}^3$ worse compared to the primary validation. The biases are >10% of the accuracy and are therefore significant.

The validation results for sensor PMSA003_8F33 are extremely bad. According to table 3, the correlations of the PN classes between sensor PMSA003_9290 and PMSA003_9492 show comparable sensitivity but the correlations between PMSA003_9492 and PMSA003_8F33 show much more sensitivity for the latter sensor. This has a high impact on the validation results.

Based on the results of table 9 and 10 it can be concluded that the transferability of the models based on "PM+RH+T" gives better performance compared to the "PN+RH+T" models. A possible improvement of the transferability of the "PN+RH+T" models could be a standardization of the PN classes. This will be discussed in 8.6.

8.5.1 Real-time experiment model transfer PMSA003 sensor

The PM2.5- and PM10 MLR model developed for the PMSA003_9492 sensor and based on "PM+RH+T" is transferred to a live PMSA003 sensor. The raw PM2.5- and PM10 values of the sensor are compared with the MLR predicted values and with the official PM2.5- and PM10 monitors at two RIVM locations. The MLR models are applied on the 10th of October on a PMSA003 sensor (62F3) active at location 's-Gravenpolder in Zeeland. The RIVM locations are 'Ossendrecht' and 'Breda', respectively 40km and 90km east from 's-Gravenpolder.

The results of this experiment are presented in the graphs below. The graphs shows the hourly averaged values for PM2.5, PM10, temperature and relative humidity for different days. The blue line is the raw PM sensor output, the lilac line is the PM prediction by the MLR model. The URL to the real time graph is https://openiod.org/SCAPE604/images/R/apri-sensor/aprisensor_sgravenpolder-mlr.png.

The results can be influenced by temporary increases from local sources such as wood-burning stoves. Larger deviations may then occur temporarily with the official monitors. The general picture shows that the post-calculation using the MLR model for both PM2.5 and PM10, the sensor value comes closer to the official monitor value.

Real-time MLR calibration

The Multi Linear Regression model (MLR) compensates for the influence of RH and T and predicts the value as measured with the BAM1020 reference monitor.

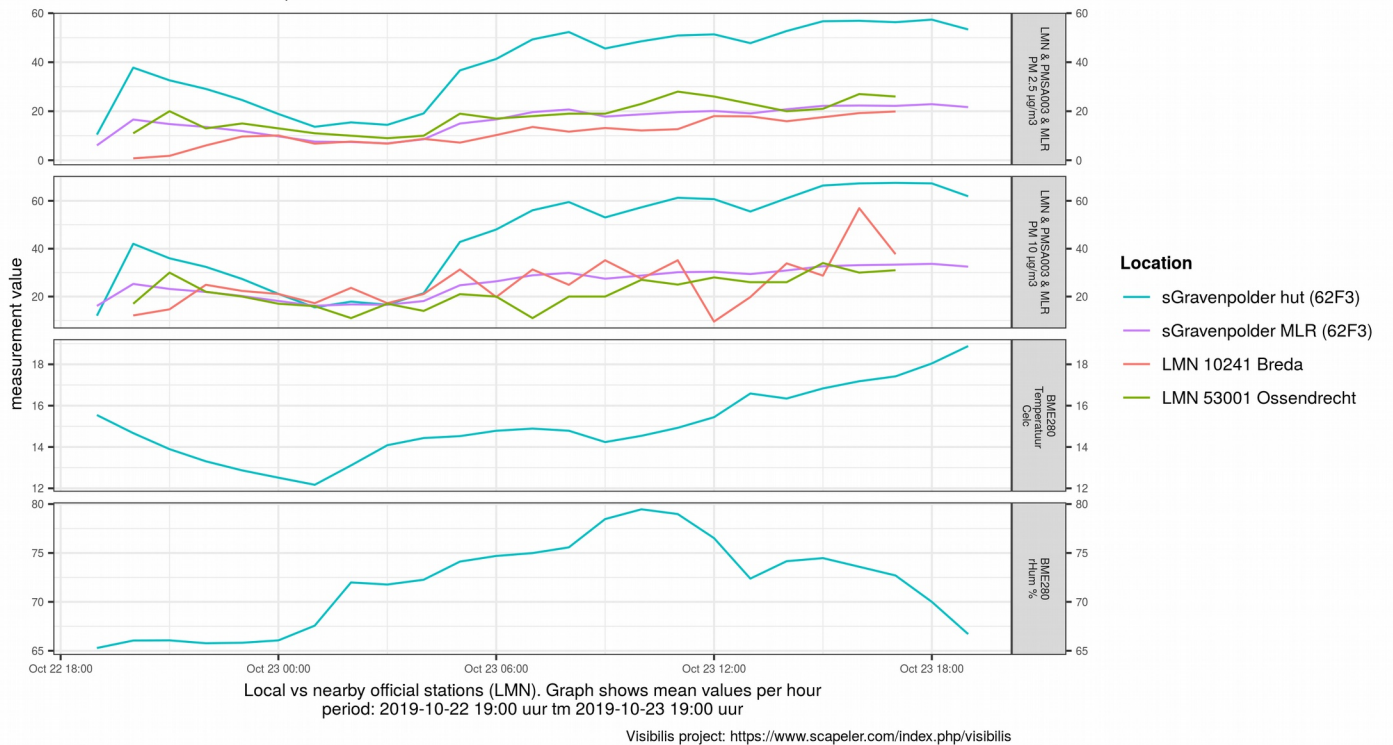


Figure 54: Real-time MLR calibration - Example 1

Real-time MLR calibration

The Multi Linear Regression model (MLR) compensates for the influence of RH and T and predicts the value as measured with the BAM1020 reference monitor.

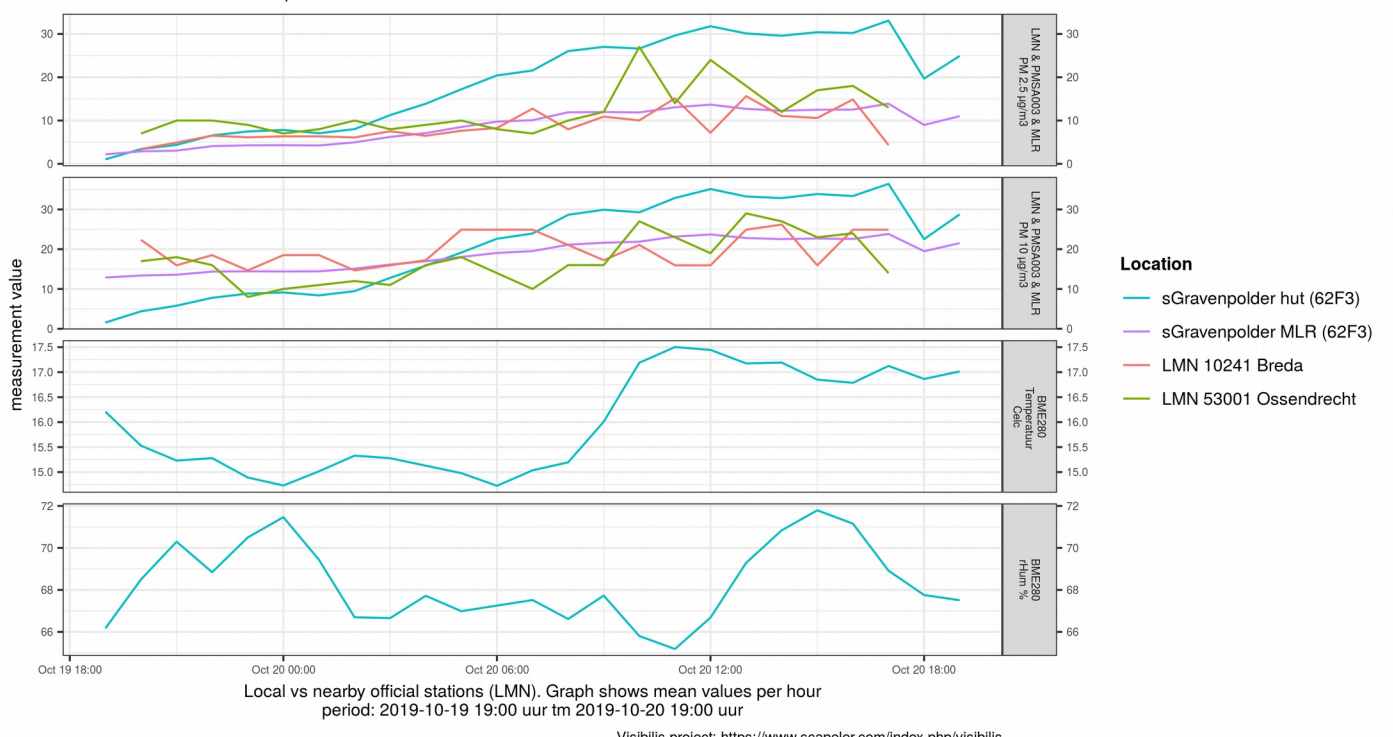


Figure 55: Real-time MLR calibration - Example 2

Real-time MLR calibration

The Multi Linear Regression model (MLR) compensates for the influence of RH and T and predicts the value as measured with the BAM1020 reference monitor.

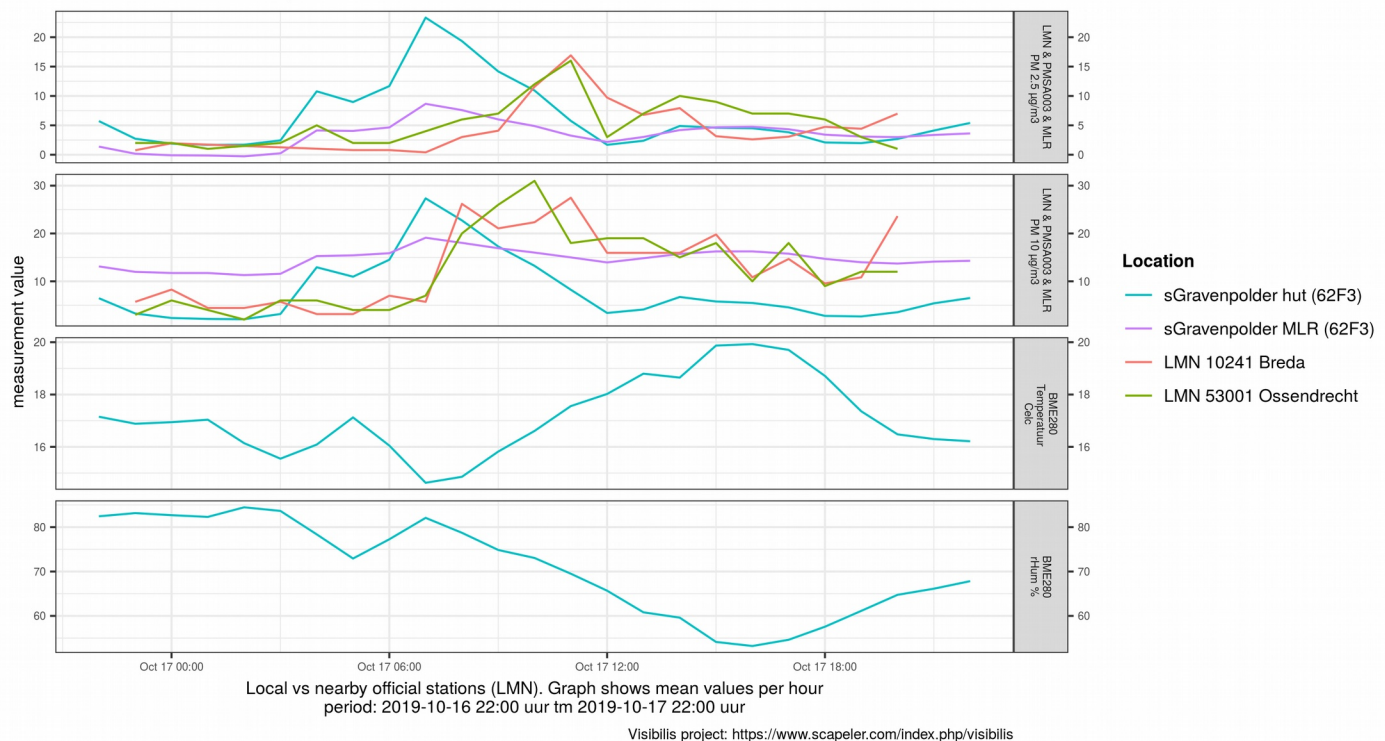


Figure 56: Real-time MLR calibration - Example 3

Real-time MLR calibration

The Multi Linear Regression model (MLR) compensates for the influence of RH and T and predicts the value as measured with the BAM1020 reference monitor.

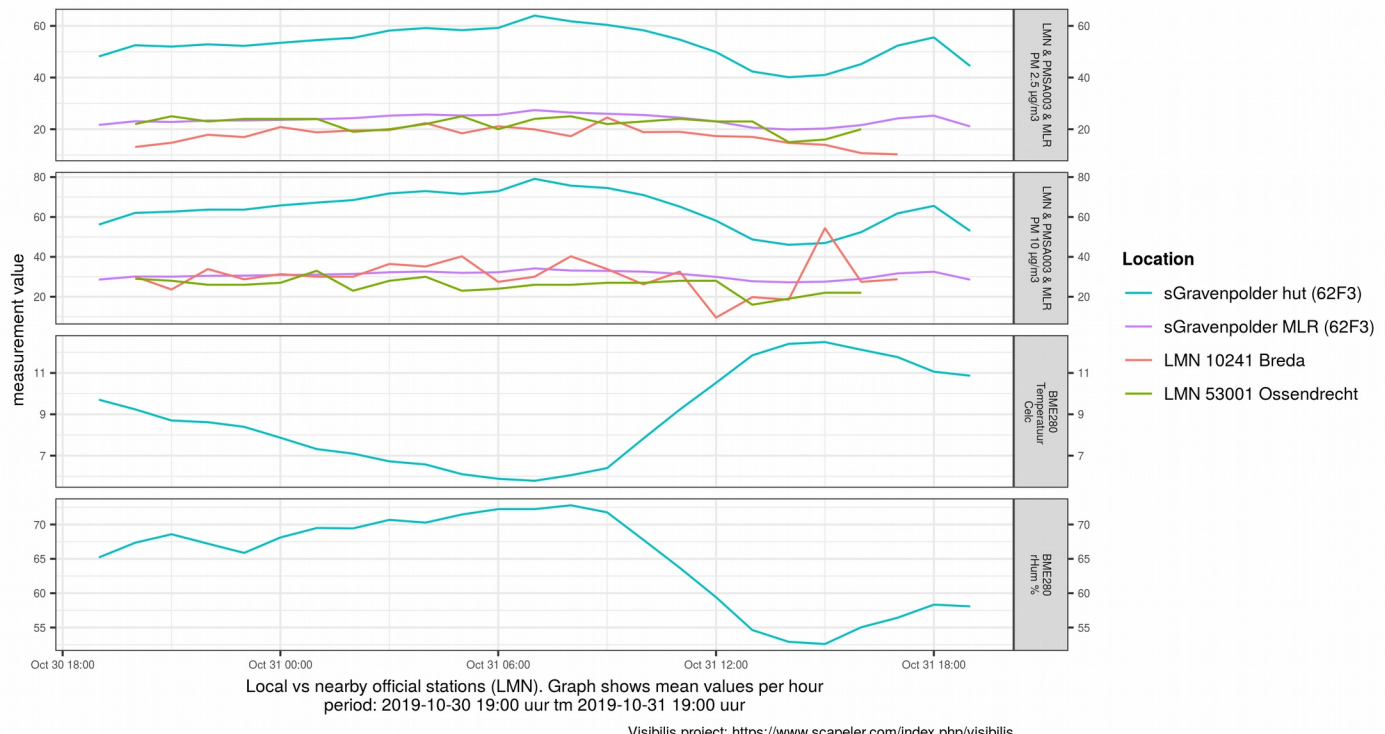


Figure 57: Real-time MLR calibration - Example 4

8.6 Standardization of the MLR Calibration Model based on particle numbers

The overall performance of the calibrations and validations for the PMSA003 MLR models based on "PN+RH+T" is better compared to the MLR models based on "PM+RH+T". However, transferred models based on "PM+RH+T" give better validation performance compared to the "PN+RH+T" models. The success rate of the model transfer can possibly be improved by standardization of the PN classes to a specific 'reference sensor'. For this experiment, sensor PMSA003_9492 is chosen as the reference. The PN classes of the other two PMSA003 sensors are recalculated by use of the parameters as given in table 3. After standardization of the PN classes, the MLR models constructed for sensor PMSA003_9492 can be applied on the other two PMSA003 sensors.

The recalculation is implemented by applying the linear regression coefficients slope and offset from table 3 on the PN classes of the sensors to be standardized against sensor PMSA003_9492.

As an example, the standardization of PN class 2.5 μm of sensor PMSA003_9290 to PMSA003_9492 is implemented as follows:

$$\text{PN class } 2.5\mu\text{m}_\text{PMSA003_9492} = 1.790 * \text{PN class } 2.5\mu\text{m}_\text{PMSA003_9290} - 0.95$$

The slope and offset in this calculation are derived from the correlation plot as given in figure 58.

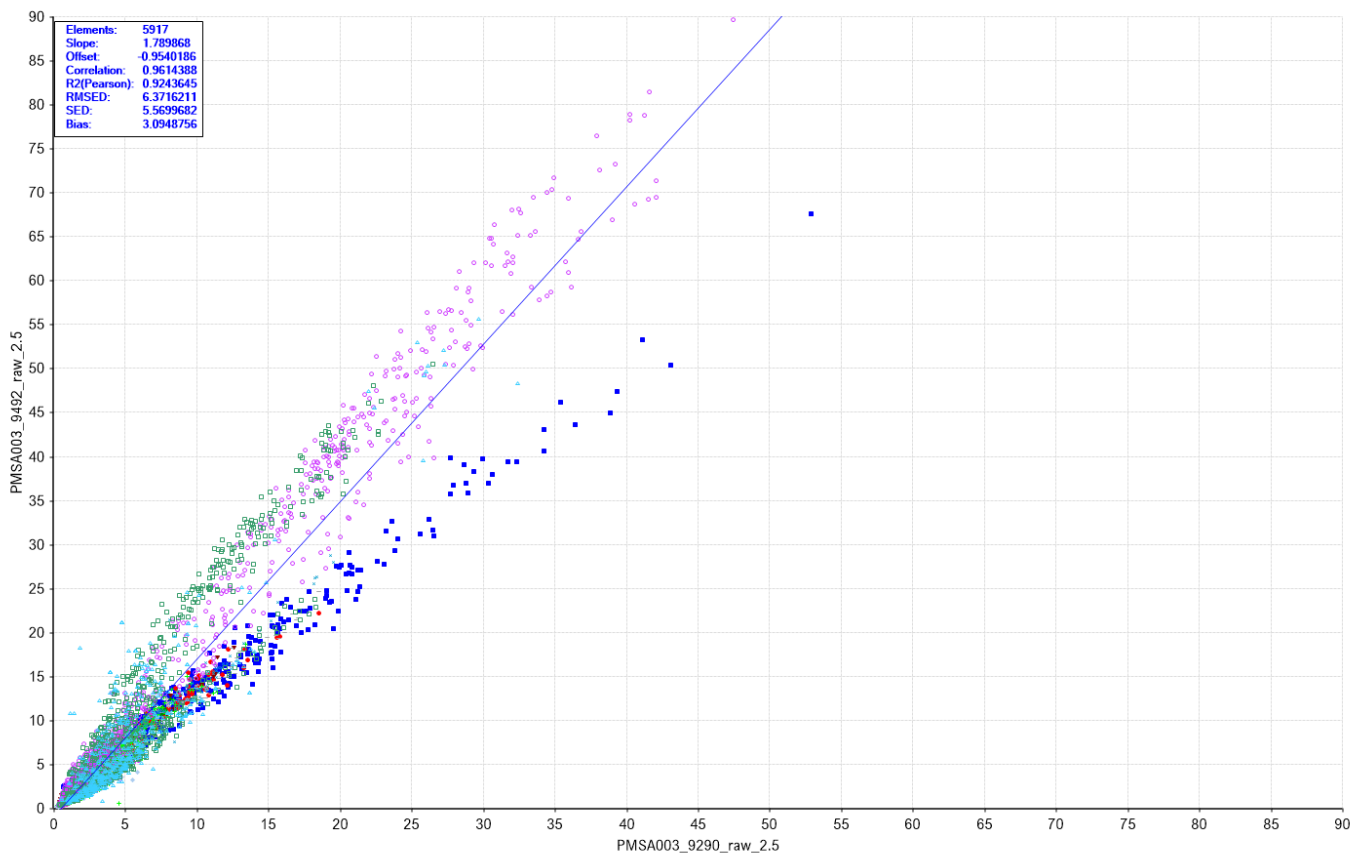


Figure 58: Correlation plot PN Class 2.5 μm between PMSA003_9290 and PMSA003_9492

After standardization of the PN classes of sensor PMSA003_8F33 and PMSA003_9290 the validation of the two sensors is carried out by use of the "PN+RH+T" model calibrated for sensor PMSA003_9492. The validation results after standardization are compared with both the primary validation of the sensors as given in table 6 and the validation results without standardization as given in table 12. An overview of the results is given in table 13. A graphical presentation of the validations after PN standardization is given in figures 59, 60, 61 and 62.

	PMSA003_8F33		PMSA003_8F33		PMSA003_8F33		PMSA003_9290		PMSA003_9290		PMSA003_9290	
	primary validation		model transfer		PN standardization		primary validation		model transfer		PN standardization	
	PM2.5	PM10	PM2.5	PM10	PM2.5	PM10	PM2.5	PM10	PM2.5	PM10	PM2.5	PM10
N	420	422	420	422	420	422	968	970	968	970	968	970
Range ($\mu\text{g}/\text{m}^3$)	0.1-45.4	2.8-60.3	0.1-45.4	2.8-60.3	0.1-45.4	2.8-60.3	0.1-50.9	1.0-60.3	0.1-50.9	1.0-60.3	0.1-50.9	1.0-60.3
Slope	0.799	0.676	-0.218	-0.243	0.81	0.660	0.831	0.651	0.911	0.701	0.783	0.554
Offset ($\mu\text{g}/\text{m}^3$)	1.52	6.77	-2.65	4.00	1.55	7.63	1.42	7.35	0.35	4.43	1.87	9.34
R-square	0.818	0.645	NA	NA	0.765	0.571	0.851	0.615	0.803	0.492	0.826	0.526
Accuracy ($\mu\text{g}/\text{m}^3$)	2.8	5.9	8.5	13.3	3.2	6.6	3.1	6.0	3.7	7.4	3.3	6.7
BIAS ($\mu\text{g}/\text{m}^3$)	-0.1	0.2	-12.4	-21.3	0.0	0.7	-0.2	0.1	-0.5	-1.8	-0.2	0.1

Table 13: Comparison of the primary validation results of the "PN+RH+T" models for sensors PMSA003_8F33 and PMSA003_9290 with model transfer and after PN standardization

Based on the data from table 13, it can be concluded that the validation results after standardization correspond well with the primary validations of the models. The accuracy after standardization is slightly poorer, but the bias is <10% of the accuracy and therefore not significant. The results show that standardization of the PN classes can be a good alternative if one wants to use a model calibrated with the particle classes of one particular 'reference' sensor.

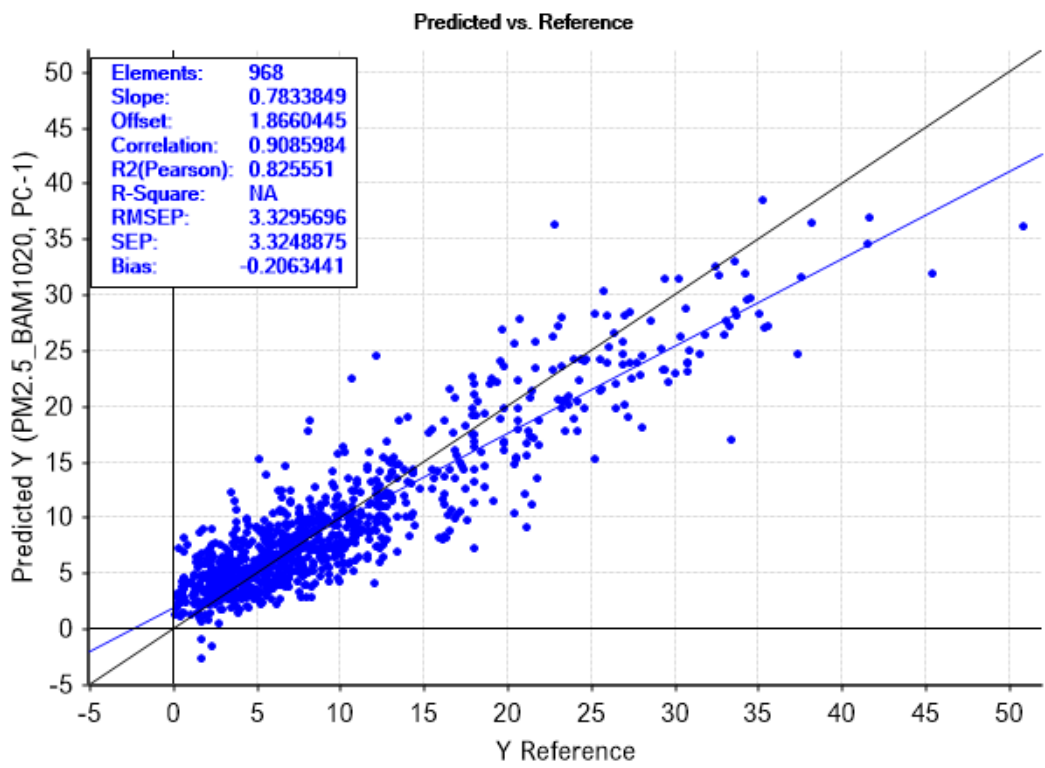


Figure 59: Validation of the "PN+RH+T" PM2.5 model for sensor PMSA003_9290 after standardization of the PN classes

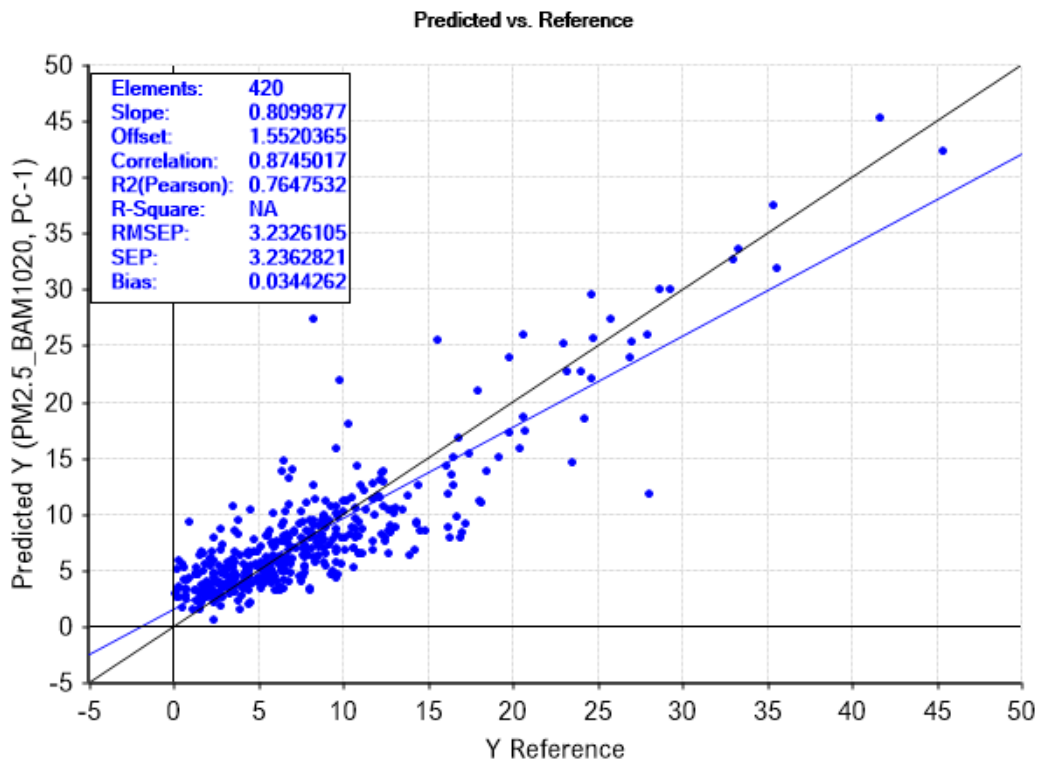


Figure 60: Validation of the "PN+RH+T" PM2.5 model for sensor PMSA003_8F33 after standardization of the PN classes

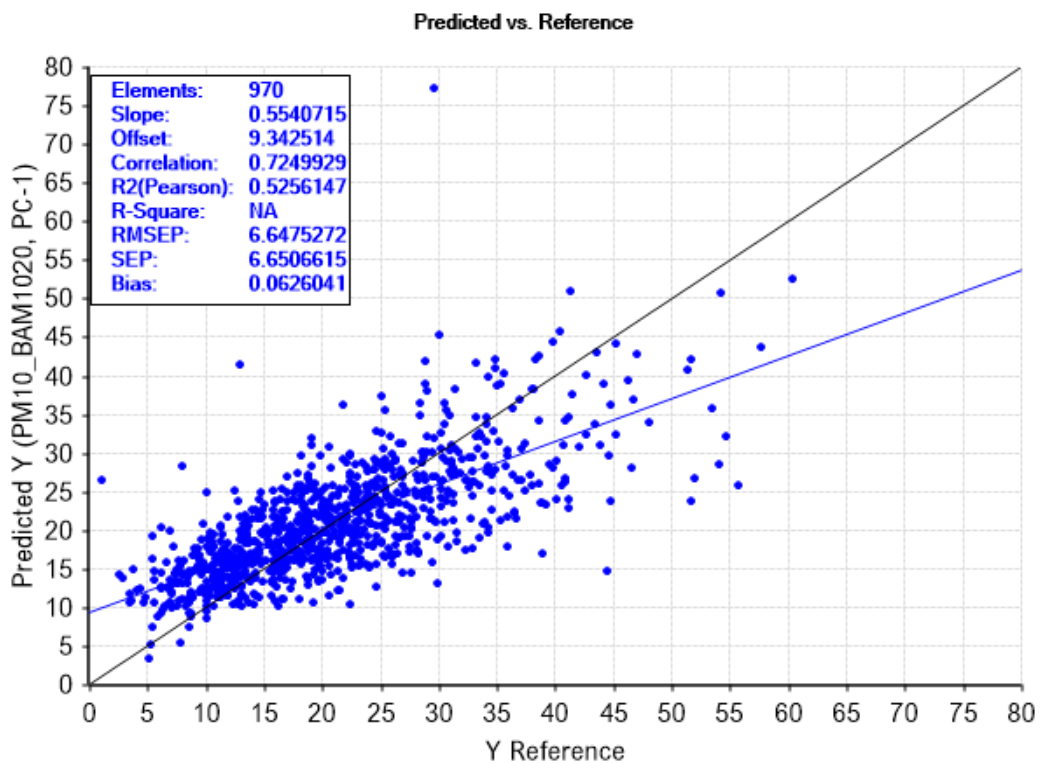


Figure 61: Validation of the "PN+RH+T" PM10 model for sensor PMSA003_9290 after standardization of the PN classes

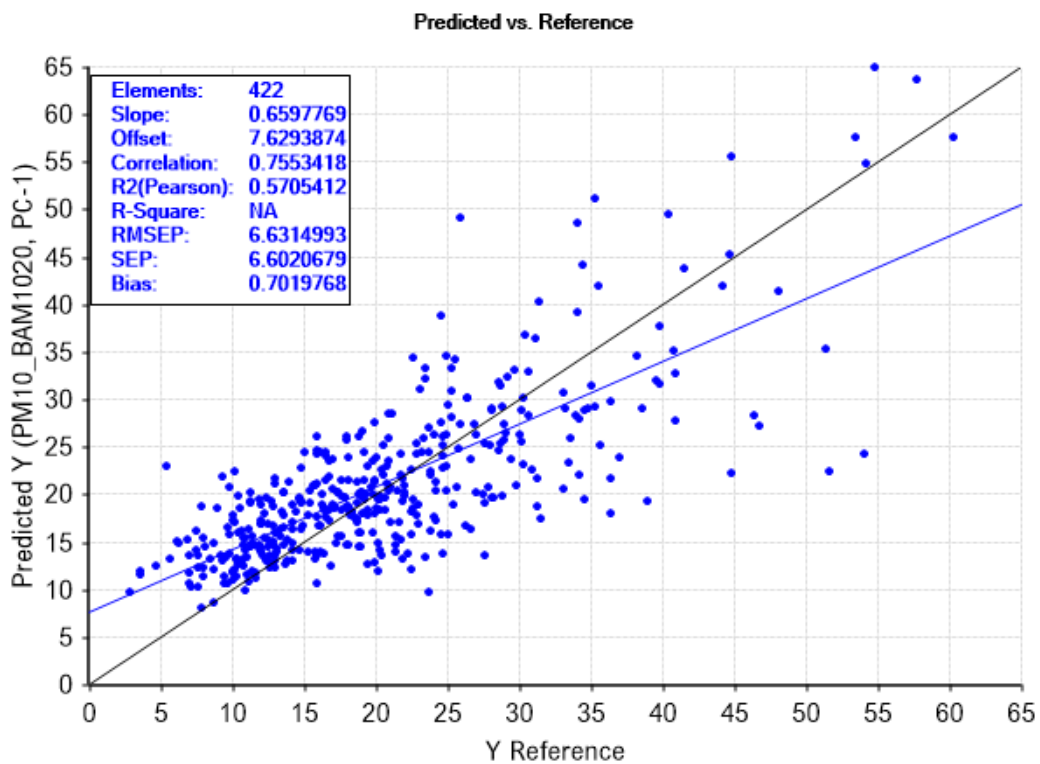


Figure 62: Validation of the "PN+RH+T" PM10 model for sensor PMSA003_8F33 after standardization of the PN classes

9 Conclusions & Recommendations

The reliability of relatively cheap particulate matter (PM) sensors can be improved by using the multiple linear regression (MLR) technique. The PM value from the sensor is read in by a model and the output of the model is the prediction for the PM value as it was measured by the official monitor Met One BAM1020. The MLR models are calibrated separately for PM2.5 and PM10. As input variables the PM value, relative humidity (RH) and temperature (T) are used. For the PMSA003 sensor also the particle number concentrations (PN), RH and T are used. For the Dylos DC1100 sensor, only PN, RH and T could be used.

It is well known that PM sensors with laser technology are sensitive to mainly relative humidity and to less extend the temperature of the ambient air. The MLR model corrects the calibrated PM value for the temperature and relative humidity of the ambient air, which further improves the reliability of the PM sensor. The input for temperature and relative humidity can be provided by sensors that are mounted together with the PM sensor in the same measuring box.

The accuracy of the calibration models for the PMSA003- and SDS011 sensors is $4 \mu\text{g}/\text{m}^3$ for PM2.5 and $8 \mu\text{g}/\text{m}^3$ for PM10. The accuracy of the PM2.5 models is good in line with the reproducibility of $4 \mu\text{g}/\text{m}^3$ of the BAM1020 monitor. The PM10 calibration models show an overall bad performance, possibly due to lack of sensitivity for particles $>2.5 \mu\text{m}$. The validation of the models show an accuracy of $4 \mu\text{g}/\text{m}^3$ for PM2.5 and $8 \mu\text{g}/\text{m}^3$ for PM10.

9.1 Improvement of the model

The accuracy of the MLR calibration models can be further improved by performing the calibration on the PN concentrations. This is only possible for the PMSA003- and Dylos DC1100 sensors where the Dylos DC1100 sensor only supports PN. The accuracy of the calibration models for the PMSA003 sensors is $3 \mu\text{g}/\text{m}^3$ for PM2.5 and $6 \mu\text{g}/\text{m}^3$ for PM10. For the Dylos DC1100 sensor the accuracies are respectively $5 \mu\text{g}/\text{m}^3$ for PM2.5 and $9 \mu\text{g}/\text{m}^3$ for PM10. The validation of the models for the PMSA003 sensor show an accuracy of $3 \mu\text{g}/\text{m}^3$ for PM2.5 and $6 \mu\text{g}/\text{m}^3$ for PM10. The validation of the models for the Dylos DC1100 sensor shows an accuracy of $5 \mu\text{g}/\text{m}^3$ for PM2.5 and $8 \mu\text{g}/\text{m}^3$ for PM10.

The reliability of the MLR model can be further improved by applying ASTM D6708. This option has been investigated for PM2.5 of one PMSA003 sensor with PN, RH and T as input variables. The ASTM D6708 application reduces the bias to zero with a small increase in the model error. It is recommended to investigate the application of ASTM D6708 for multiple sensors. The ASTM D6708 application is an arithmetic post calculation and must be seen as a correction to the fitting of the model.

9.2 Transferability of the model

The transferability of the MLR model has been investigated for the PMSA003 sensors for PM, RH and T as well as PN, RH and T as input variables. Transferability is successful for the MLR model based on PM, RH and T where independent validation has shown that the accuracy remains comparable to the primary validation. The transferability of the MLR model based on PN, RH and T is not successful and is caused by large differences in sensitivity to PN between the sensors.

The transferability of the MLR model based on PN, RH and T can be improved by standardizing the PN classes. This option has been investigated for the PMSA003 sensors, whereby the PN classes are standardized against one specific sensor. It has been demonstrated through independent validation that the accuracy through standardization is comparable to the primary validation of the sensors.

Calibration, standardization and model transfer of a MLR model based on PN, RH and T produces a more accurate prediction. However, a disadvantage of this process is that one specific sensor must be available against which the standardization of other sensors can be performed. Calibration and transfer of a MLR model based on PM, RH and T produces a less accurate prediction. An advantage of this process is that it can be applied directly on other sensors of the same kind.

9.3 Recommendations

Model transfer has not been investigated for the SDS011 sensor, but it is recommended to perform this in a follow-up investigation.

It is strongly recommended to re-calibrate and re-validate the MLR models under extended meteorological conditions. The conditions must be chosen in a way that they are outside the ranges as have been used for this project.

The Visibilis project has been carried out at one location, close to the sea and in the vicinity of industry and shipping. It is strongly recommended to repeat the project at other locations, preferably inland, but also at locations where other particulate matter sources are present. By repeating the project at different locations, the models can be made more robust and accurate, because then more different particulate matter particles are included in the calibration and validation of the models.

It is recommended to test the models over a longer period of time. Sensors can deviate slowly over time and these effects can affect the reliability of the models.

Contact

Correspondence: info@scapeler.com

Website: <https://www.scapeler.com/index.php/visibilis/>

License



© 2019 by the authors. This work is licensed under the Creative Commons Attribution 4.0 International License. To view a copy of this license, visit <http://creativecommons.org/licenses/by/4.0/> or send a letter to Creative Commons, PO Box 1866, Mountain View, CA 94042, USA.

Tables

Index of Tables

Table 1: Properties of the particulate matter sensor.....	10
Table 2: Properties of the meteorological sensors.....	10
Table 3: Between sensor correlation statistics for the PN classes of the PMSA003 sensors.....	23
Table 4: Standard errors in the regression coefficients and intercepts of the MLR models PM2.5 and PM10.....	28
Table 5: properties MLR models against BAM1020 with PM, RH% and T as X-variables.....	30
Table 6: Errors regression coefficients.....	30
Table 7: Properties MLR models against BAM1020 with “PN+RH+T” as X-variables.....	34
Table 8: Errors regression coefficients.....	34
Table 9: Validation results MLR models based on “PM+RH+T”.....	42
Table 10: Validation results MLR models based on “PN+RH+T”.....	46
Table 11: Validation results transfer of PMSA003_9492 models “PM+RH+T” to other PMSA003 sensors	50
Table 12: Validation results transfer of PMSA003_9492 models “PN+RH+T” to other PMSA003 sensors	50
Table 13: Comparison of the primary validation results of the “PN+RH+T” models for sensors PMSA003_8F33 and PMSA003_9290 with model transfer and after PN standardization.....	55

Figures

Table of Figures

Figure 1: Location Visibilis Project.....	7
Figure 2: Berghaven, Hoek van Holland.....	7
Figure 3: Sensor case.....	8
Figure 4: Sven Leckel SEQ47/50 (www.leckel.de).....	9
Figure 5: Met One BAM1020 (www.metone.com).....	9
Figure 6: PM2.5 & PM10 data for the BAM1020 monitors at DCMR Berghaven.....	13
Figure 7: Correlation between PM2.5 & PM10 for the BAM1020 monitors at DCMR Berghaven.....	14
Figure 8: Nova SDS011 correlation plot between PM2.5 & PM10.....	15
Figure 9: Nova SDS011 ‘Luftdaten’ correlation plot between PM2.5 & PM10.....	15
Figure 10: Plantower PMSA003_9492 correlation plot between PM2.5 & PM10.....	16
Figure 11: Dylos DC1100 (particles/0.01 cubic foot) correlation plot between PM2.5 & PM10.....	16
Figure 12: Comparison PM2.5 between BAM1020 and sensors.....	17
Figure 13: Comparison PM10 between BAM1020 and sensors.....	18
Figure 14: Difference PM2.5 between sensors and BAM1020.....	19
Figure 15: Difference PM10 between sensors and BAM1020.....	19
Figure 16: Difference PM2.5 between PMSA003 sensors and BAM1020.....	20
Figure 17: Particle number data of the Plantower PMSA003_9492 sensor 0.3µm, 0.5µm and 1.0µm particles.....	21
Figure 18: Particle number data of the Plantower PMSA003_9492 sensor 1.0µm, 2.5µm and 10.0µm particles.....	21
Figure 19: Correlation plot PN 1.0µm versus PN 2.5µm for sensor PMSA003_9492.....	22
Figure 20: Temperature and relative humidity data of KNMI monitors and sensors.....	24
Figure 21: Air pressure Bosch BME280 sensor.....	25
Figure 22: MLR model for PM2.5 against PN, sensor PMSA003_9492.....	27
Figure 23: MLR model for PM10 against PN, sensor PMSA003_9492.....	27
Figure 24: MLR regression coefficients for PM2.5 for sensor PMSA003_9492.....	28
Figure 25: MLR regression coefficients for PM10 for sensor PMSA003_9492.....	28
Figure 26: PMSA003 - MLR model PM2.5 against BAM1020 with PM, RH% and T as X-variables.....	32

Figure 27: SDS011 basic config - MLR model PM2.5 against BAM1020 with PM, RH% and T as X-variables.....	32
Figure 28: SDS011 Luftdaten - MLR model PM2.5 against BAM1020 with PM, RH% and T as X-variables.....	32
Figure 29: PMSA003 - MLR model PM10 against BAM1020 with PM, RH% and T as X-variables.....	33
Figure 30: SDS011 basic config - MLR model PM10 against BAM1020 with PM, RH% and T as X-variables.....	33
Figure 31: SDS011 Luftdaten - MLR model PM10 against BAM1020 with PM, RH% and T as X-variables.....	33
Figure 32: PMSA003 - MLR model PM2.5 against BAM1020 with "PN+RH+T" as X-variables.....	36
Figure 33: Dylos DC1100 (A) - MLR model PM2.5 against BAM1020 with "PN+RH+T" as X-variables....	36
Figure 34: Dylos DC1100 (B) - MLR model PM2.5 against BAM1020 with "PN+RH+T" as X-variables....	36
Figure 35: PMSA003 - MLR model PM10 against BAM1020 with "PN+RH+T" as X-variables.....	37
Figure 36: Dylos DC1100 (A) - MLR model PM10 against BAM1020 with "PN+RH+T" as X-variables....	37
Figure 37: Dylos DC1100 (B) - MLR model PM10 against BAM1020 with "PN+RH+T" as X-variables.....	37
Figure 38: Outcome of ASTM D6708 improvement on PM2.5 model PMSA003_8F33 "PN+RH+T".....	39
Figure 39: Residuals versus level of different ASTM D6708 calculations on PM2.5 model PMSA003_8F33 "PN+RH+T"	39
Figure 40: PM2.5 BAM1020, MLR, (MLR+Class2) for PMSA003_8F33 Validation Set.....	40
Figure 41: Difference PM2.5 versus BAM1020 for MLR, (MLR+Class2) for PMSA003_8F33 Validation Set	40
Figure 42: PMSA003 - Validation of MLR model PM2.5 against BAM1020 with "PM+RH+T" as X-variables.....	43
Figure 43: SDS011 basic config - Validation of MLR model PM2.5 against BAM1020 with "PM+RH+T" as X-variables.....	43
Figure 44: SDS011 Luftdaten - Validation of MLR model PM2.5 against BAM1020 with "PM+RH+T" as X-variables.....	44
Figure 45: PMSA003 - Validation of MLR model PM10 against BAM1020 with "PM+RH+T" as X-variables	44
Figure 46: SDS011 basic config - Validation of MLR model PM10 against BAM1020 with "PM+RH+T" as X-variables.....	45
Figure 47: SDS011 Luftdate - Validation of MLR model PM10 against BAM1020 with "PM+RH+T" as X-variables.....	45
Figure 48: PMSA003 - Validation MLR model PM2.5 against BAM1020 with "PN+RH+T" as X-variables	47
Figure 49: Dylos DC1100 (A) - Validation MLR model PM2.5 against BAM1020 with "PN+RH+T" as X-variables.....	47

Figure 50: Dylos DC1100 (B) - Validation MLR model PM2.5 against BAM1020 with “PN+RH+T” as X-variables.....	48
Figure 51: PMSA003 - Validation of MLR model PM10 against BAM1020 with “PN+RH+T” as X-variables.....	48
Figure 52: Dylos DC1100 (A) - Validation of MLR model PM10 against BAM1020 with “PN+RH+T” as X-variables.....	49
Figure 53: Dylos DC1100 (B) - Validation of MLR model PM10 against BAM1020 with “PN+RH+T” as X-variables.....	49
Figure 54: Real-time MLR calibration - Example 1.....	52
Figure 55: Real-time MLR calibration - Example 2.....	52
Figure 56: Real-time MLR calibration - Example 3.....	53
Figure 57: Real-time MLR calibration - Example 4.....	53
Figure 58: Correlation plot PN Class 2.5 μ m between PMSA003_9290 and PMSA003_9492.....	54
Figure 59: Validation of the “PN+RH+T” PM2.5 model for sensor PMSA003_9290 after standardization of the PN classes.....	56
Figure 60: Validation of the “PN+RH+T” PM2.5 model for sensor PMSA003_8F33 after standardization of the PN classes.....	56
Figure 61: Validation of the “PN+RH+T” PM10 model for sensor PMSA003_9290 after standardization of the PN classes.....	57
Figure 62: Validation of the “PN+RH+T” PM10 model for sensor PMSA003_8F33 after standardization of the PN classes.....	57

Appendix 1

Coding and properties of the sensors and official monitors

Code	Monitor/Sensor	Parameter	Unit
PM2.5_BAM1020	BAM1020	PM2.5	µg/m³
PM10_BAM1020	BAM1020	PM10	µg/m³
PM2.5_SDS011	SDS011 basic	PM2.5	µg/m³
PM10_SDS011	SDS011 basic	PM10	µg/m³
PM2.5_SDS011_Luft	SDS011 Luftdaten	PM2.5	µg/m³
PM10_SDS011_Luft	SDS011 Luftdaten	PM10	µg/m³
PM2.5_PMSA003_8F33/9290/9492	PMSA003 sensor 1/2/3	PM2.5	µg/m³
PM10_PMSA003_8F33/9290/9492	PMSA003 sensor 1/2/3	PM10	µg/m³
DylosDC1100>0.5µm	Dylos DC1100	>0.5 µm	Particles / 0.01 cubic foot
DylosDC1100>2.5µm	Dylos DC1100	>2.5 µm	Particles / 0.01 cubic foot
PMSA003_8F33/9290/9492_RAW_0.3	PMSA003 sensor 1/2/3	>0.3 µm	Particles per 0.1 L
PMSA003_8F33/9290/9492_RAW_0.5	PMSA003 sensor 1/2/3	>0.5 µm	Particles per 0.1 L
PMSA003_8F33/9290/9492_RAW_1.0	PMSA003 sensor 1/2/3	>1.0 µm	Particles per 0.1 L
PMSA003_8F33/9290/9492_RAW_2.5	PMSA003 sensor 1/2/3	>2.5 µm	Particles per 0.1 L
PMSA003_8F33/9290/9492_RAW_5.0	PMSA003 sensor 1/2/3	>5.0 µm	Particles per 0.1 L
PMSA003_8F33/9290/9492_RAW_10.0	PMSA003 sensor 1/2/3	>10.0 µm	Particles per 0.1 L
Dallas_EXT_T°C	Dallas external sensor	Temperature	°C
BME280_8F33/9290/9492_T°C	Meteo sensor 1/2/3	Temperature	°C
BME280_8F33/9290/9492_RH%	Meteo sensor 1/2/3	Relative Humidity	%
BME280_8F33/9290/9492_Pi	Meteo sensor 1/2/3	Air Pressure	hPa
KNMI_T°C	KNMI Hoek van Holland	Temperature	°C
KNMI_RH%	KNMI Hoek van Holland	Relative Humidity	%

SDS011 = Nova SDS011

PMSA003 = Plantower PMSA003

BME280 = Bosch BME280

References

1. The influence of humidity on the performance of a low-cost air particle mass sensor and the effect of atmospheric fog, Rohan Jayaratne, Xiaoting Liu, Phong Tai, Matthew Dunbabin, Lidia Morawska, International Laboratory for air quality and health, and Institute for future environments. Queensland University of Technology, Brisbane, Australia. 27 August 2018.
2. Fine particle mass monitoring with low-cost sensors: Corrections and longterm performance evaluation, Carl Malings , Rebecca Tanzer, Aliaksei Hauryliuk, Provat K. Saha, Allen L. Robinson , Albert A. Presto , and R Subramanian, Center for Atmospheric Particle Studies, Carnegie Mellon University, Pittsburgh, Pennsylvania, USA, 10 June 2019.
3. Met One Technical Bulletin, Dennis Hart, 30 December 2010.

